1961-05

A flight test determination of the static longitudinal stability of the Cessna 310d airplane

Lenox, Glen W.; Lindell, Clifford A.

Princeton University

A FLIGHT TEST DETERMINATION OF THE STATIC LONGITUDINAL STABILITY OF THE CESSNA 310d AIRPLANE

GLEN W. LENOX
and
CLIFFORD A. LINDELL

A FLIGHT TEST DETERMINATION OF THE STATIC LONGITUDINAL STABILITY OF THE CESSNA 310d AIRPLANE

By

Lt. Glen W. Lenox, USN
Capt. Clifford A. Lindell, USMC

Aeronautical Engineering Report No. 547

May 1961

Submitted in partial fulfillment of the requirements for the Degree of Master of Science in Engineering from Princeton University, June 1961

ACKNOWLEDGEMENTS

The authors wish to commend Princeton University for providing the excellent opportunities for gaining actual experience in the flight testing of aircraft for stability. The authors' sincere appreciation is extended to Professor Courtland D. Perkins, under whose inspiration and guidance this investigation was conducted. In addition, the authors wish to express their humble thanks to Professor Perkins for making the test aircraft available for their exclusive use during the flight test phase of this investigation, a significant factor in the smooth conduct and rapid completion of the flight tests.

The authors acknowledge with gratitude the opportunities for postgraduate education provided by the United States Navy and the United States Marine Corps.

Appreciation is further extended to Mr. Thomas E. Sweeney and the hangar staff for their assistance in the design and installation of the required instrumentation and in providing excellent maintenance of the test aircraft during this investigation.

Special thanks are due Mrs. Elizabeth Kenney who typed the manuscript and whose enthusiasm and assistance in preparation added materially to the progress of this report.

TABLE OF CONTENTS

LIST OF FIGURES

LIST OF SYMBOLS

a.c.	Aerodynamic center
a_t	tail lift curve slope
a_w	wing lift curve slope
c	mean aerodynamic chord, (ft.)
c_e	elevator chord, (ft.)
C_{h_α}	$\partial C_h / \partial \alpha_t$
C_{h_δ}	$\partial C_h / \partial \delta_e$
C_L	lift coefficient
C_m	pitching moment coefficient
C_{m_δ}	elevator power derivative
C_{N_A}	normal force coefficient, nC_L
C_{n_p}	propeller normal force coefficient
dC_m / dC_L	stick fixed stability
D	propeller diameter, (ft.)
F_s	stick force, (lbs.)
G_e	elevator to stick gearing, (rad./ft.)
h	distance from c.g. to N_o, (ft.)
ℓ_e	distance from c.g. to center of pressure of tail, (ft.)
ℓ_p	propeller moment arm, (ft.)

l_t	distance from wing a.c. to tail a.c., (ft.)
MAC	mean aerodynamic chord, (ft.)
n	normal load factor
N_m	stick fixed maneuver point, (% MAC)
N_m'	stick free maneuver point, (% MAC)
N_o	stick fixed neutral point
N_o'	stick free neutral point
ΔP	stick force increment due to downspring, (lbs.)
q	dynamic pressure
S or S_w	wing area, (sq. ft.)
S_p	propeller disc area, (sq. ft.)
S_t	tail area, (sq. ft.)
T_c	thrust coefficient
V	velocity, (mph)
$\bar{V}$	tail volume coefficient
W	airplane gross weight, (lbs.)
x_a	distance of a.c. from $x_{c.g.}$ (ft.)
$x_{c.g.}$	distance of c.g. from leading edge of MAC, (ft.)
z	vertical location of thrust line, measured from c.g., (ft.)

GREEK SYMBOLS

α	angle of attack, (deg. or rad.)
δ_e	elevator deflection, (deg.)
$\left\lvert \frac{d\beta}{d\alpha} \right\rvert_{prop}$	wing upwash derivative evaluated at the propeller
$d\varepsilon/d\alpha$	wing downwash derivative
$d\varepsilon_p/d\alpha$	propeller downwash derivative
η_p	propeller efficiency
η_t	tail efficiency, q_t/q
ρ	air density, (slugs/cu. ft.)
τ	elevator effectiveness

SUBSCRIPTS

a.c.	aerodynamic center
c.g.	center of gravity
e	elevator
i	indicated
p	propeller
s	stick or slipstream
t	tail
w	wing

A FLIGHT TEST DETERMINATION OF THE STATIC LONGITUDINAL STABILITY OF THE CESSNA 310d AIRPLANE

SUMMARY

The purpose of this investigation was to determine the static longitudinal stability of the Cessna 310d airplane through steady state flight tests.

The flight test method used to determine the location of the neutral points was that in which the equilibrium elevator angle and stock force were measured at various steady state airspeeds and center of gravity locations. The maneuver points were determined from measurements of equilibrium elevator angle and stick force for various load factors and center of gravity locations in steady turns.

Through analysis of the flight test data, the variations of the neutral points with lift coefficient were determined for the cruise configuration and the approach configuration, both power on and power off. The maneuver points were determined for the power on cruise configuration. Elevator power was determined by analysis of the "1 g" elevator position trim curves. A theoretical analysis was conducted to check the validity of the flight test results.

The major results of this investigation are:

1. Close correlation exists between the theoretical and the

flight test results except for stick free maneuvering stability and elevator power.

2. The airplane has a satisfactory level of stick fixed stability and an unusually high level of stick free stability throughout the flight test regime.

3. Maneuvering stability is relatively high and is normal in all respects.

4. Elevator power varies slightly with lift coefficient.

A FLIGHT TEST DETERMINATION OF THE STATIC LONGITUDINAL STABILITY OF THE CESSNA 310d AIRPLANE

INTRODUCTION

The purpose of this investigation was to determine the variation of the Neutral Points (N_o and N_o') and the Maneuver Points (N_m and N_m') with lift coefficient for a variety of airplane configurations and power settings. A secondary objective was to devise an instrumentation setup which would be as simple and as portable as possible and still provide data with sufficient accuracy.

The stick fixed (control position) and stick free (control force) static stability of an airplane can be determined from steady state flight tests by measuring the deflection of the longitudinal control surface and the stick or wheel force at various airspeeds and normal force coefficients. Analysis of these data can yield the stability levels of the airplane in the form of the variations of the neutral and maneuver points with lift coefficient.

There are three flight test methods currently used by various organizations to determine the location of the neutral points. These are: the "Effective Weight Moment" method, as described in Ref. 1; the "Tab Angle" method, (Refs. 2 and 3); and the elevator angle and stick force vs. airspeed method.

The elevator angle and stick force vs. airspeed method was used in this investigation. This method was selected in order to avoid the instrumentation difficulties of the Effective Weight Moment method and the excessive time required for data collection and reduction with the "tab angle" method. Ref. 3 gives a good description and evaluation of these various methods of flight testing for neutral points.

In the determination of airplane maneuver points, there are three flight test techniques that can be used to obtain the necessary elevator angle and stick force vs. normal acceleration data. These are the steady pull-up, the wind-up turn, and the steady turn. These methods are well described in Ref. 2.

The steady turn was chosen for this investigation. The steady turn is a constant acceleration, constant airspeed turn. Since steady airspeed and accelerations exist throughout the maneuver, a simplified instrumentation can be used. The altitude variation is less in this maneuver than in either of the above maneuvers. More accurate stick force data are available than in the wind-up turns where stick forces are trimmed to zero at only the highest test airspeed. The instrumentation requirements are less severe than in the wind-up turns and less flight time is required than in the steady pull-ups.

The Elevator Power derivative, C_{m_δ}, was determined by an analysis of the "1 g" elevator trim curves.

For purposes of comparison with flight results, theoretical values of the neutral points, maneuver points, and the elevator power were determined for the cruising configuration at an appropriate lift coefficient. This theoretical analysis is included as an Appendix to this report.

All phases of this investigation were conducted at the Forrestal Research Center during the Spring Semester of the 1960-61 Academic Year.

EQUIPMENT

TEST AIRPLANE

The airplane used for the flight test program was a standard Cessna Model 310d, Registration No. N 6954T, powered by two Continental I0-470-D engines. The Continental I0-470-D is an horizontally opposed, six cylinder reciprocating engine and has a rated power of 260 horsepower at 2625 RPM. The airplane is equipped with two all-metal, hydraulically operated, constant speed, full-feathering, two-bladed propellers. Conventional wheel and rudder pedal controls operate the primary flight control surfaces. Each surface has an adjustable trim tab and the elevator is fitted with a downspring. The landing gear is of the fully-retractable, tricycle type, incorporating a steerable nosewheel.

The following general specifications and dimensions for the Cessna 310d are taken from manuals and reports published by the Cessna Aircraft Company.

Airplane, general

Length (overall)	29.50 ft.
Height	9.33 ft.
Design Gross Weight	4830 lb.

Wing

Area (total)	175 sq. ft.
Span	35.77 ft.

Type	Full Cantilever
Airfoil (centerline)	NACA 23018
Airfoil (tip)	NACA 23009
Airfoil (nacelle)	NACA 23012
Incidence (root)	$+2^{\circ}$ 30'
Incidence (tip)	-0° 30'
Mean Aerodynamic Chord	61 in.
Taper Ratio	1.517
Aspect Ratio	7.0
Area (flap)	22.9 sq. ft.
Angular Travel (flap down)	$45^{\circ} + 1^{\circ} - 0^{\circ}$
Leading edge of MAC from Datum plane	22.25 in.

Horizontal Tail

Span (total)	17 ft.
Airfoil (root)	NACA 0009
Airfoil (tip)	NACA 0006
Incidence	-1° 45'
Area (total)	54.25 sq. ft.
Area (stabilizer)	32.15 sq. ft.
Area (elevator)	22.10 sq. ft.
Tail a.c. from wing a.c.	175 in.
Elevator to stick gearing ratio	.98 rad./ft.
Elevator chord (average)	1.3 ft.

INSTRUMENTATION

GENERAL

The only instrumentation devices required for neutral point, maneuver point, and elevator power determination, other than those contained in the aircraft's standard instrument panel, were for the measurement of stick force, elevator angle, and normal acceleration. A small portable box, containing instrumentation for reading elevator angle and stick force, was designed specifically for this investigation to meet the test objective of the use of simplified instrumentation. The box was held by the recorder. The portable feature enabled the recorder to move about in the aircraft cabin for purposes of shifting the c.g. location, and permitted quick and easy removal of the extra instrumentation when the aircraft was not being utilized for flight test purposes. The portable instrumentation box is shown in Fig. 3. The circuit diagram for the instrumentation system is shown as Fig. 4.

POWER SUPPLY

A 22.5 volt dry cell storage battery provided the electrical power for the measurement of stick force and elevator angle.

STICK FORCE

The standard pilot's control wheel was replaced by a special wheel built for stick force measurement. See Fig. 5 for a picture showing the force measuring wheel installed in the aircraft. Four

Baldwin SR-4, type A-7, strain gages were installed on the cross beam of the wheel, and connected as shown in Fig. 4. The strain gages were supplied with a maximum of 15 volts potential throughout the tests. The use of a ten turn potentiometer in the balancing circuit permitted the nulling of the stick force signal on a microammeter, thus eliminating any errors due to supply voltage variation. The system was then calibrated for potentiometer setting versus applied stick force in pounds as shown in Fig. 6.

ELEVATOR ANGLE

A one turn potentiometer, supplied with approximately 20 volts potential through an adjustable pot, was mounted on the tail section fuselage bulkhead. A 6.5 to 1 ratio of elevator movement to potentiometer movement was obtained by using a waxed nylon line wrapped around a small pulley on the potentiometer shaft. One end of this string was secured to a clamp on the elevator hinge bar, and the other end was attached to a small wire spring fastened to a bulkhead in the tail section. The tension on the line provided by the spring enabled the wiper of the potentiometer to follow elevator movement with a minimum of "play" and "backlash" in the system.

The output of the potentiometer was brought up to a cannon plug at the rear bulkhead of the aircraft cabin to permit easy connection to or removal from the portable instrumentation box held by the data recorder. A ten turn potentiometer was used in the measuring circuit

to null the output of the elevator potentiometer which was displayed on a microammeter. This nulling feature, as that in the force circuit, eliminated errors due to supply voltage variation. The system was calibrated for setting of the ten turn potentiometer vs. elevator angle. Elevator angle was determined using a propeller protractor mounted on the top surface of the elevator. The calibration curve is shown in Fig. 7.

ACCELEROMETER

A mechanical accelerometer, consisting of a cylindrical lead weight supported by a small coiled wire spring, was mounted inside a 16 inch long glass tube. The spring was attached to a rubber stopper placed in the top of the glass tube. The accelerometer was then calibrated in units of 0.1 g with appropriate marks inscribed on the outside of the tube. The accelerometer was mounted in the airplane by the use of a hook attached to the top of the cabin and placed so it could be easily observed by the pilot.

STANDARD AIRCRAFT INSTRUMENTS

Airspeed, altitude, and fuel quantity were determined by using the airplane's standard instruments. Airspeed calibration data were taken from a manual published by the manufacturer. Spot checks were made of the data by the speed course method and substantiated the published data. Airspeed calibration curves are presented in Figs. 8 and 9. The fuel quantify gage was calibrated by first draining the main

tanks, then reading the indicated fuel quantity for several measured amounts of fuel as the tank was refilled. The fuel gage calibration is shown in Fig. 10. No attempt was made to calibrate the altimeter for accuracy since it was used for general reference only.

CENTER OF GRAVITY DETERMINATION

The airplane was placed on scales in a gear down configuration and weighed in order to determine the basic weight and c.g. location. The moment of the airplane was calculated with respect to Station 0.0, hereafter known as the Datum. By using a variety of loading conditions the moment arms were found for each of the seat locations and for the baggage compartment. The values so obtained confirmed those published by the manufacturer.

The effect on the c.g. location of actuating the landing gear was determined by jacking up the airplane with the two front jacks (of a four point arrangement) mounted on scales. Scale readings were taken with the landing gear in the up and down positions. Knowing the basic weight from previous measurements, the effect of actuating the landing gear was calculated as a net moment change about the datum.

The moment arm of the fuel in the main tanks was not calculated, the value provided by the manufacturer was used in all computations in this report. The auxiliary fuel tanks contained approximately five gallons each. Special care was taken to ensure that no fuel was added to or consumed out of the auxiliary tanks. Hence, no computations or measurements were required for auxiliary fuel.

Having the values for the basic airplane moment, basic airplane weight, weight of pilots, passengers, and/or ballast, and also knowing the moment arms for fuel and each location in the cabin, the weight and moment (hence, c.g. location) can be calculated for the airplane under any loading condition.

Weight and balance information is summarized in the following table.

	Weight	Moment about Datum
Basic airplane, gear up (includes oil and 10 gal. aux. fuel)	3328 lb.	115,628 in.-lb.
Basic airplane, gear down	3328 lb.	113,813 in.-lb.

Moment arms from datum for variable loads:

Main fuel	35 in.
Pilot	38 in.
Middle passenger seat	69 in.
Rear passenger seat	96 in.
Ballast	96 in.

PROCEDURE

In general, the procedures used in this investigation for both flight testing and data reduction follow the guide lines set forth in Ref. 2. Although only two center of gravity locations are theoretically needed, five were used in each test in order to account for any possible nonlinearities and to reduce experimental error. The variation in c.g. location was obtained by moving one of the investigators (or a passenger) from seat to seat in the cabin with and without ballast in the baggage compartment. A total shift in c.g. location of nine to ten percent was thus obtained in each configuration.

Two airplane configurations were investigated: the Cruise configuration, and the Landing Approach configuration. Each configuration was tested for both Power On and Power Off conditions in order to determine the power effects on static stability. Maneuvering tests were performed in only the cruise configuration since maneuvering stability in the Approach configuration is normally of no interest.

The cruise configuration, as used herein, was with landing gear and flaps up and a trim speed of 180 mph. The cruise power setting used was that required for level flight at the trim airspeed at an altitude of 8000 feet (approx. 52% power).

In the approach configuration, the landing gear were down and flaps were full down (45°). The trim speed was 110 mph. The power setting desired for the approach configuration tests was that which

would give level flight at the trim speed at low altitudes -- sea level to about 3000 feet. Approximately 55% power was used in this investigation. It is normally desirable that the approach configuration tests be conducted at a relatively low altitude, but an average test altitude of 7500 feet was used in this investigation. It was found that even the very low levels of turbulence encountered at low altitudes caused a lightly damped yawing oscillation which created difficulties in obtaining reliable steady state data. Thus it was necessary to conduct the flight tests above a prevailing cloud layer in order to be in smooth air.

In both configurations the "power off" engine setting was that which was estimated to give zero thrust.

NEUTRAL POINTS, Flight Tests

As mentioned above, the neutral points were found for both power on and power off in each airplane configuration. The same flight test procedure was used for each condition. First, the airplane and power configurations were selected. Next, the c.g. condition was selected by positioning the recorder and his portable instrumentation box in a given seat. The most forward c.g. condition was usually tested first to take advantage of the rearward shift in c.g. as fuel was consumed. Three c.g. positions were obtained by moving the recorder from seat to seat. For the remaining two c.g. positions it was necessary to land and install the ballast in the baggage compartment. The change in c.g. location was again obtained by shifting the recorder from one seat to another.

After selecting the c.g. location, the airplane was trimmed for hands-off flight at the trim speed, 180 mph, and at the test altitude, 8000 feet. Once the power and trim settings were made for a given condition, neither was changed for the remainder of the test at that c.g. condition. The airspeed was then changed by a small increment and stabilized. When steady conditions were reached, the elevator position and stick force indicator readings were recorded. This process was repeated over the full speed range of the airplane for the configuration being tested. In each case, data were taken for ten or more steady state airspeeds in order to reduce experimental error and account for nonlinearities. Special care (and rudder action) was taken by the pilot to ensure that zero sideslip was maintained for all the test airspeeds.

NEUTRAL POINTS, Data Reduction

All of the recorded data were corrected or put into proper form by referring to the appropriate calibration curves and the c.g. location was computed as a percentage of the mean aerodynamic chord for each c.g. condition. The subsequent analysis follows the same procedure for each configuration.

Elevator position and stick force were plotted against calibrated airspeed for each c.g. location as a first step in the analysis. By plotting against airspeed rather than Lift Coefficient, the curves were smoothed through points which were relatively evenly spaced throughout the speed range tested. Then more accurate curves of elevator angle

vs. lift coefficient and stick force divided by dynamic pressure vs. lift coefficient could be drawn. See, for instance, Figs. 20, 21, 23, and 24. Slopes of the above curves were then taken at various values of lift coefficient and plots were made of $\frac{d\delta_e}{dC_L}$ vs. % MAC and of $\frac{d\ F_s/_q}{dC_L}$ vs. % MAC for the various values of lift coefficient. See Figs. 22 and 25. By definition, the neutral points, N_o and N_o', are the c.g. locations at which $\frac{d\delta_e}{dC_L}$ and $\frac{d\ F_s/_q}{dC_L}$, respectively, are zero. Hence, the neutral points were at once determined for the various lift coefficients. As mentioned above, this same procedure of analysis is used for each configuration. See Fig. 27 for a summary of the neutral points for the cruise configuration and Fig. 42 for the neutral points for the approach configuration.

MANEUVER POINTS, Flight Tests

The maneuver points were determined by an analysis of elevator angle and stick force data taken at various values of normal acceleration -- all at the same airspeed. There is often a small difference in the data obtained in left hand and right hand turns due to gyroscopic effects when using the steady turn maneuver. A preliminary test showed this difference to be minor in the Cessna 310d and all the data for this investigation were taken in left hand turns.

The maneuver points were found for the same cruise configuration as used in the neutral points flight tests, i.e., same trim airspeed,

test altitude, and power setting. The c.g. conditions were selected as described for the neutral points flight tests and the airplane trimmed for hands off flight. The power and trim settings remained unaltered throughout the test at any one c.g. condition. The airplane was placed in a left hand turn and when steady flight conditions were established (constant airspeed at V_{trim}, zero sideslip, and a constant level of normal acceleration, n), the elevator position and the stick force indications were recorded. This process was repeated for several values of normal acceleration evenly spaced between 1.0 and 2.0.

MANEUVER POINTS, Data Reduction

As in the neutral point analysis, the recorded data were corrected and put into the proper form by referring to the appropriate calibration curves and the c.g. location was computed as a percentage of MAC for each of the five c.g. conditions tested. One additional correction was made. Where the airspeed in the steady turn varied from V_{trim}, the elevator trim curves for the neutral point investigation were consulted for the same c.g. location. From these curves the elevator angle and stick force in level flight could be determined for the airspeed recorded in the maneuver and these values used as a basis for correction of the recorded maneuvering elevator angle and stick force. Although the steady airspeed attained in the maneuver never varied more than 2 mph from V_{trim}, the resulting correction was often significant.

The elevator angle and the stick force were each plotted (Figs. 43 and 46) against normal force factor, n. These curves provided smoothed data for plotting (Figs. 44 and 47) δ_e and F_s/q against normal force coefficient, C_{N_A}, ($C_{N_A} = nC_L$) for each c.g. condition. The slopes of these curves were then taken at various values of normal force coefficient and plotted against % MAC (Figs. 45 and 48) resulting in the maneuver points as the intersections on the abscissa of each graph. See Fig. 49 for a summary plot showing the variation of N_m and N_m' with C_{N_A}.

ELEVATOR POWER

The 1 g elevator trim curves yield not only the neutral points, but also the elevator power derivative, C_{m_δ}. In short, the elevator power can be considered as a measure of the moment developed by elevator deflection in balancing the effective pitching moment increment produced by a c.g. shift. Then, from Ref. 2, the following expression can be used to determine the elevator power from the elevator trim curves:

$$C_{m_\delta} = -\frac{\Delta X_{cg}}{\Delta \delta_e} C_L$$

This expression is based on the airplane C_L and, as a result, neglects the tail lift effect. A correction factor was developed in Ref. 4 to account for the tail lift effect and is included as follows:

$$C_{m_\delta} = -\frac{\Delta X_{cg}}{\Delta \delta_e} C_L \frac{\ell_e/c}{\ell_e/c - h/c}$$

where C_L is the airplane lift coefficient,
c is the mean aerodynamic chord,
h is the distance from the c.g. to the neutral point, and
ℓ_e is the distance from the c.g. to the center of pressure of the tail, which for calculations was assumed to coincide with the quarter chord of the tail.

With the above expression, the elevator power was determined for both the cruise and approach configurations, power on and power off. Due to the nature of the tail correction factor, C_{m_δ} will vary slightly with c.g. position. C_{m_δ} was determined for the most forward and most aft c.g. locations in each test and it was found that these extreme values differ by only .001. Curves of elevator power variation with airplane lift coefficient are shown in Fig. 50. These curves represent the mean values in each case and the maximum error encountered due to c.g. shift will be about 1.5%.

DISCUSSION OF RESULTS

The main results of this investigation are summarized on Figs. 27, 42, 49, and 50, copies of which are included in this section of the report for easy reference. For comparison, values of theoretical and flight test results, at similar flight conditions, are shown below in tabular form. These results are for the power on, cruise configuration only.

Parameter	Theoretical	Flight Test
N_o	.477	.460
N_o'	.634	.617
N_m	.564	.550
N_m'	.526	.412
C_{m_δ}	-.0356	-.0282

Close agreement between theoretical and flight test values is observed for all but the stick free maneuver point and elevator power. This difference is probably due to the difficulties in accurately estimating values of tail efficiency and elevator hinge moment derivatives.

NEUTRAL POINT SUMMARY, Cruise Configuration, Fig. 27

The most apparent result shown on Fig. 27 is that the airplane is much more stable "stick-free" than "stick-fixed", due to the action of the strong downspring installed in the elevator control system.

Fig. 27 also shows the effect predicted by Gilruth in Ref. 5,

that low wing monoplanes will have a decrease in stability with increased angle of attack in the power on configuration.

The normal trend of increasingly detrimental power effects with C_L on N_o is seen by comparing the "N_o, power on" and "N_o, power off" curves. The fact that these curves cross at low C_L cannot be fully explained. It is expected that these curves would be close together normally, since the de-stabilizing effects of slipstream and propeller normal force are relatively small at low values of C_L. The crossing of these curves at low C_L could possibly be attributed to:

1. Unusual flow effects on the tail
2. Experimental error
3. Other unknown factors

In any case, the net effect is not pronounced.

The effects of power on N_o' with increasing C_L are reversed from the power effects on N_o. This suggests a strong nonlinearity in C_{h_α} and C_{h_δ} due possibly to slipstream and nacelle wake effects on the horn balance of the elevator. The difference between N_o' and N_o, in the "power off" case, tends to decrease as C_L increases. This trend is probably due to reduction of downspring force as the elevator is raised, and to the variation in C_{m_δ} with C_L, as shown in Fig. 50.

NEUTRAL POINT SUMMARY, Approach Configuration, Fig. 42

The effect of the heavy downspring is also seen in the approach

configuration, since the stick-free neutral point is about 8 to 10% MAC aft of the stick-fixed neutral point.

The other important result seen in Fig. 42 is that the power effects are very large, especially when compared to results for the cruise configuration. This is probably due to the effect of the flaps increasing the upwash in front of the wing in the vicinity of the nacelles and propellers. The increased upwash would accentuate the de-stabilizing effect of propeller normal force and nacelle pitching moment derivatives.

By comparing Figs. 27 and 42, it is observed that the gear and flap extension has little effect on the power-off stick-fixed neutral point. The power-off stick-free neutral point moves forward about 7% MAC, which further suggests nonlinearities in C_{h_α} and C_{h_δ}.

For the power-on case, the divergence in N_o' and N_o with increased C_L is similar to that observed in the cruise configuration, and can presumably be accounted for by the same reasons.

MANEUVER POINTS, Cruise Configuration, Fig. 49

The maneuver points showed the normal trend in that N_m' is forward of N_m. The stick-fixed maneuver point, N_m, shows a favorable comparison with the theoretical value, while the stick-free neutral point, N_m', differs by approximately 10% MAC from the theoretical value. This indicates a variation from theory in the

elevator hinge-moment derivatives, C_{h_α} and C_{h_δ}, and points up the difficulty in theoretically estimating their values.

ELEVATOR POWER, C_{m_δ}

From Fig. 50 it is observed that elevator power increases with C_L in the power on configurations. It is believed this is due to the increased tail efficiency caused by the increased slipstream velocity ratio at lower airspeeds, as predicted by Gilruth in Ref. 5. The decrease in slope at higher C_L for the power on cruise configuration is probably caused by the tail becoming more immersed in the nacelle and wing wake.

From a study of measurements made on the airplane, it is apparent that the flow over the tail will be affected by the nacelle wake, particularly in nose-up attitudes.

The power off configurations demonstrate a slight increase in elevator power with increased C_L. This is difficult to explain fully, but is probably caused by the wing and nacelle wake effects on flow over the tail.

FIG. 2.7
NEUTRAL POINT SUMMARY

CRUISE CONFIGURATION

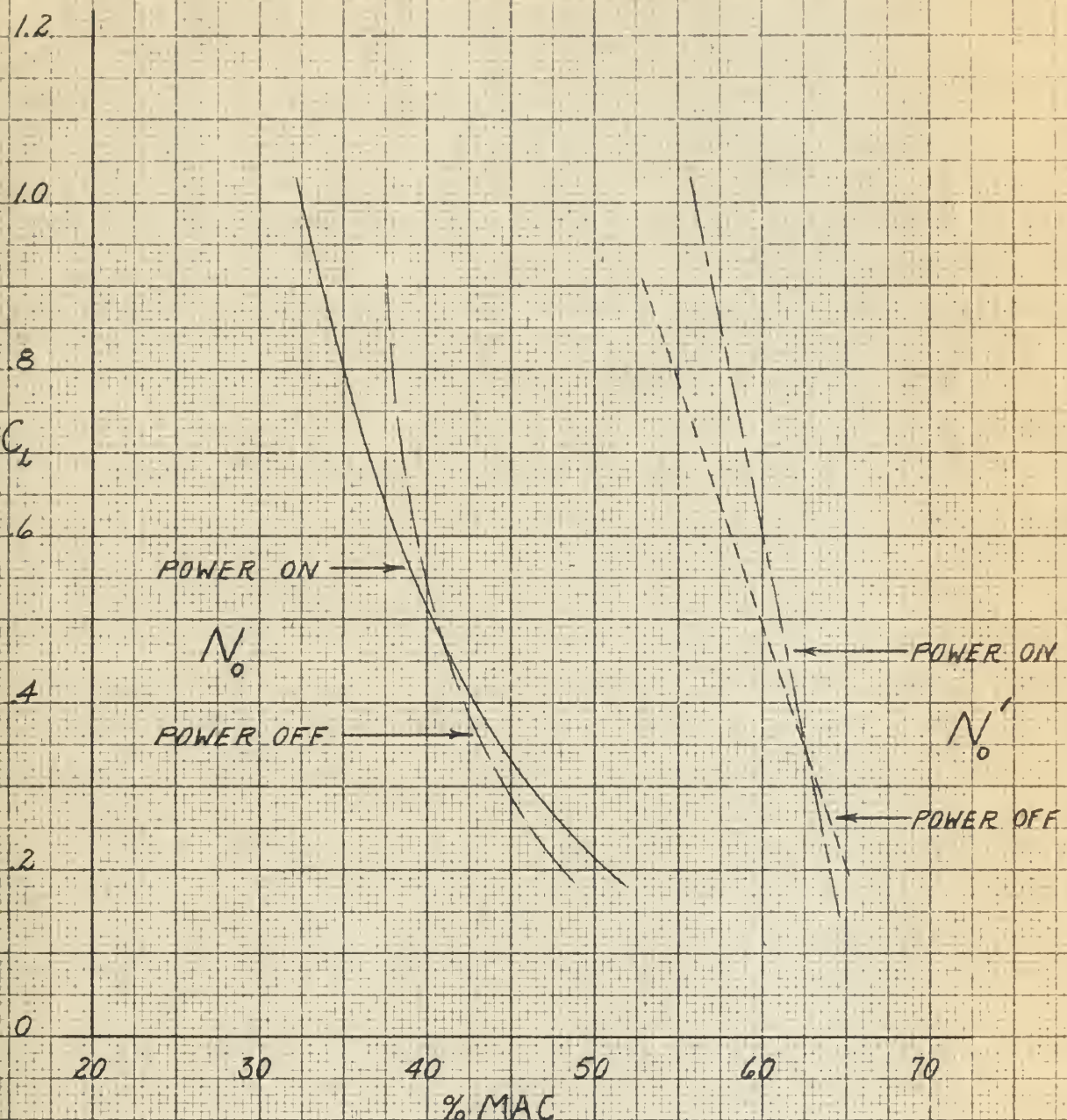

FIG. 42

NEUTRAL POINT SUMMARY

APPROACH CONFIGURATION

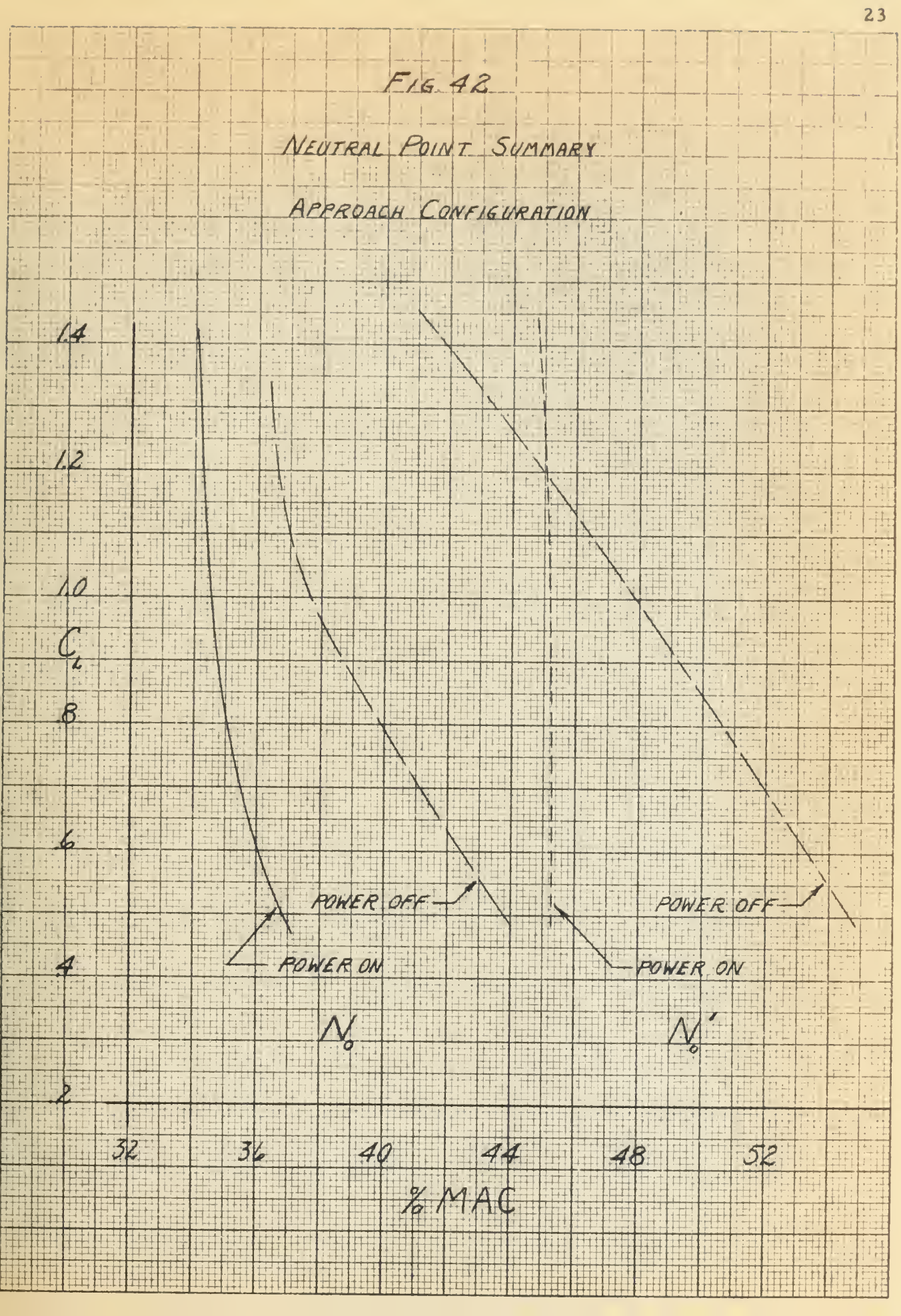

FIG. 49
MANEUVER POINTS

CRUISE CONFIGURATION

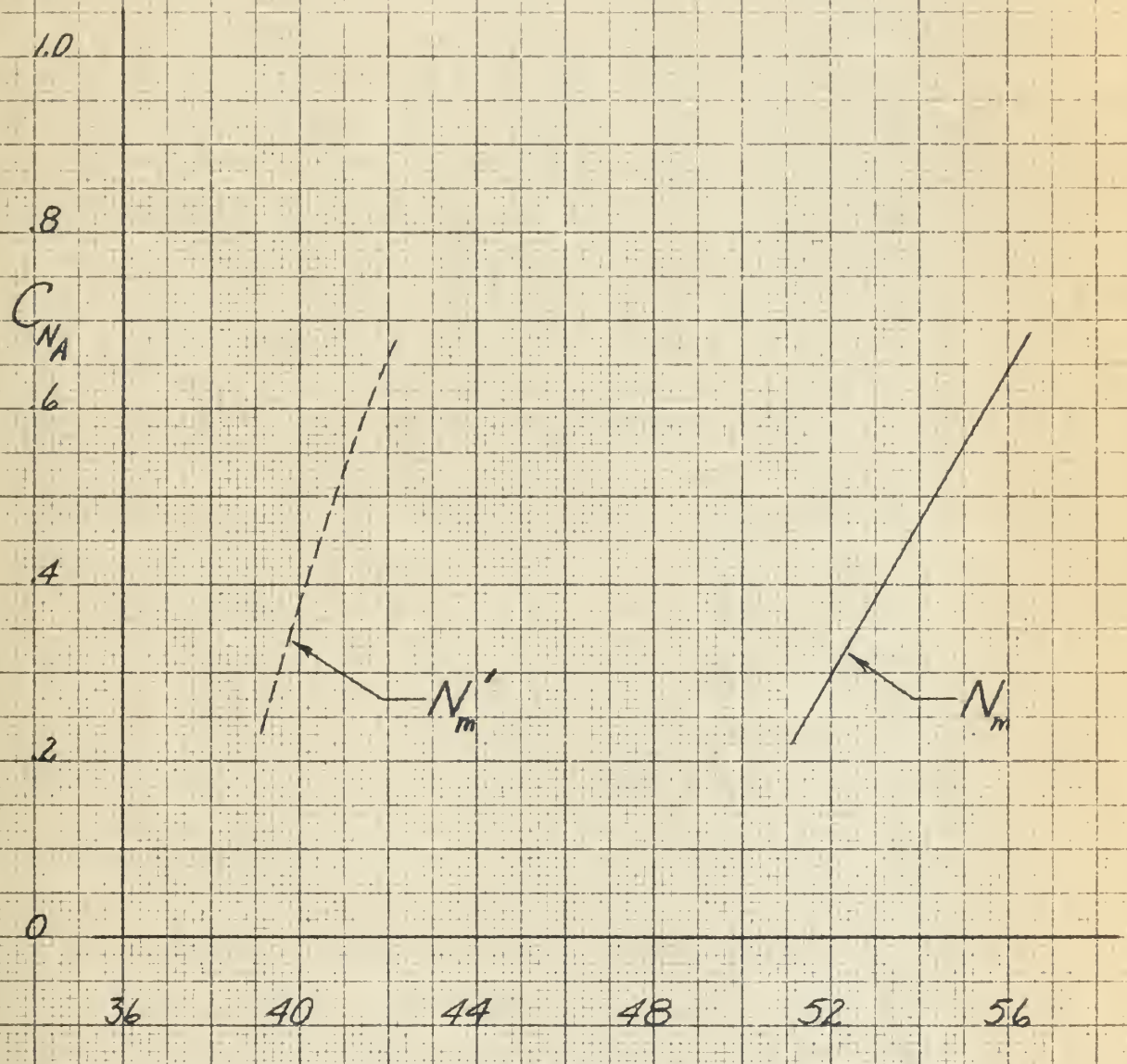

FLIGHT TEST 4-4-61

FIG 50

ELEVATOR POWER

C_{m_δ} VS C_L

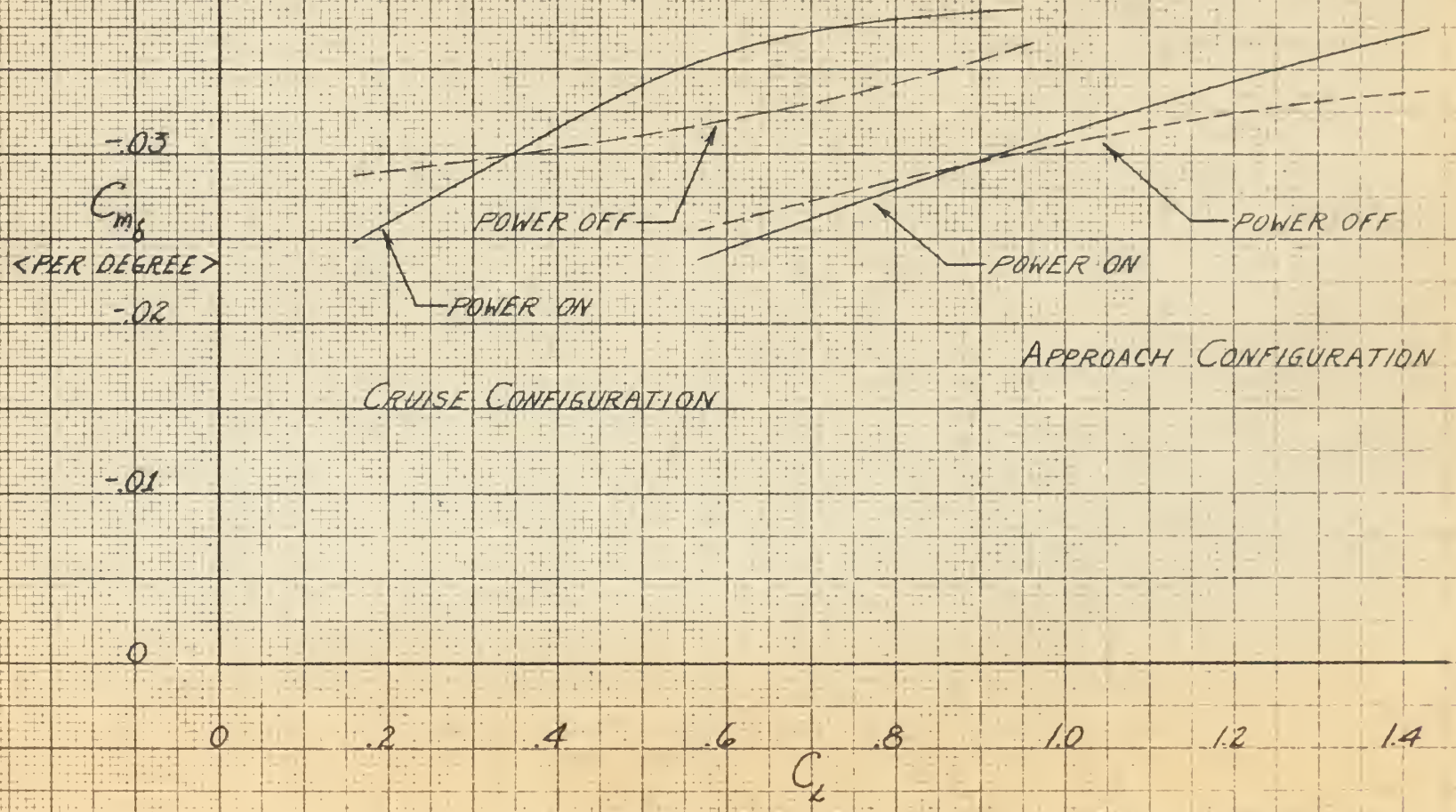

CONCLUSIONS

It is concluded that:

1. The simplified, portable instrumentation system developed for this investigation is reliable and capable of supplying sufficiently accurate steady state flight test data.

2. Close correlation exists between theoretical and flight test results except for stick free maneuvering stability and elevator power.

3. The Cessna 310d airplane has a satisfactory level of control-fixed stability throughout the flight test regime and the stability variation with lift coefficient and power follows the normal pattern.

4. The Cessna 310d airplane has an unusually high level of control-free stability due to the effect of the strong downspring.

5. The unusual variation of control-free stability with power is due to nonlinearities in the elevator hinge moment derivatives.

6. The power effects on static longitudinal stability are more pronounced in the approach configuration than in the cruise configuration.

7. There is a decrease in the static stability with landing gear and flap extension in the power on case.

8. The relative positions of the maneuvering points of the Cessna 310d airplane is normal in that N_m' is forward of N_m. There is a slight nonlinearity with C_{N_A} in evidence in both N_m and N_m'.

9. Due to the very small range of elevator travel encountered in the flight regimes tested and the high level of downspring force present

at those elevator angles, the nonlinearity of downspring force with elevator angle causes no appreciable adverse effects in stick-free stability.

10. Elevator power, C_{m_δ}, varies with lift coefficient. This variation is due to power effects and to the wing and nacelle wake effects on the flow over the tail.

RECOMMENDATIONS

It is recommended that:

1. The strength of the downspring be reduced by at least a factor of one half.

2. A detailed study be made of the power and attitude effects on the elevator hinge moment derivatives. It is further recommended that a study be made of the effects of wing and nacelle wake on the flow over the tail.

3. Lateral Static and Dynamic Stability be investigated. This recommendation is based on the observation, during the static longitudinal stability flight tests, that light turbulence excited a lightly-damped yawing oscillation.

REFERENCES

1. Flight Testing for Performance and Stability, Allen, Edmund T., Journal of Aeronautical Sciences, Vol. 10, No. 1, January 1943.

2. Advisory Group for Aeronautical Research and Development Flight Test Manual, Volume II, Stability and Control, Edited by Perkins, C. D.

3. Matson, R. S. and W. H. Spillers, Jr., "An Analysis of Various Methods of Flight Testing for Neutral Points," Princeton University Aeronautical Engineering Report No. 275, 1955.

4. Foxgrover, James H. and Robert C. Mandeville, "An Investigation of the Variation of Elevator Power and Damping in Pitch with Mach Number for an FJ-3B Fury Jet Airplane Through Steady State Flight Tests," Princeton University Aeronautical Engineering Report No. 453, 1959.

5. Gilruth, R. R. and M. D. White: Analysis and Prediction of Longitudinal Stability of Airplanes. N.A.C.A. Rep. 711, 1941.

6. Perkins, Courtland D. and Robert E. Hage: Airplane Performance, Stability and Control, John Wiley & Sons, Inc., New York, 1950.

7. Sears, Richard I.: Wind Tunnel Data on the Aerodynamic Characteristics of Airplane Control Surfaces. N.A.C.A. WR L-663, 1943.

8. Hartman, E. P. and D. Bierman: The Aerodynamic Characteristics of Full Scale Propellers Having 2, 3, and 4 Blades of Clark Y and RAF 6 Airfoil Sections. N.A.C.A. Report 640, 1939.

9. Goett, H. S. and H. R. Pass: Effect of Propeller Operation on the Pitching Moments of Single Engine Monoplanes. N.A.C.A. WR L-761, 1941.

10. Ribner, Herbert S.: Notes on the Propeller and Slipstream in Relation to Stability, N.A.C.A. WR L-25, 1944.

BIBLIOGRAPHY

Advisory Group for Aeronautical Research and Development Flight Test Manual, Vol. III, Instrumentation Catalog, Edited by Perkins, C. D., Princeton, N. J., 1954.

Etkin, Bernard: Dynamics of Flight Stability and Control, John Wiley & Sons, New York, 1959.

Perkins, C. D. and T. F. Walkowicz: Stability and Control Flight Test Methods, AAF TR 5242, 1945.

Schuld, Emil P. and Leonard J. Reinhart: Determination of Longitudinal Stability Parameters by Steady State Flight Testing and Theoretical Calculations for the Ryan Navion, Princeton University Aeronautical Engineering Report No. 232, 1953.

Silverstein, A. and S. Katzoff: Design Charts for Predicting Downwash Angles and Wake Characteristics Behind Plain and Flapped Wings, N.A.C.A. TR 648, 1939.

Fig. 1. Photograph of the Test Airplane

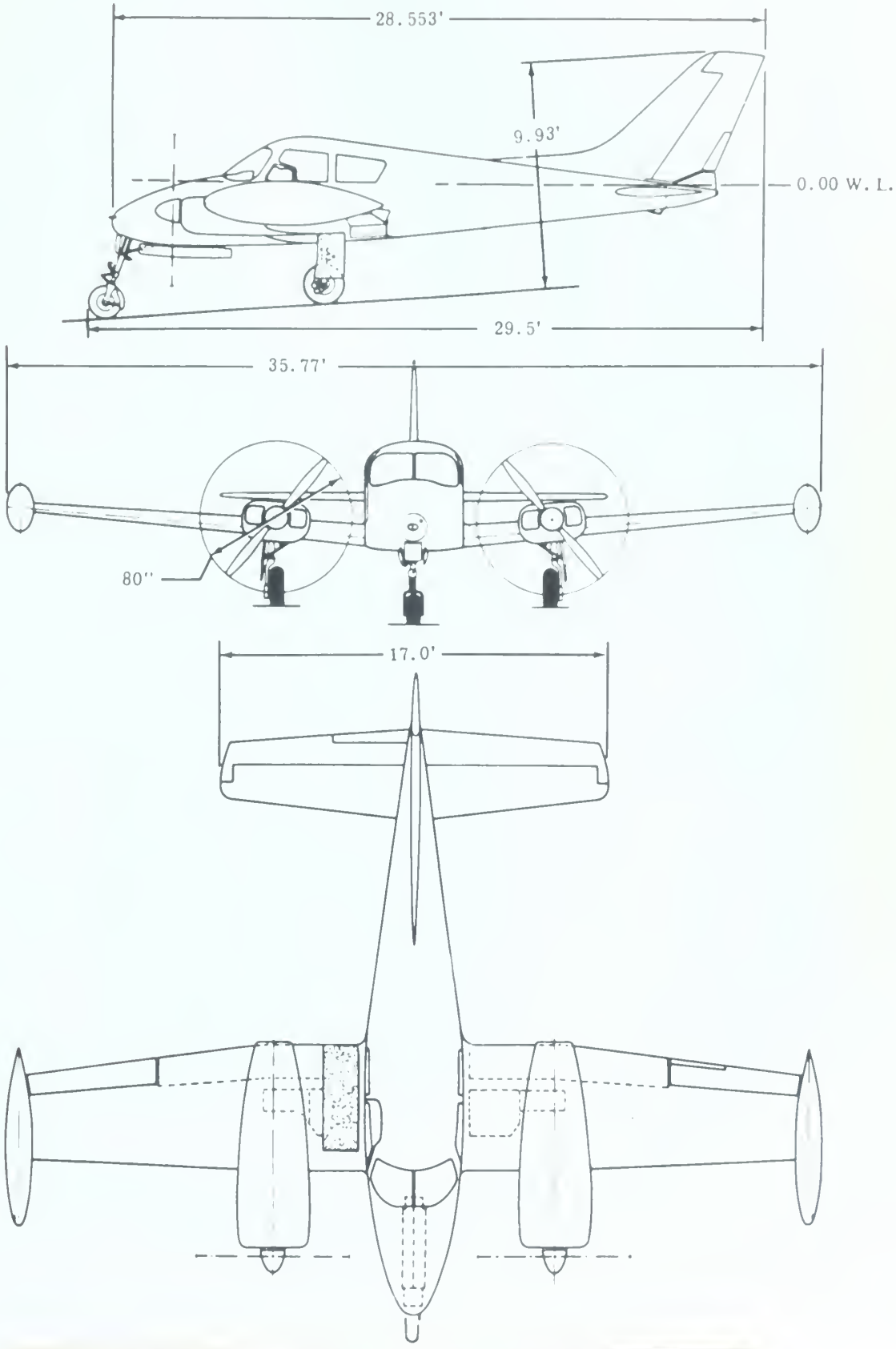

Fig. 2. Three-view Drawing of Test Airplane

Fig. 3. Photograph of the Instrumentation Box

FIG. 4
INSTRUMENTATION CIRCUIT DIAGRAM

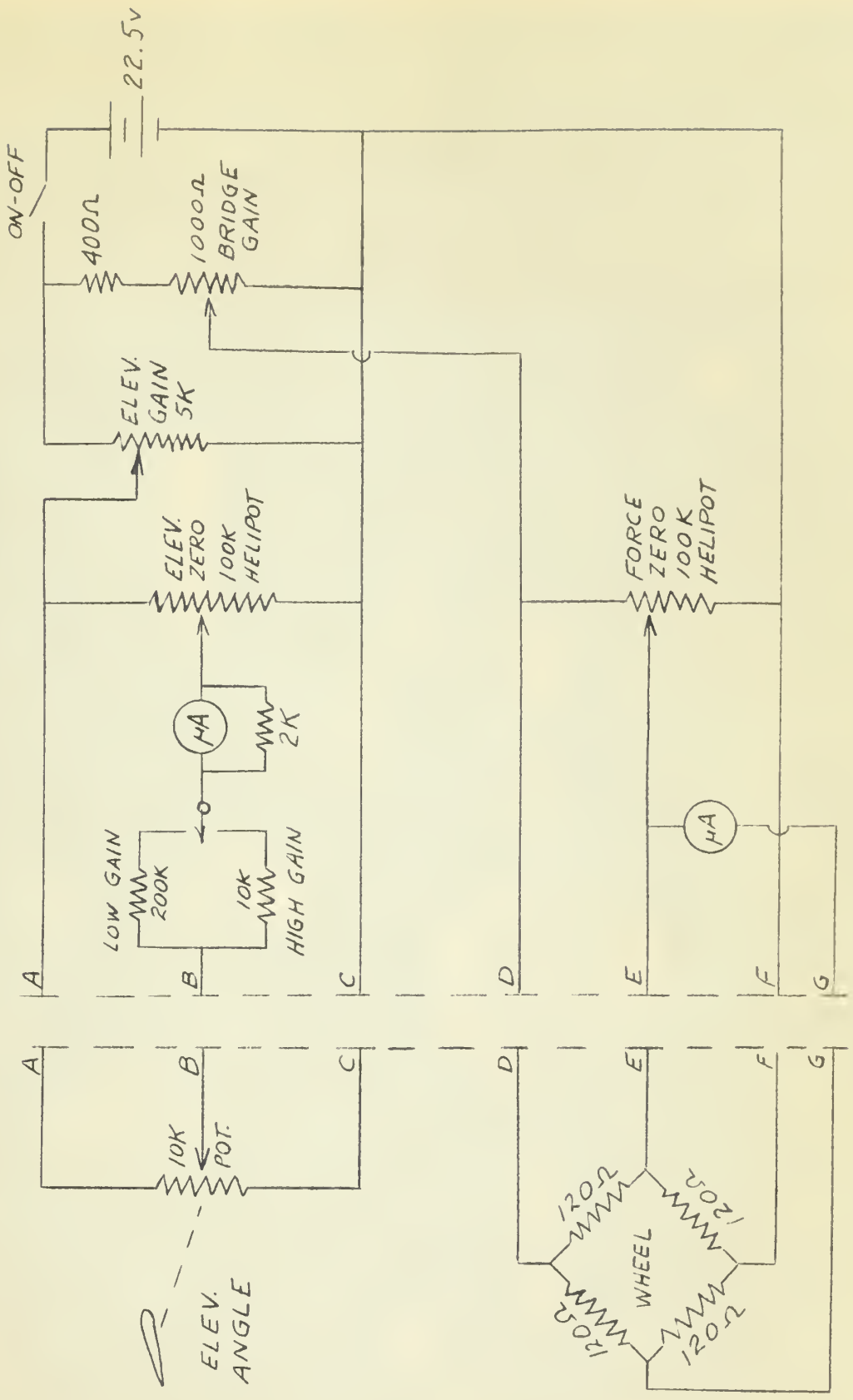

Fig. 5. Photograph of Force Measuring Wheel Installed in Test Airplane

FIG. 6

FORCE WHEEL CALIBRATION

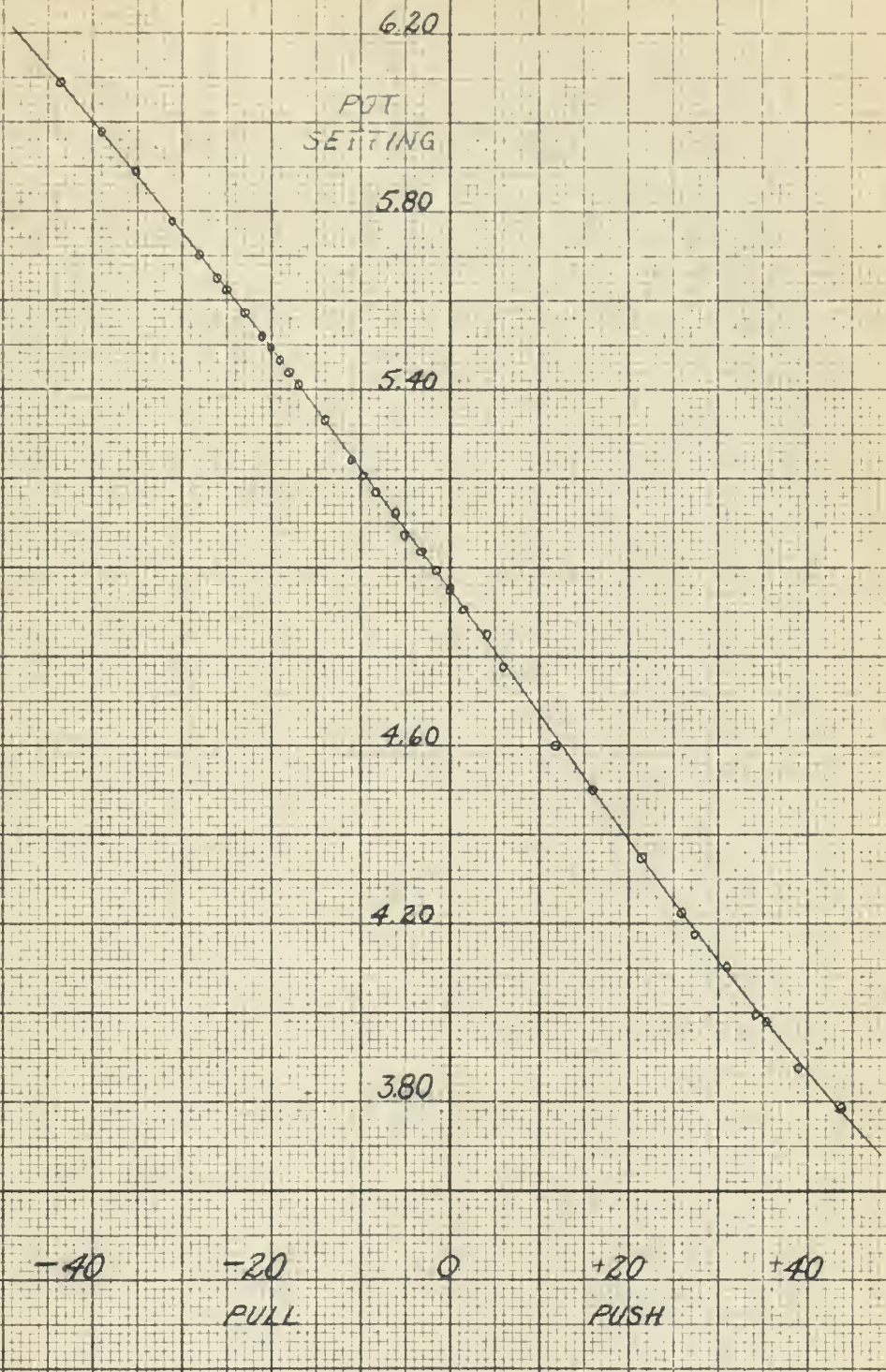

3-23-61

FIG. 7

ELEVATOR ANGLE CALIBRATION

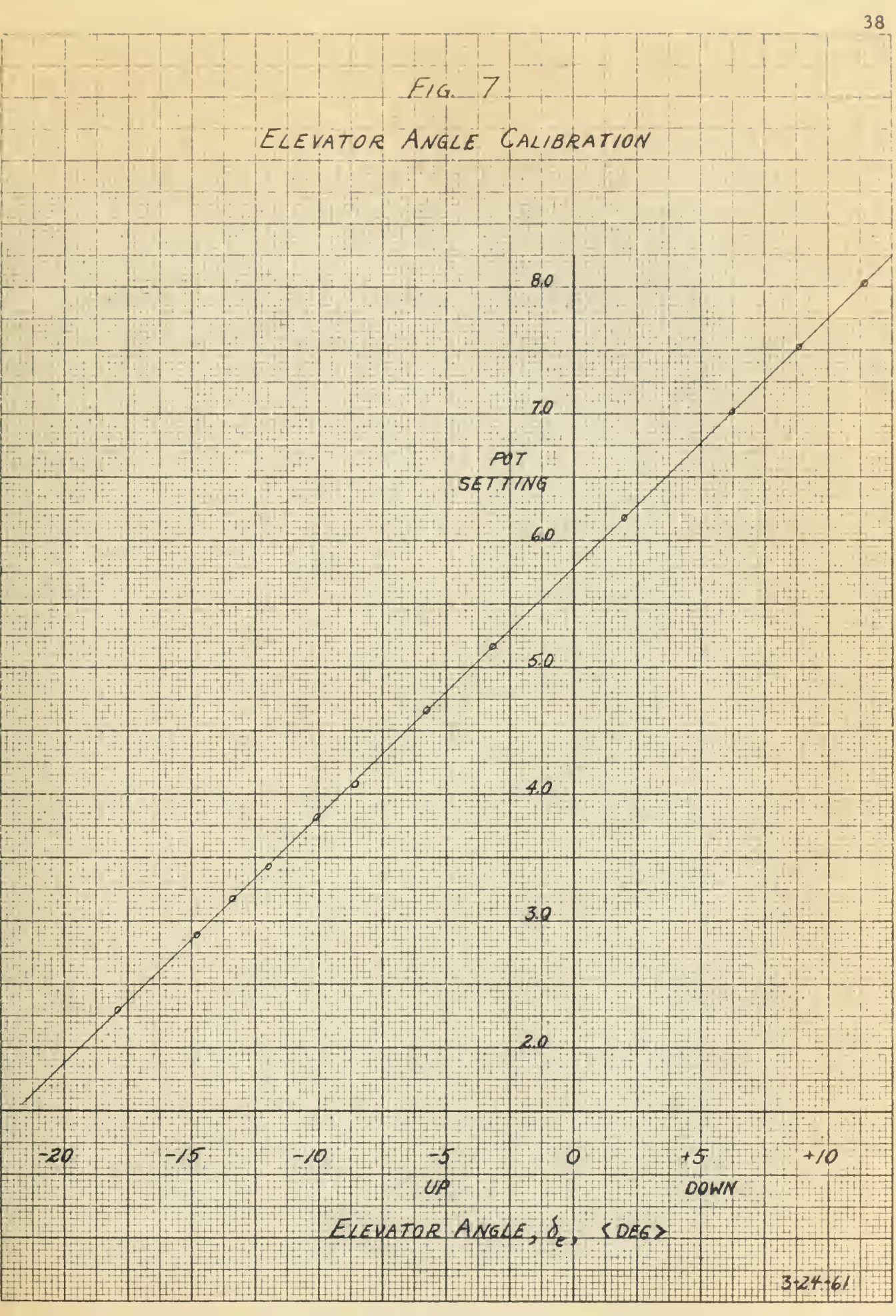

FIG. 8

AIRSPEED CALIBRATION

(FLAPS UP)

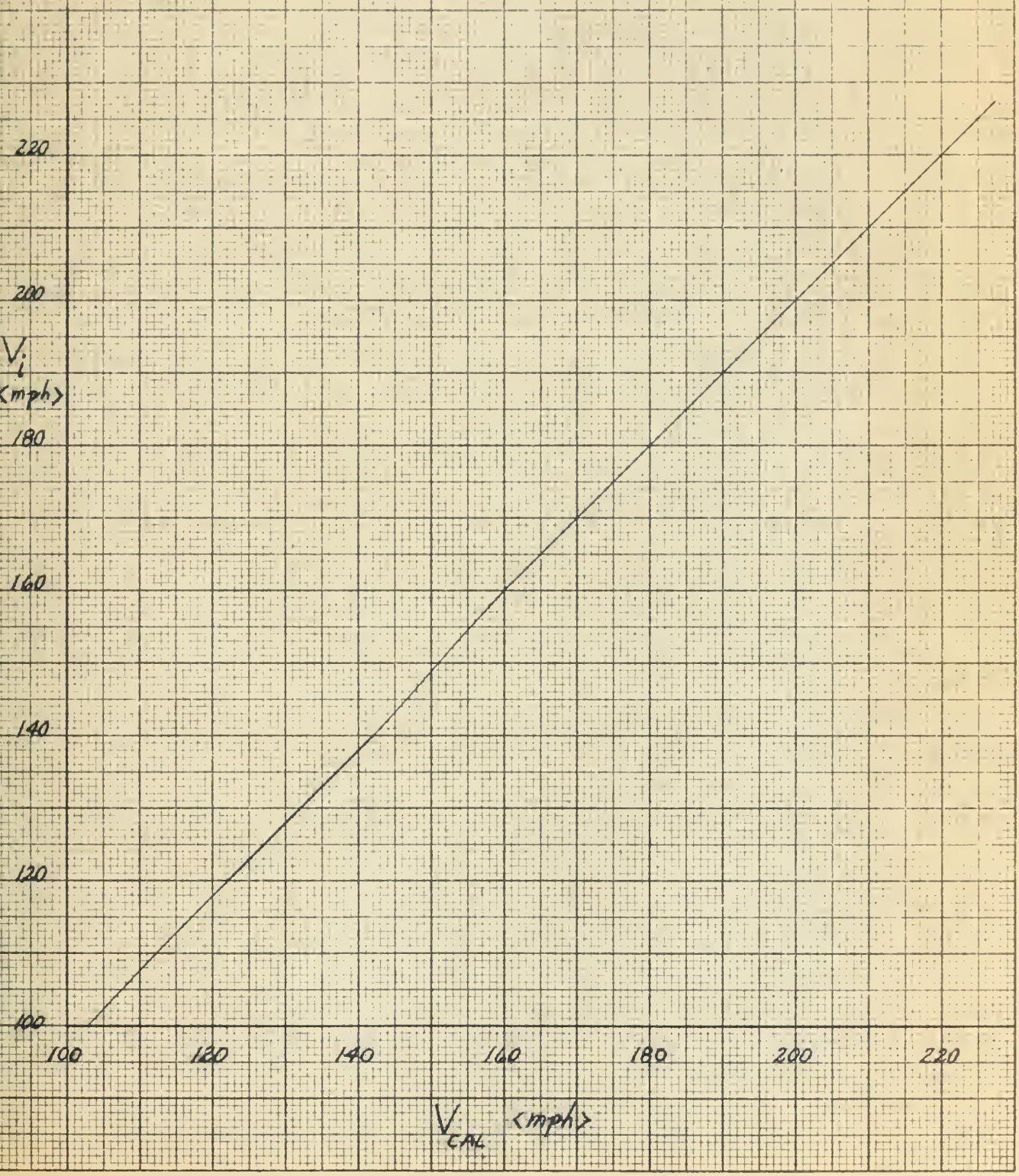

FIG. 9

AIRSPEED CALIBRATION

(45° FLAPS)

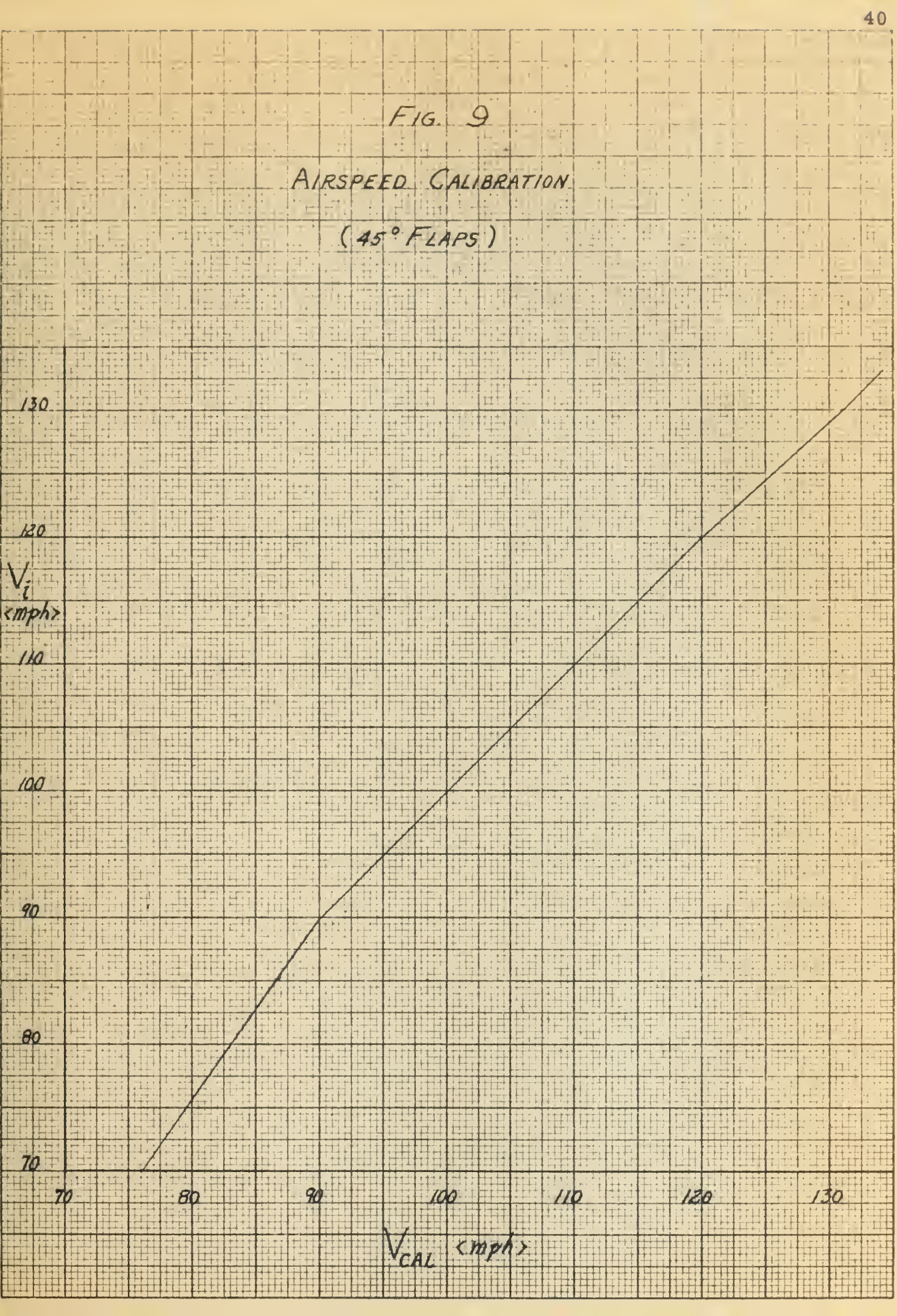

FIG. 10
FUEL GAGE CALIBRATION

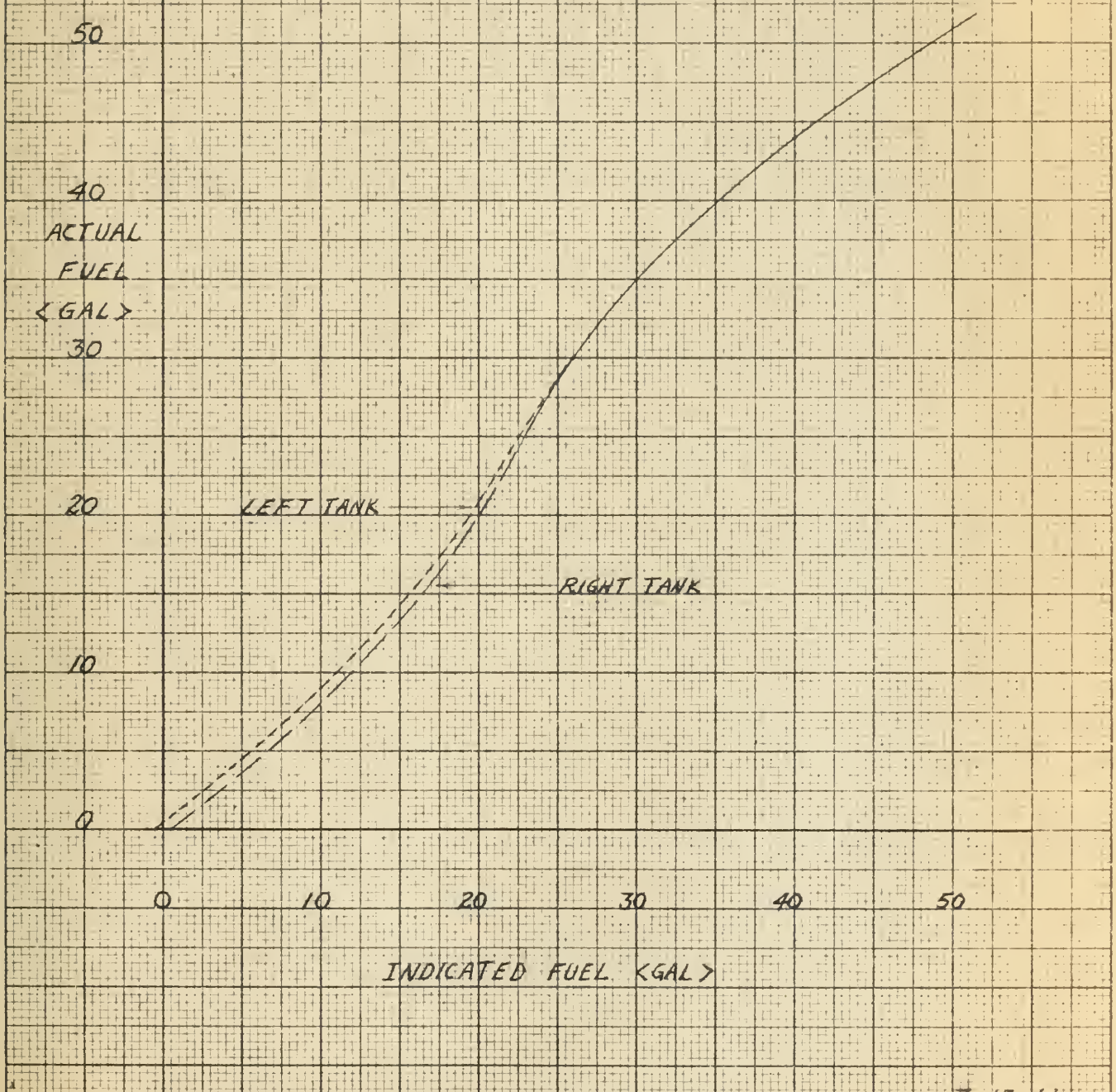

3-17-61

FIG. 11

DOWNSPRING FORCE CALIBRATION

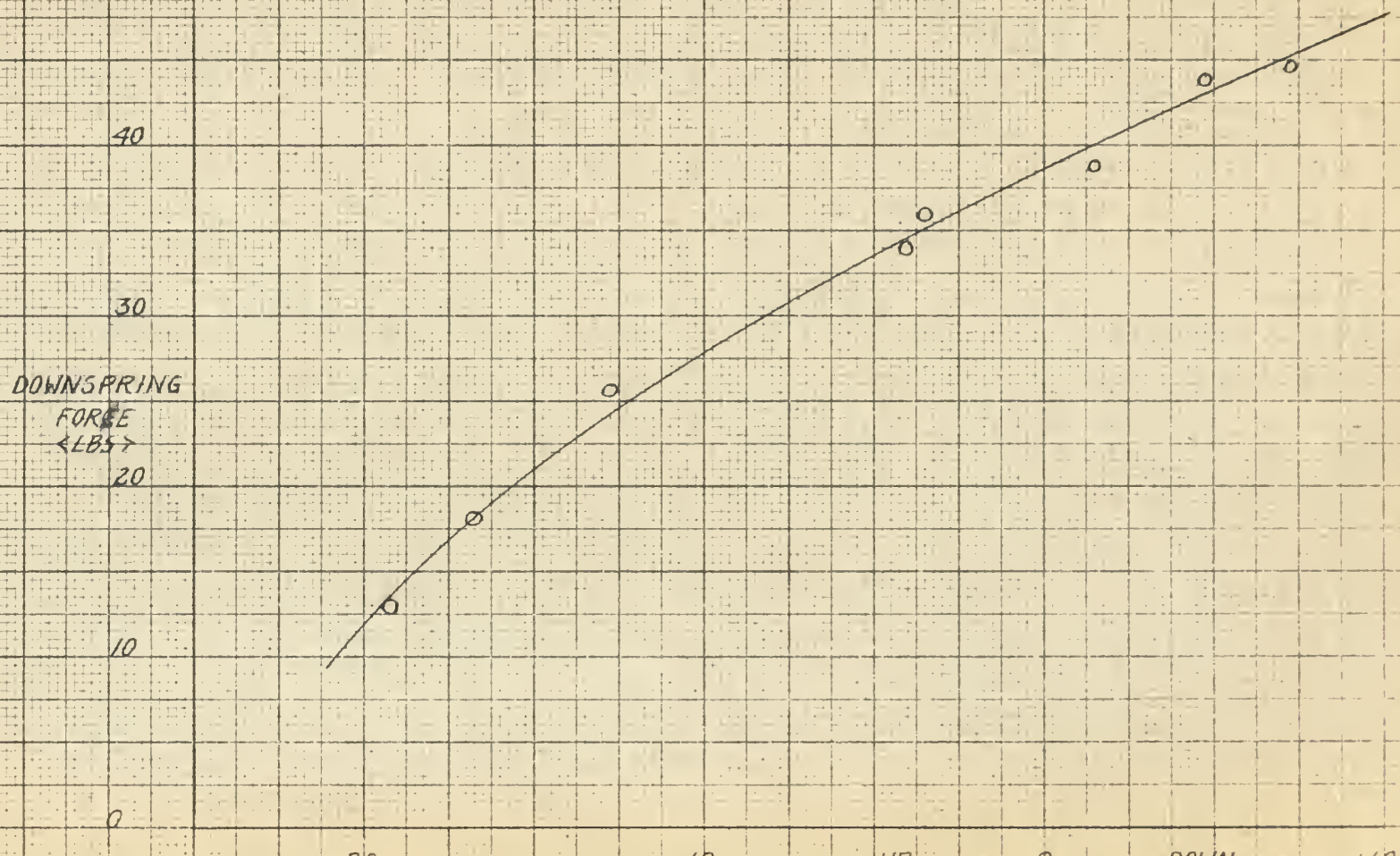

4-3-61

FIG. 12
CRUISE CONFIGURATION
POWER ON

δ_e V.S. V_{CAL}

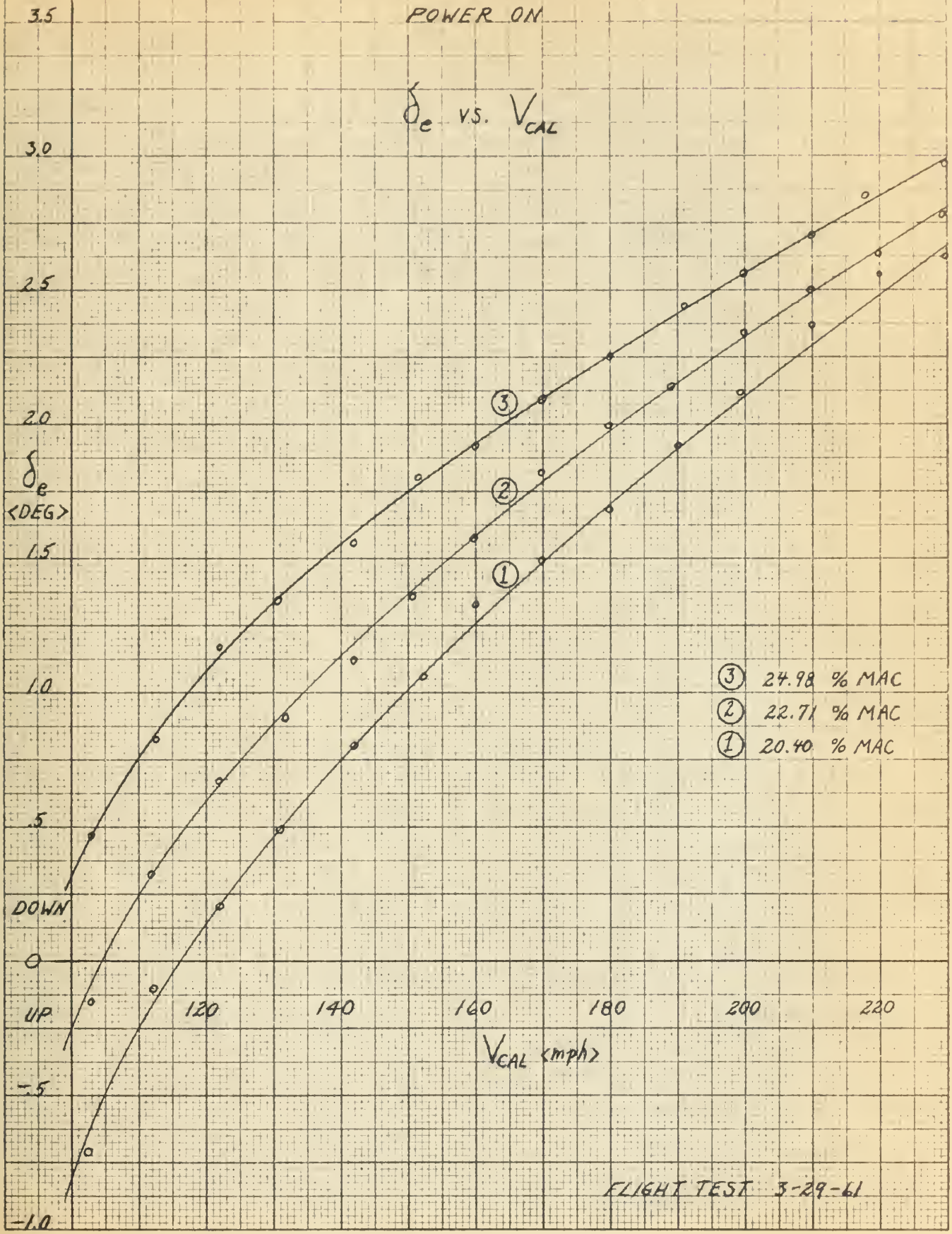

FIG. 13

CRUISE CONFIGURATION

POWER ON

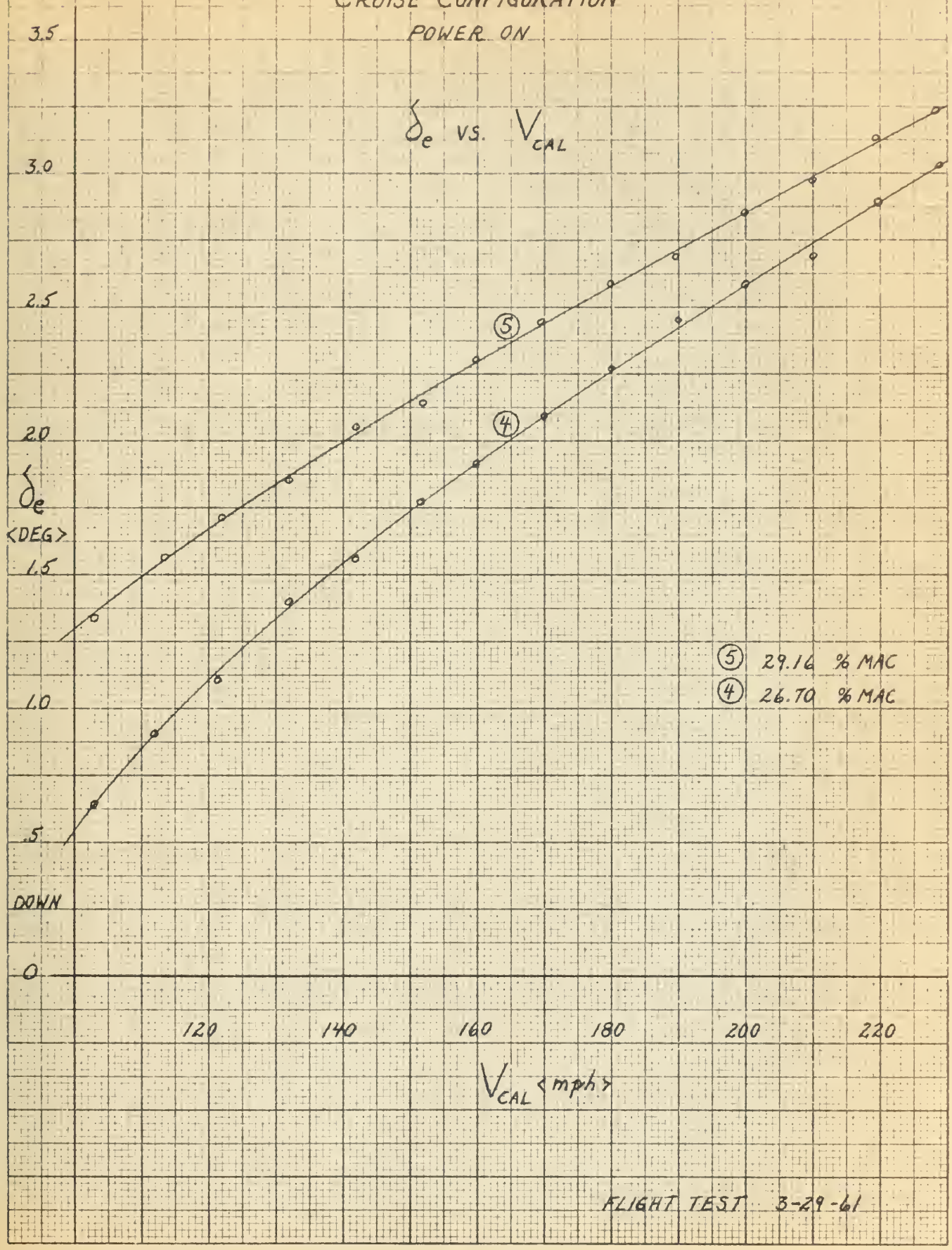

FLIGHT TEST 3-29-61

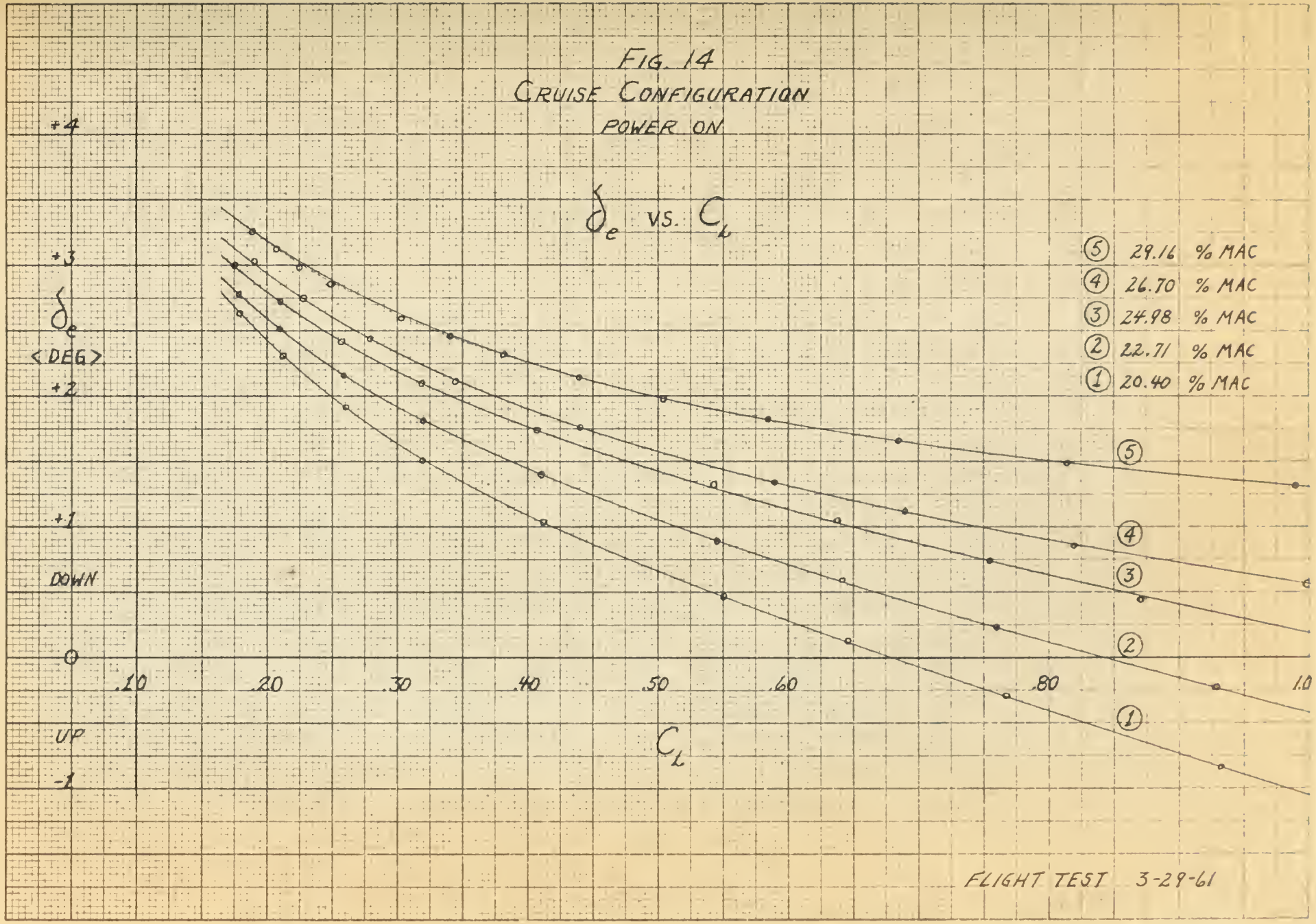
FIG. 14
CRUISE CONFIGURATION
POWER ON
δ_e VS. C_L
⑤ 29.16 % MAC
④ 26.70 % MAC
③ 24.98 % MAC
② 22.71 % MAC
① 20.40 % MAC
+4
+3
+2
+1
0
-1
δ_e <DEG>
DOWN
UP
.10
.20
.30
.40
.50
.60
.80
1.0
C_L
FLIGHT TEST 3-29-61

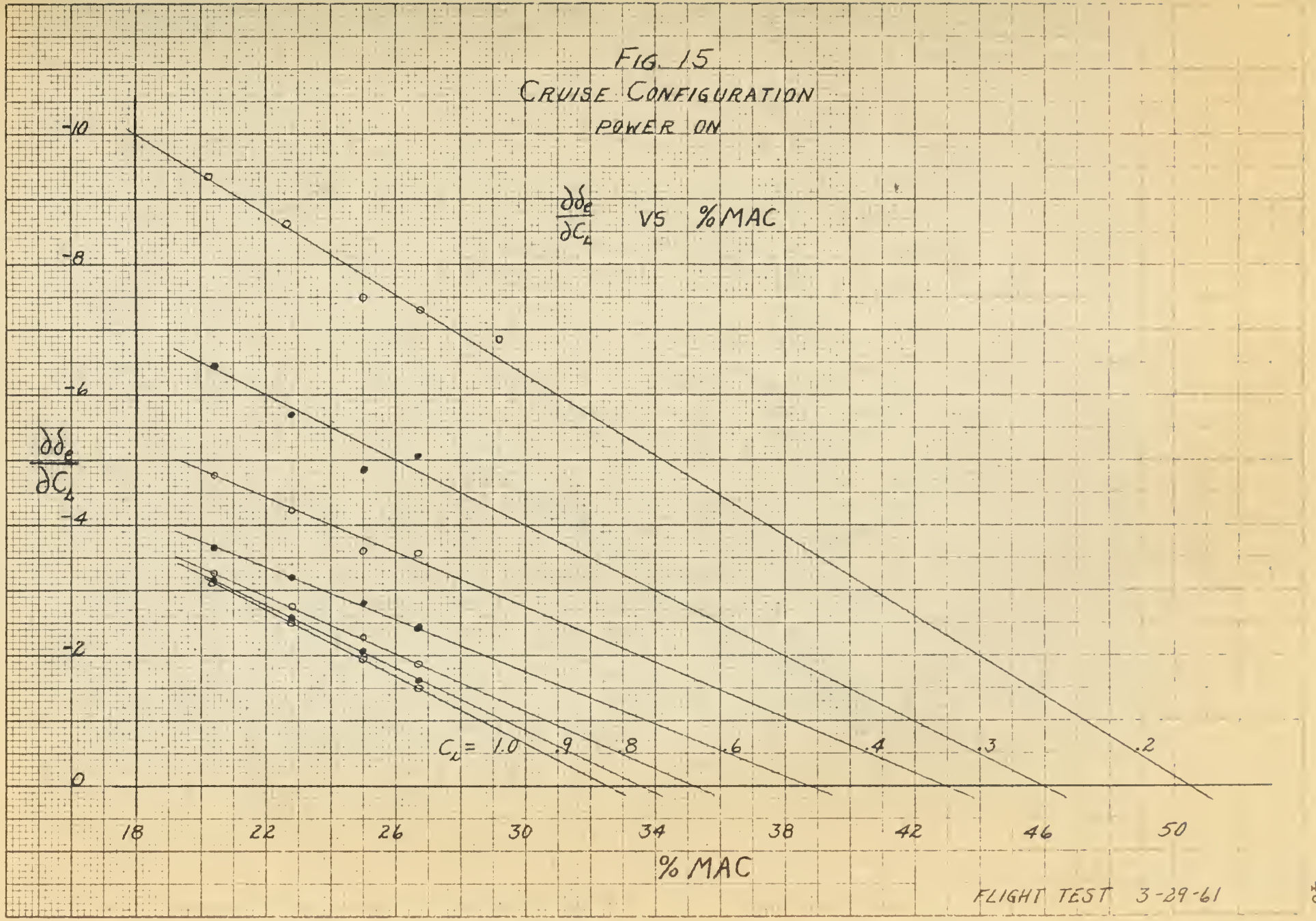
FIG. 15
CRUISE CONFIGURATION
POWER ON
$\frac{\partial \delta_e}{\partial C_L}$ VS % MAC
-10
-8
-6
-4
-2
0
$\frac{\partial \delta_e}{\partial C_L}$
C_L = 1.0 .9 .8 .6 .4 .3 .2
18
22
26
30
34
38
42
46
50
% MAC
FLIGHT TEST 3-29-61

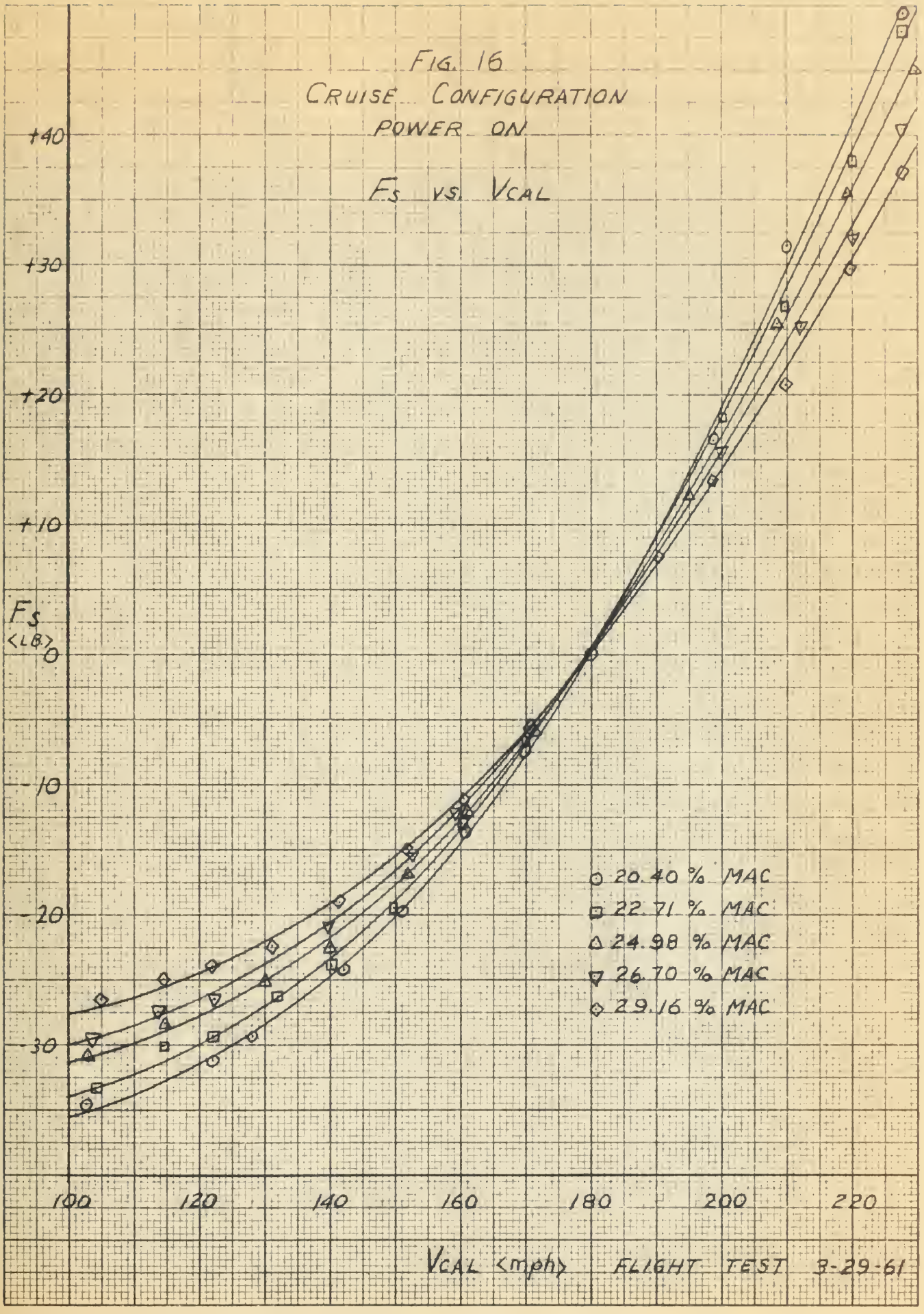
FIG. 16
CRUISE CONFIGURATION
POWER ON
FS VS. VCAL
+40
+30
+20
+10
FS <LB.> 0
-10
-20
-30
20.40 % MAC
22.71 % MAC
24.98 % MAC
26.70 % MAC
29.16 % MAC
100
120
140
160
180
200
220
VCAL <mph>
FLIGHT TEST 3-29-61

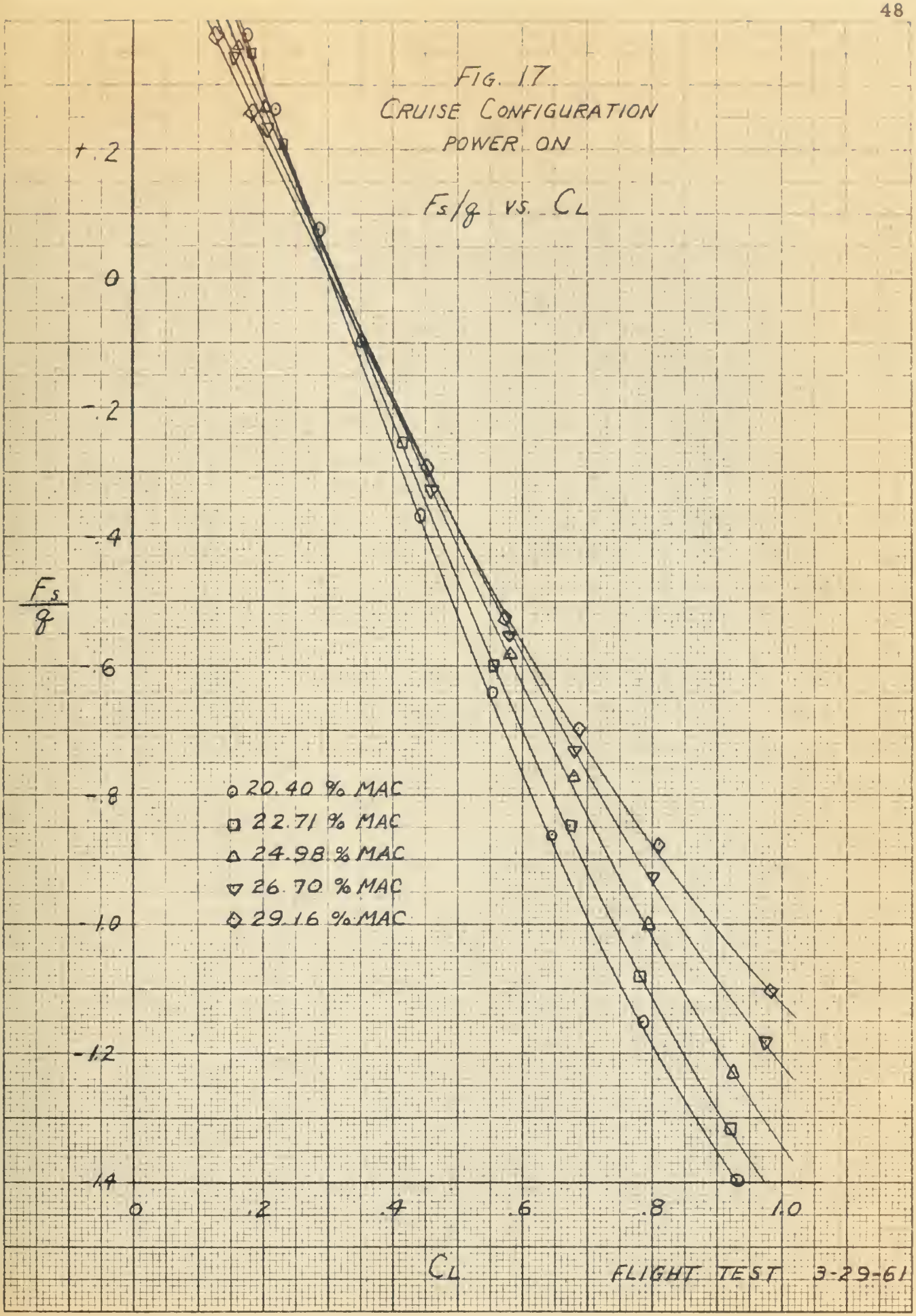
FIG. 17
CRUISE CONFIGURATION
POWER ON
Fs/q VS. CL
+.2
0
-.2
-.4
Fs/q
-.6
-.8
-1.0
-1.2
-1.4
20.40 % MAC
22.71 % MAC
24.98 % MAC
26.70 % MAC
29.16 % MAC
0
.2
.4
.6
.8
1.0
CL
FLIGHT TEST 3-29-61

FIG. 18

CRUISE CONFIGURATION

POWER ON

$\frac{d[F_s/q]}{dC_L}$ vs. % MAC

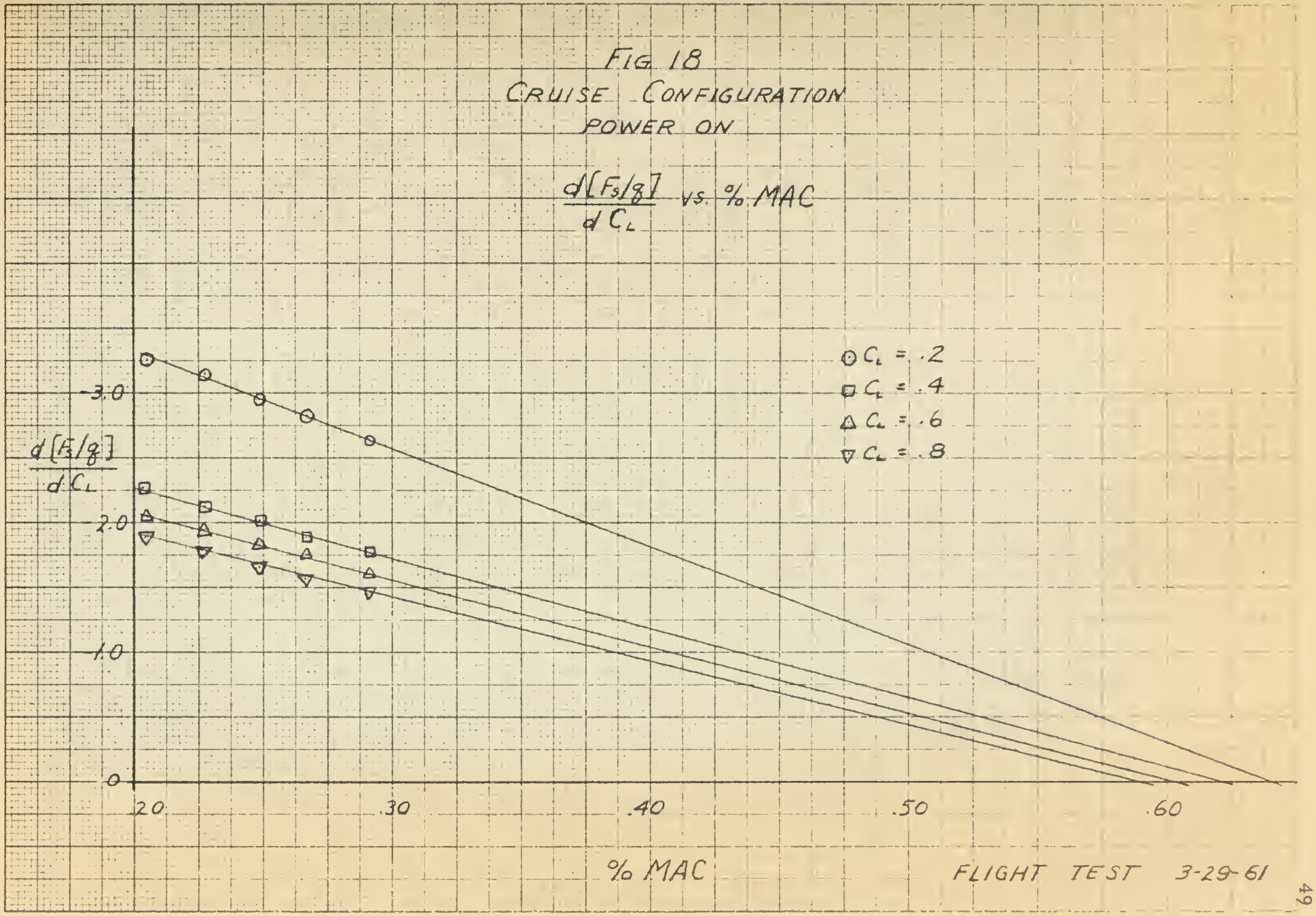

FLIGHT TEST 3-29-61

FIG. 19

CRUISE CONFIGURATION

POWER ON

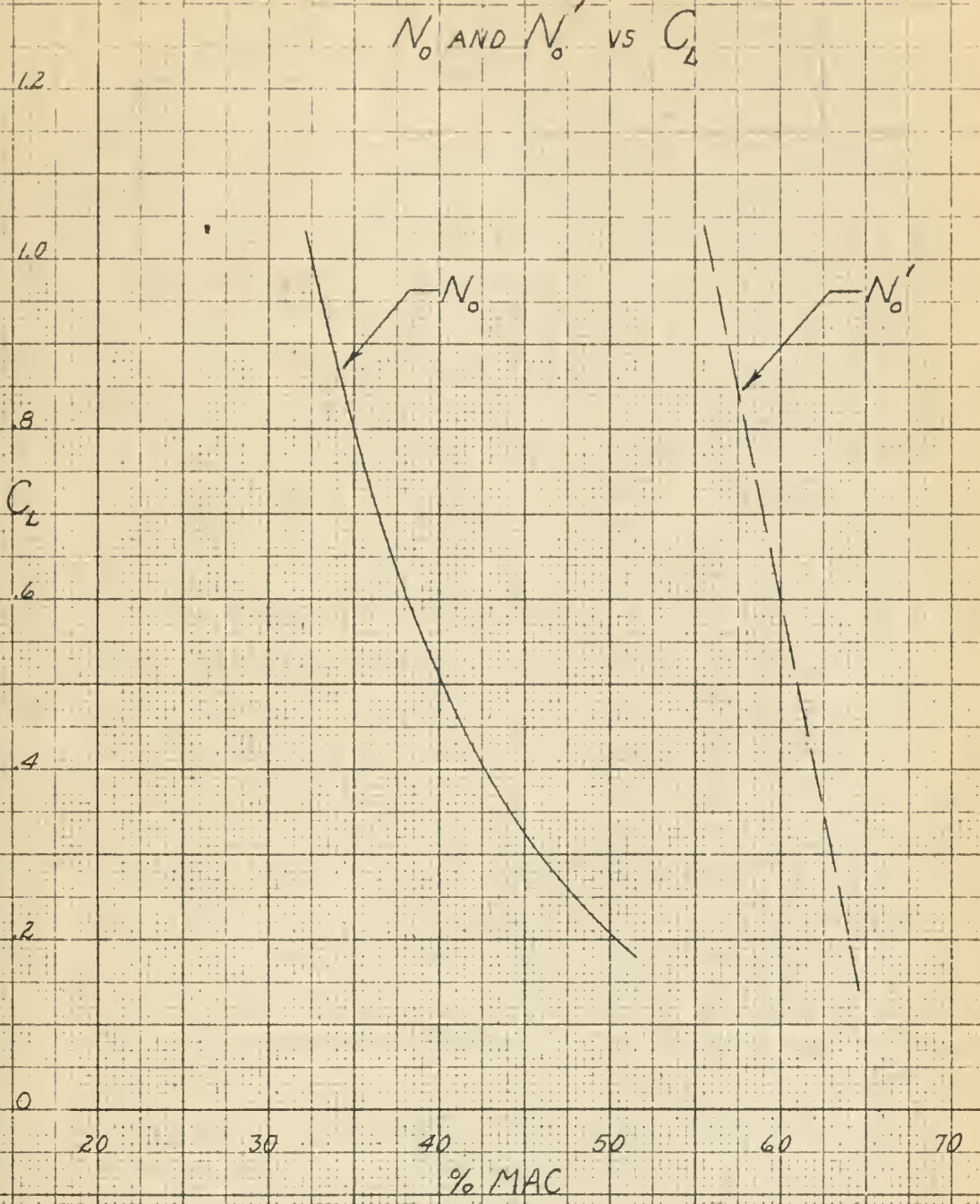

FLIGHT TEST 3-29-61

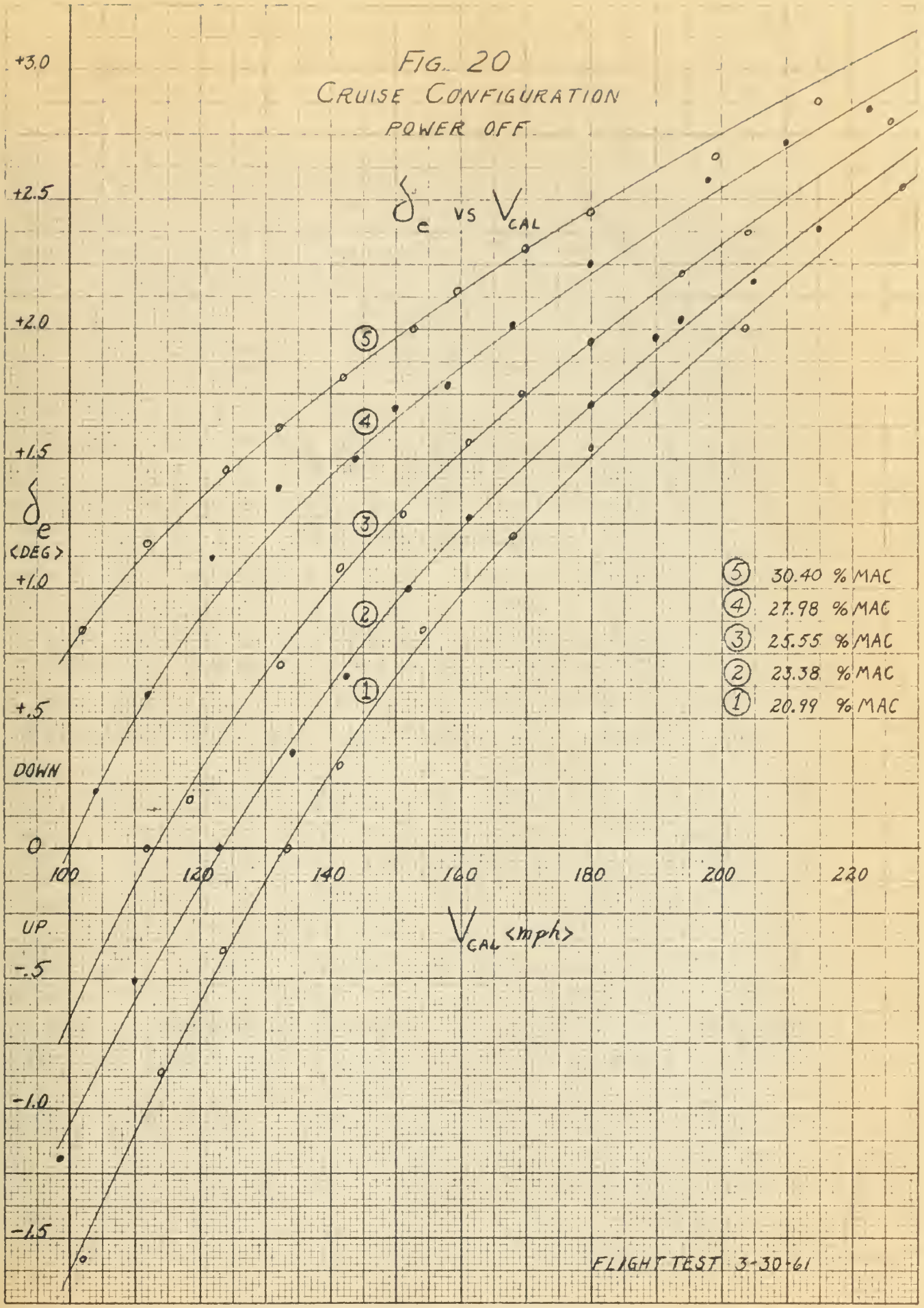
FIG. 20
CRUISE CONFIGURATION
POWER OFF
δe VS VCAL
+3.0
+2.5
+2.0
+1.5
δe (DEG)
+1.0
+.5
DOWN
0
UP
-.5
-1.0
-1.5
100
120
140
160
180
200
220
VCAL (mph)
5 30.40 % MAC
4 27.98 % MAC
3 25.55 % MAC
2 23.38 % MAC
1 20.99 % MAC
FLIGHT TEST 3-30-61

FIG. 21

CRUISE CONFIGURATION

POWER OFF

δ_e VS. C_L

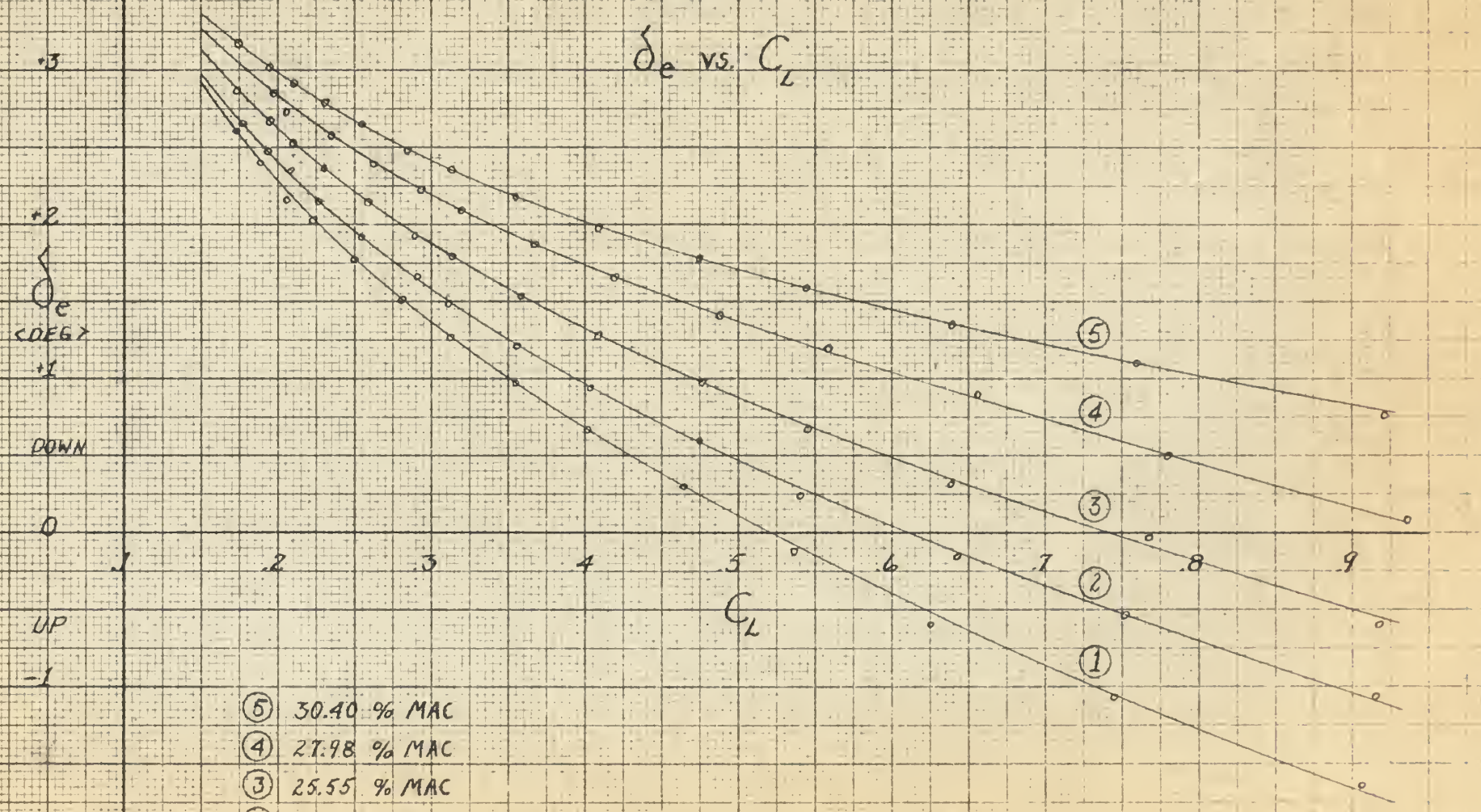

(5)	30.40 % MAC
(4)	27.98 % MAC
(3)	25.55 % MAC
(2)	23.38 % MAC
(1)	20.99 % MAC

FLIGHT TEST 3-30-61

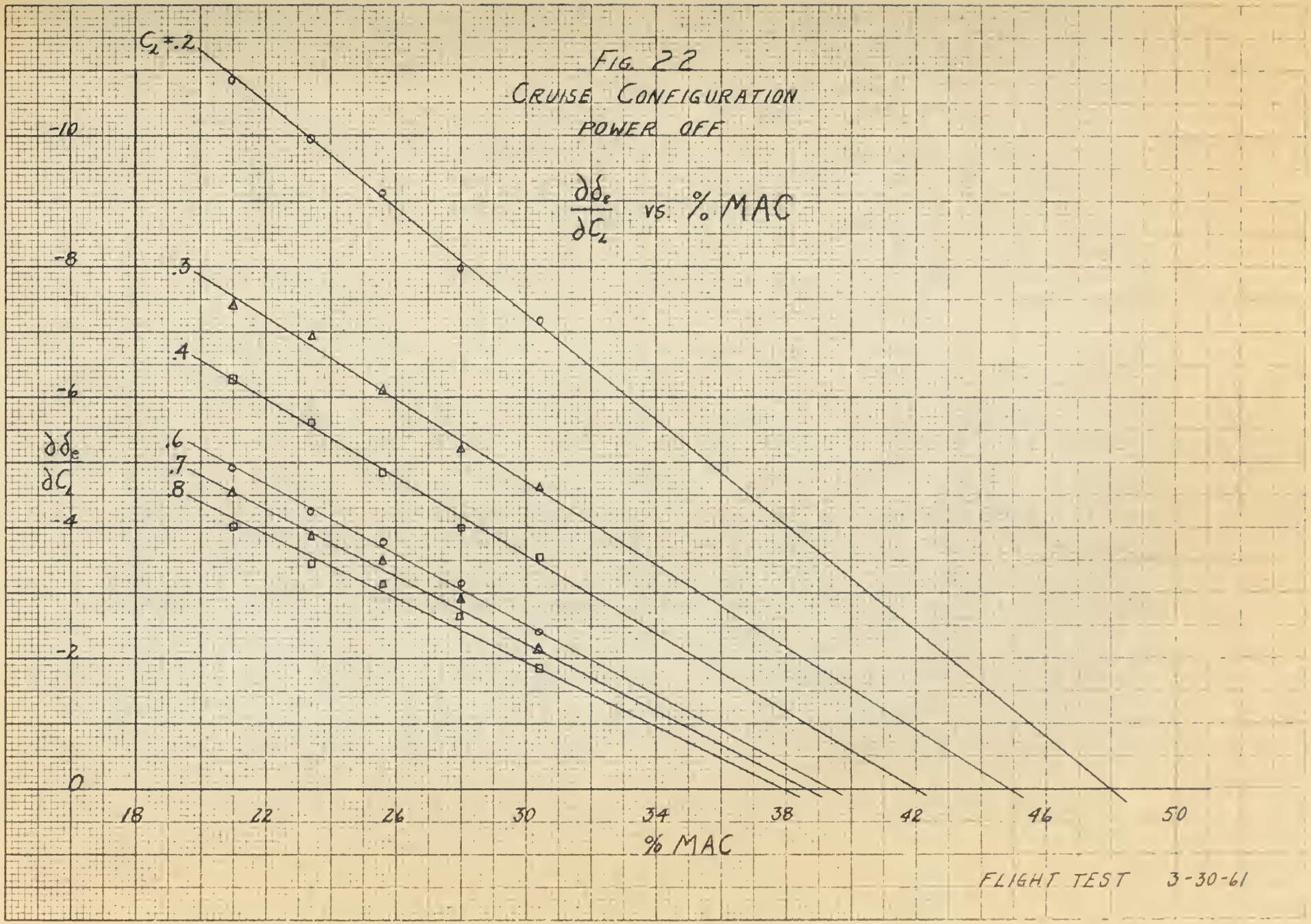
FIG. 22
CRUISE CONFIGURATION
POWER OFF
$\frac{\partial \delta_e}{\partial C_L}$ vs. % MAC
C_L = .2
.3
.4
.6
.7
.8
$\frac{\partial \delta_e}{\partial C_L}$
-10
-8
-6
-4
-2
0
18
22
26
30
34
38
42
46
50
% MAC
FLIGHT TEST 3-30-61

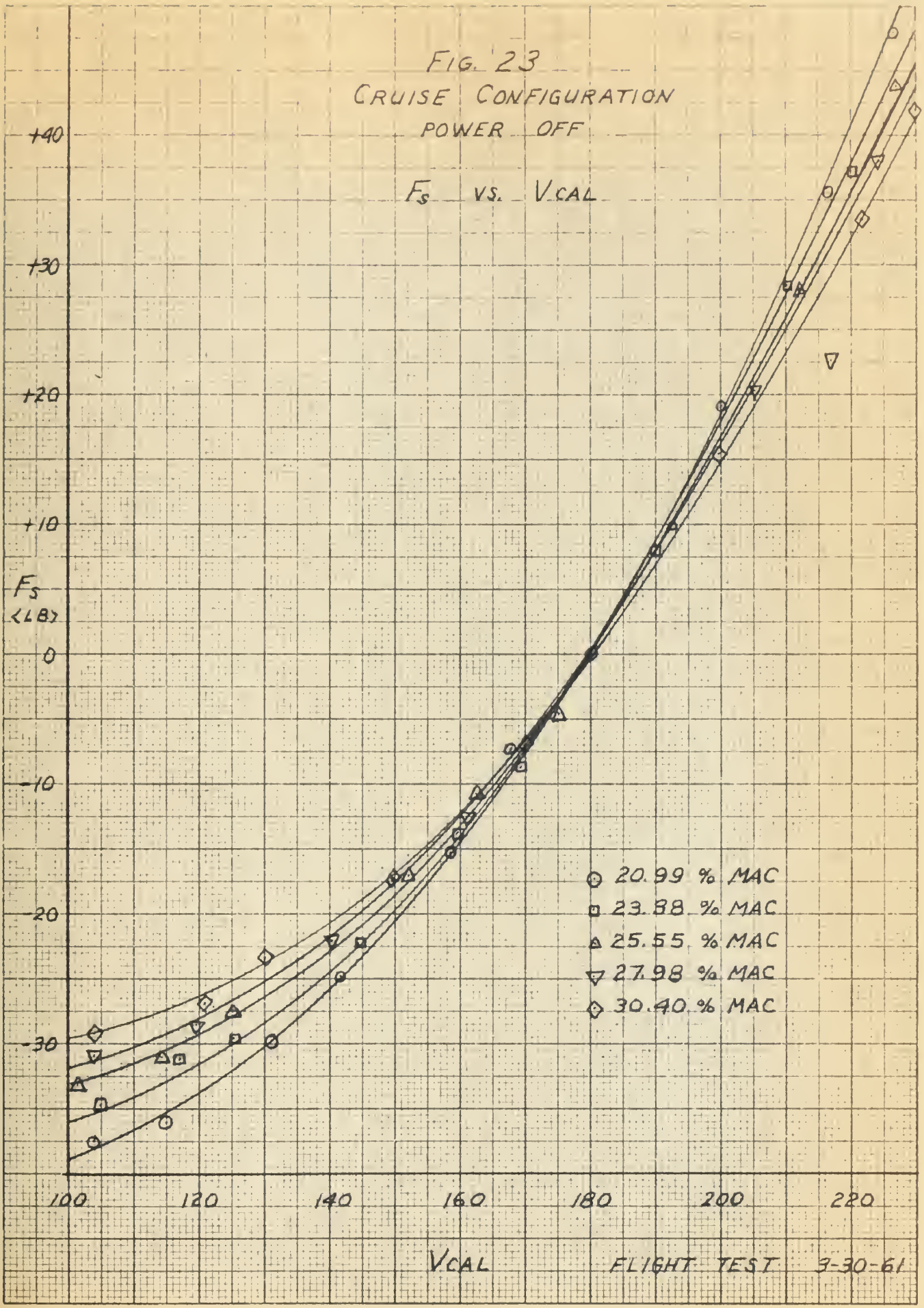
FIG. 23
CRUISE CONFIGURATION
POWER OFF
F_S VS. V_{CAL}
+40
+30
+20
+10
F_S
(LB)
0
-10
-20
-30
20.99 % MAC
23.88 % MAC
25.55 % MAC
27.98 % MAC
30.40 % MAC
100
120
140
160
180
200
220
V_{CAL}
FLIGHT TEST 3-30-61

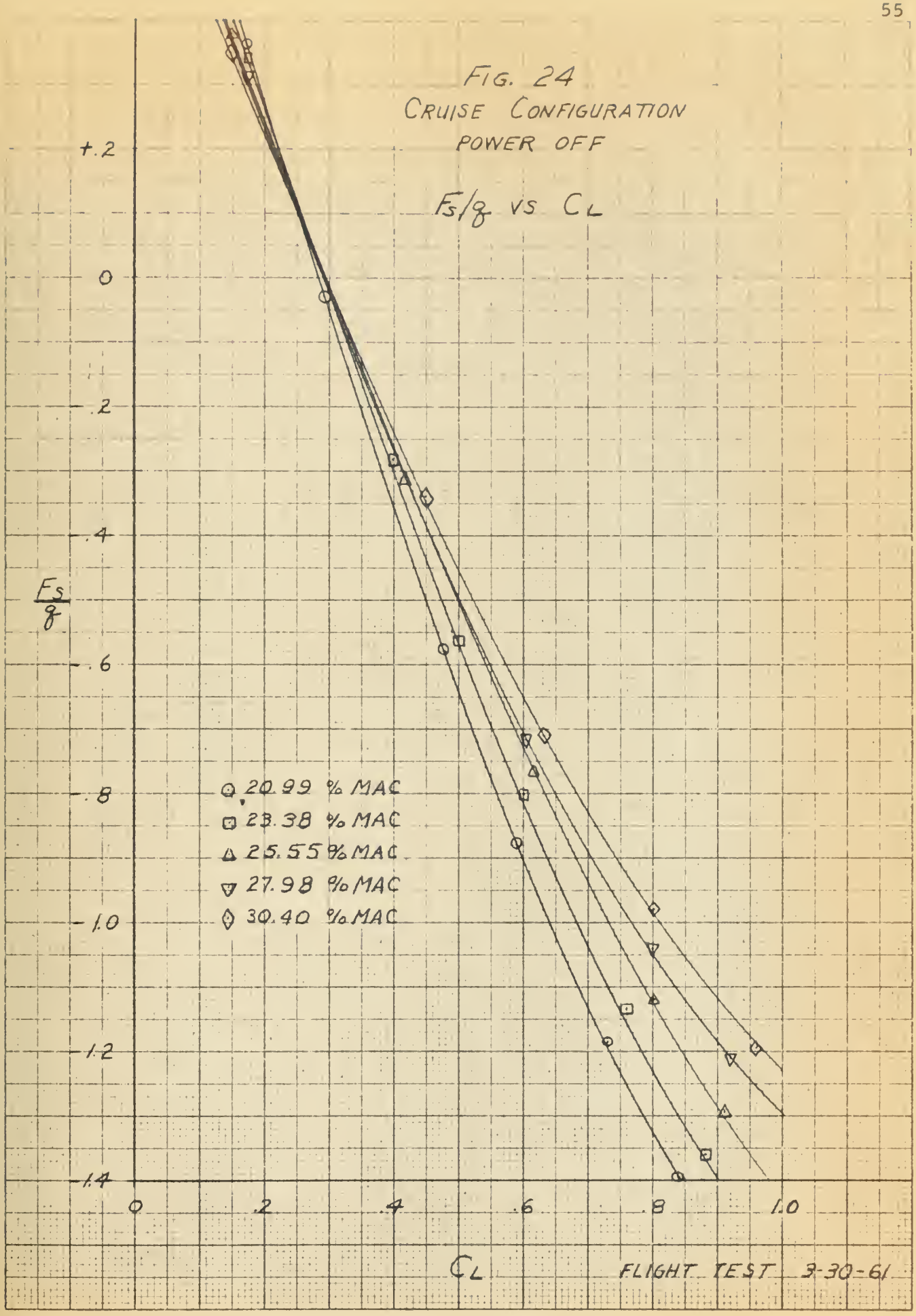
FIG. 24
CRUISE CONFIGURATION
POWER OFF
Fs/q VS CL
+.2
0
-.2
-.4
Fs/q
-.6
-.8
-1.0
-1.2
-1.4
20.99 % MAC
23.38 % MAC
25.55 % MAC
27.98 % MAC
30.40 % MAC
0
.2
.4
.6
.8
1.0
CL
FLIGHT TEST 3-30-61

FIG. 25

CRUISE CONFIGURATION

POWER OFF

$\frac{d[F_s/q]}{dC_L}$ VS. %MAC

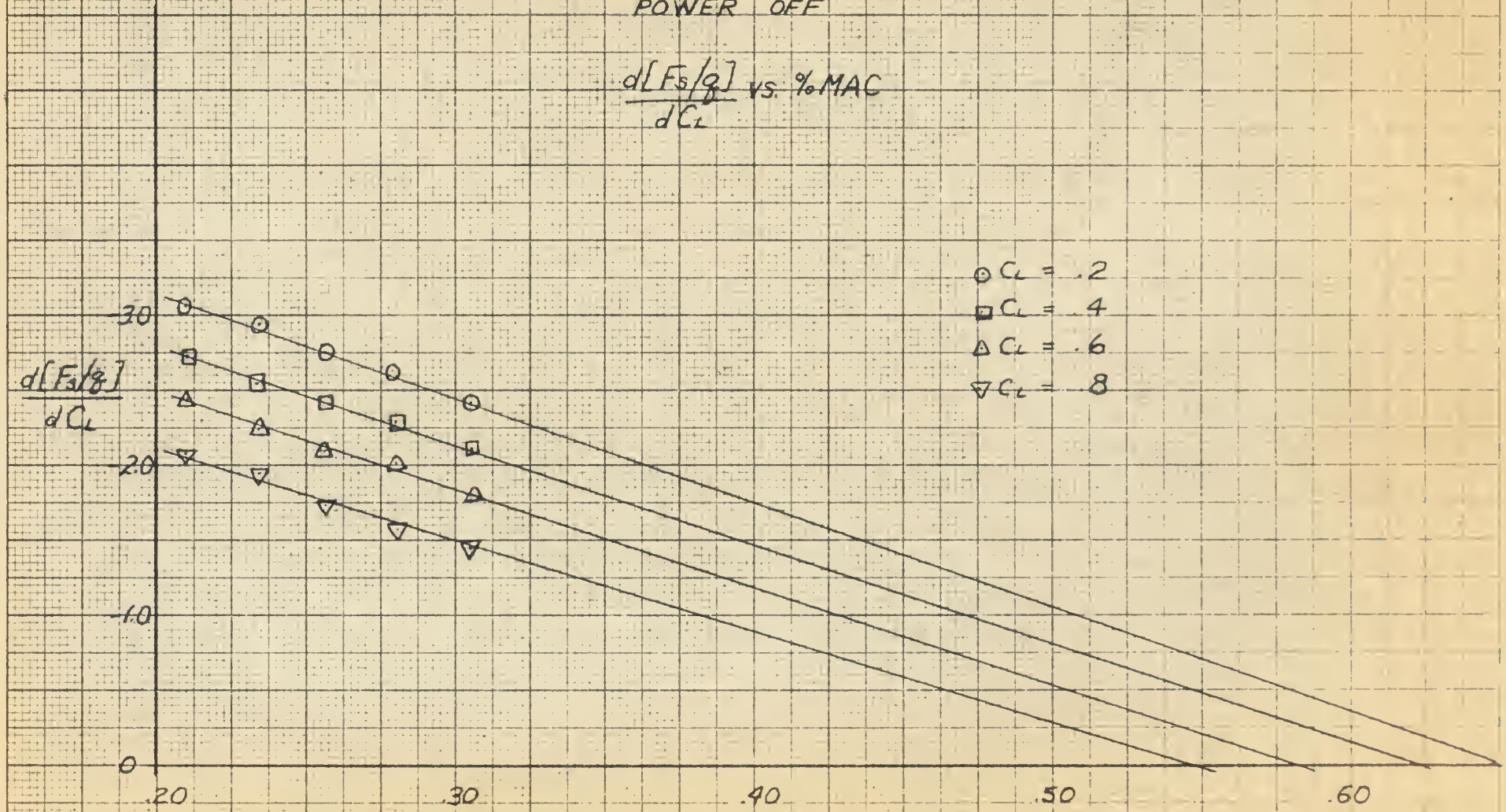

FLIGHT TEST 3-30-61

FIG. 26
CRUISE CONFIGURATION
POWER OFF

N_o AND N_o' VS. C_L

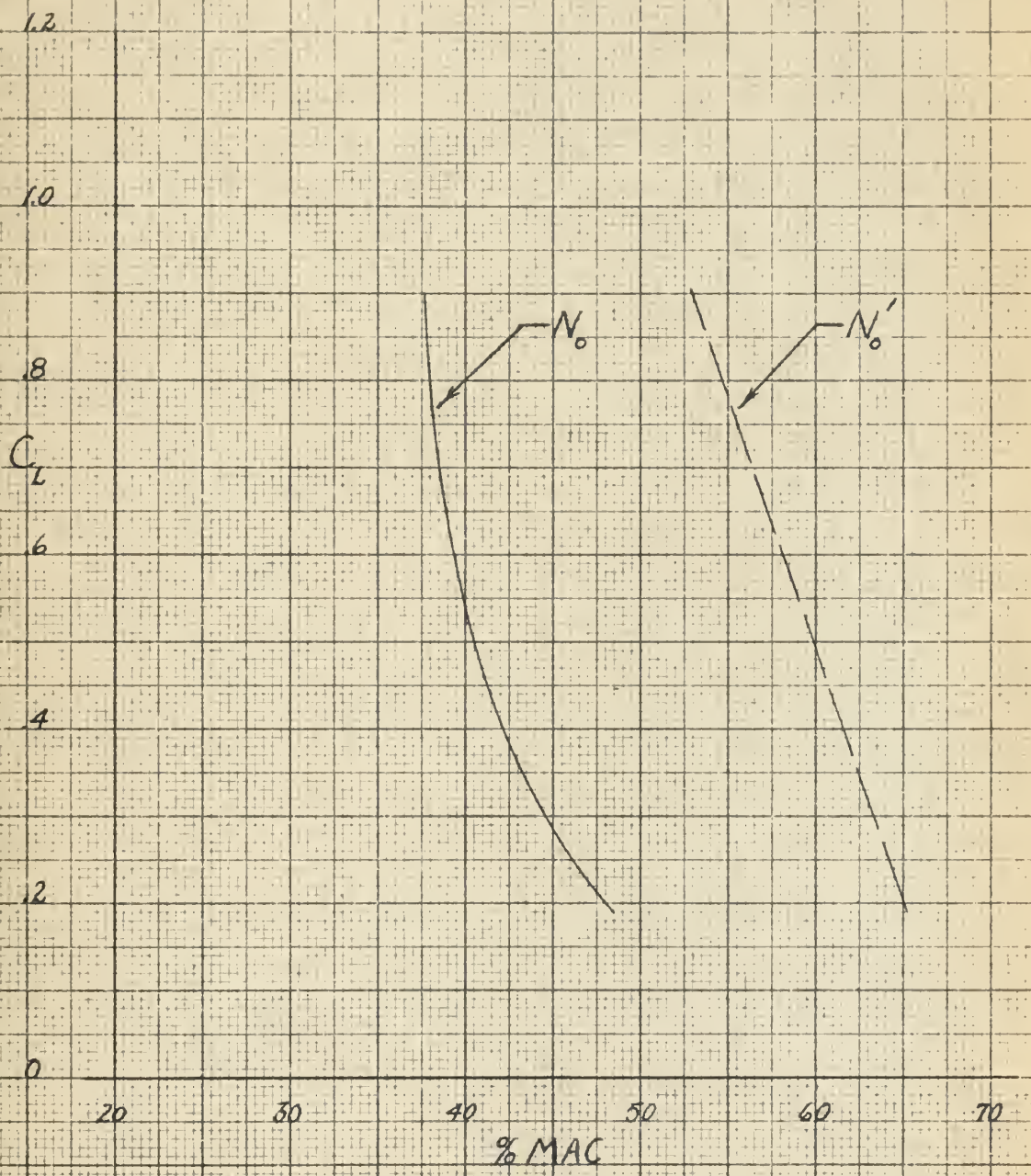

FLIGHT TEST 3-30-61

FIG. 27
NEUTRAL POINT SUMMARY

CRUISE CONFIGURATION

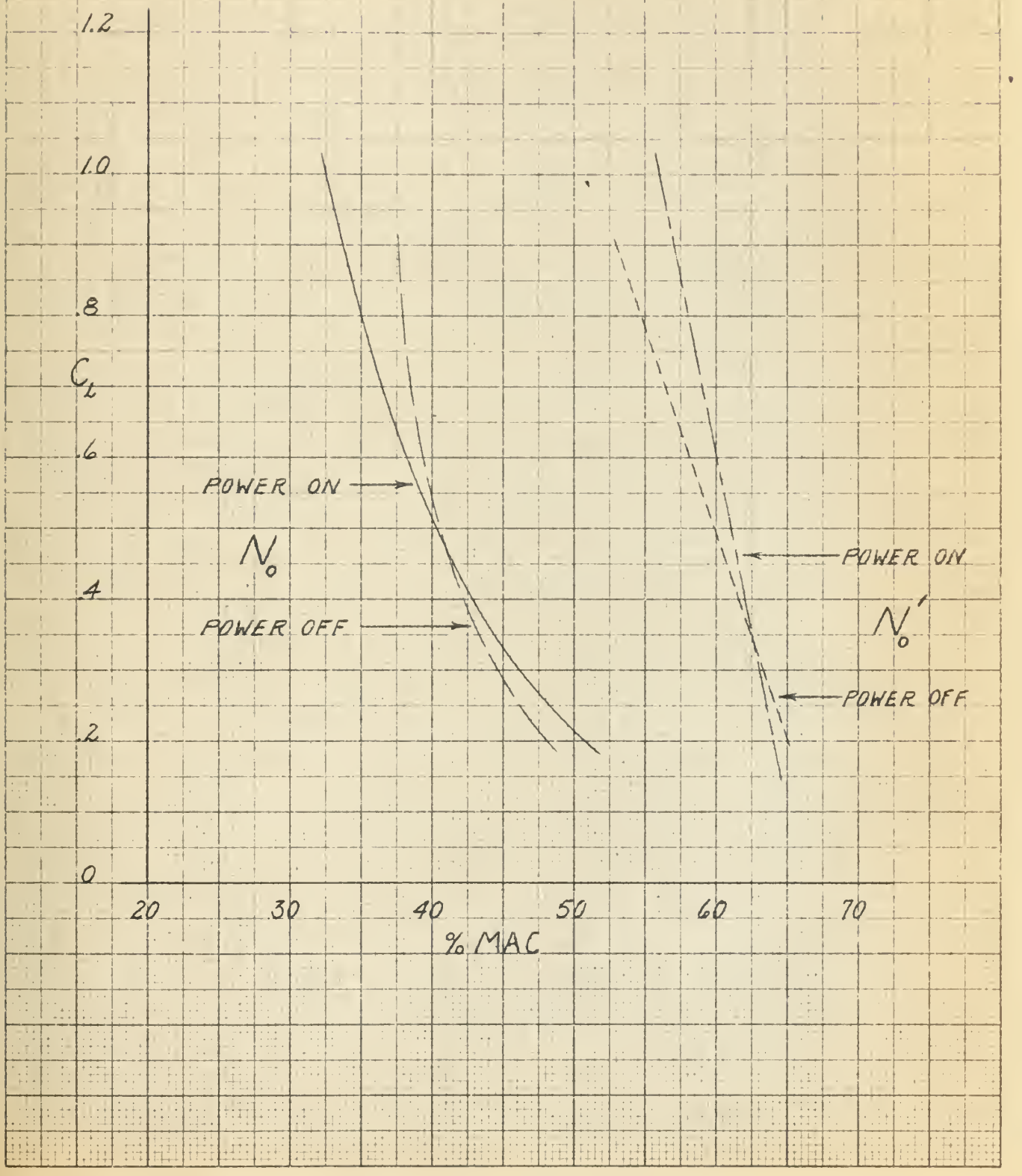

FIG. 28

APPROACH CONFIGURATION

POWER ON

δ_e VS V_{CAL}

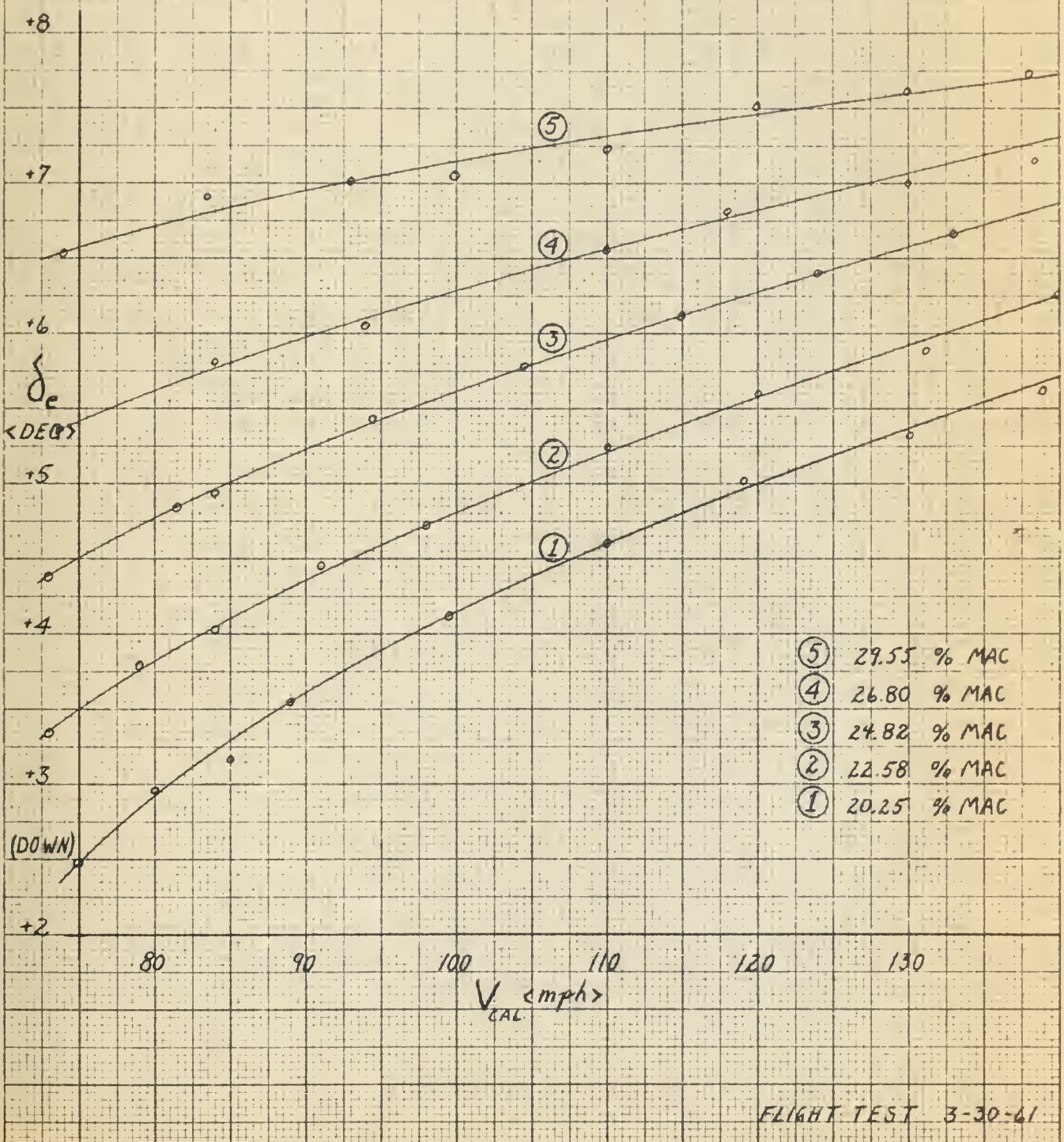

FLIGHT TEST 3-30-61

FIG. 29

APPROACH CONFIGURATION

POWER ON

δ_e VS C_L

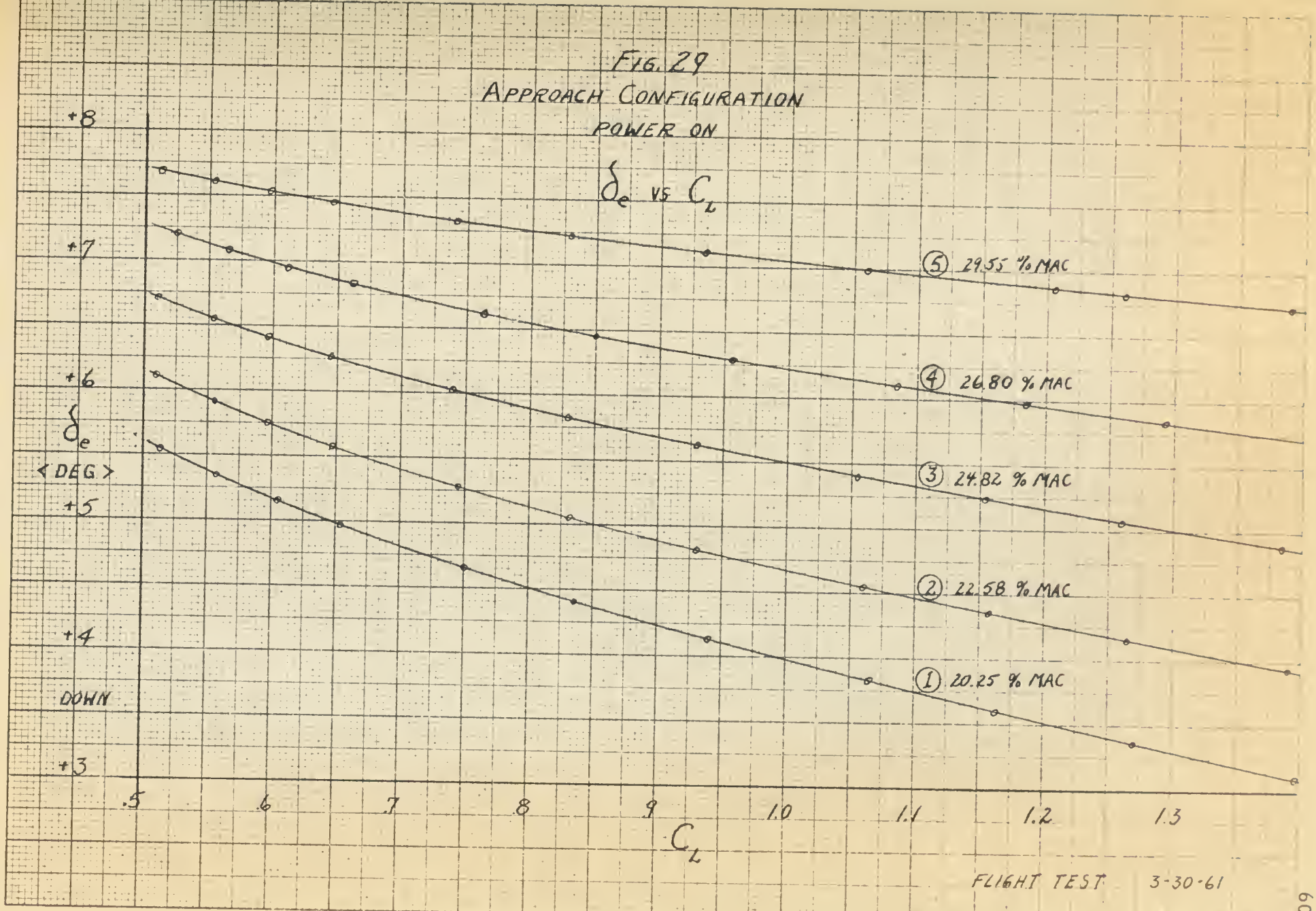

FLIGHT TEST 3-30-61

09

FIG. 30

APPROACH CONFIGURATION

POWER ON

$\frac{\partial \delta_e}{\partial C_L}$ VS. % MAC

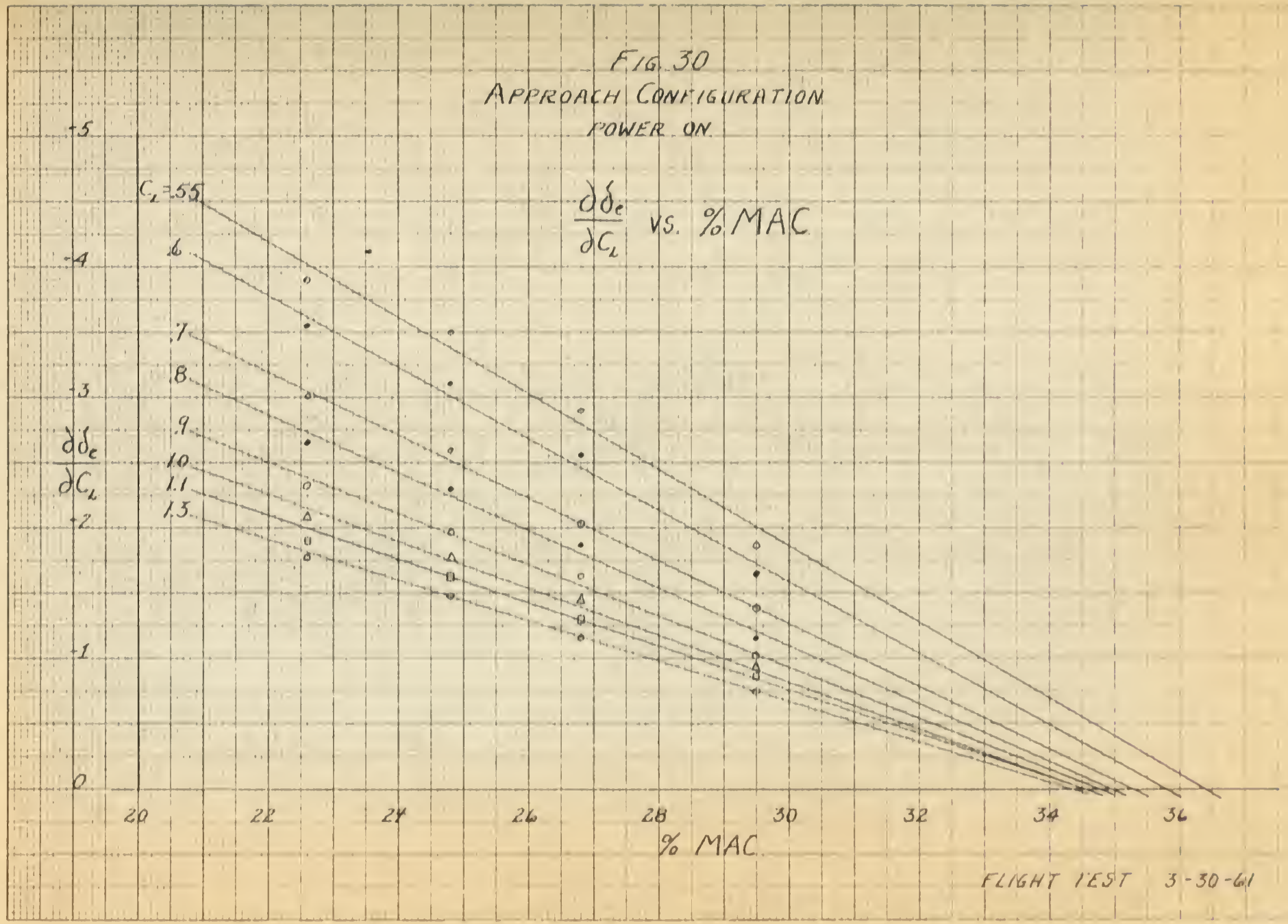

FLIGHT TEST 3-30-61

FIG 31

APPROACH CONFIGURATION

POWER ON

F_S VS. V_{CAL}

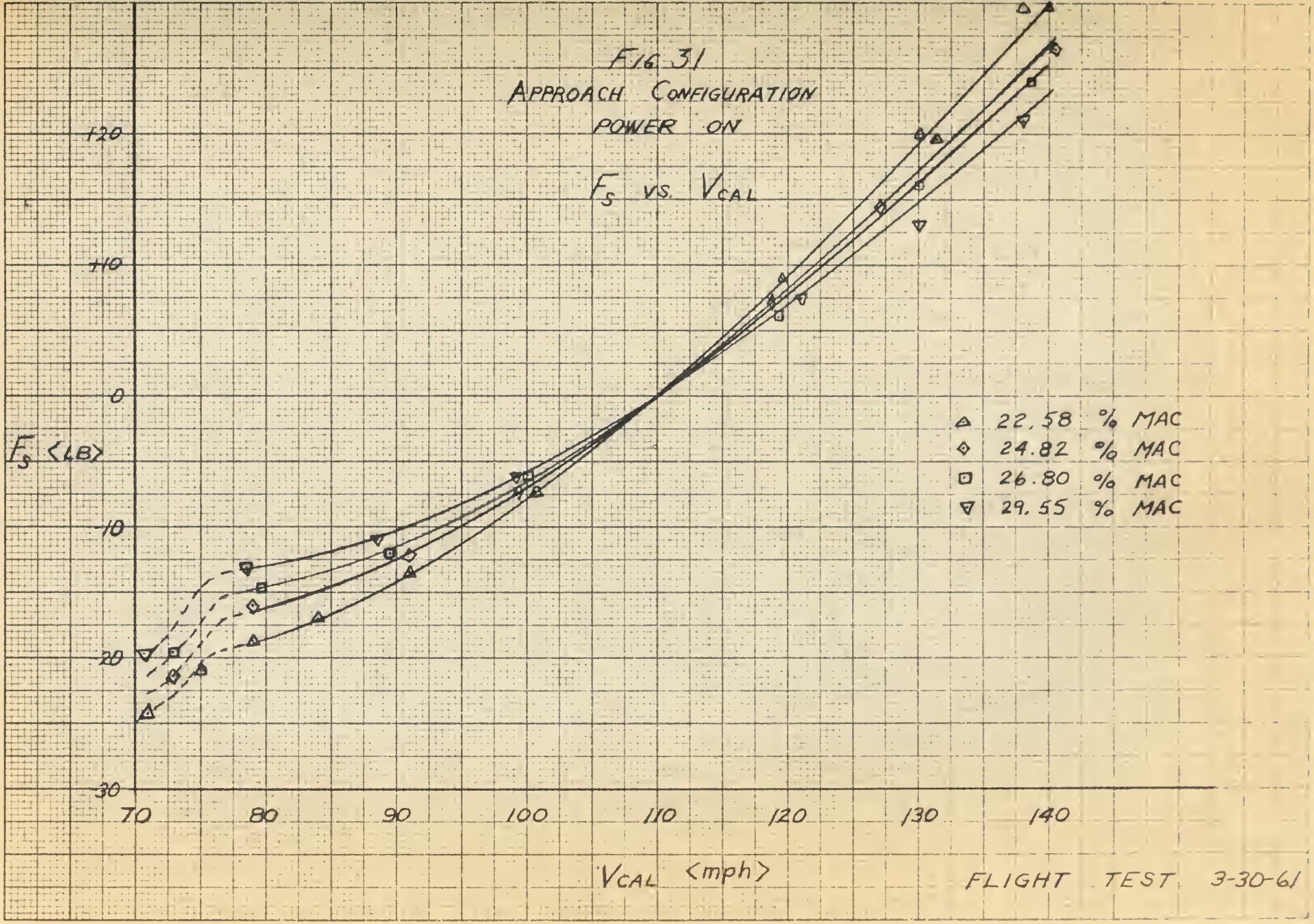

FLIGHT TEST 3-30-61

FIG. 32

APPROACH CONFIGURATION

POWER ON

F_s/δ VS. C_L

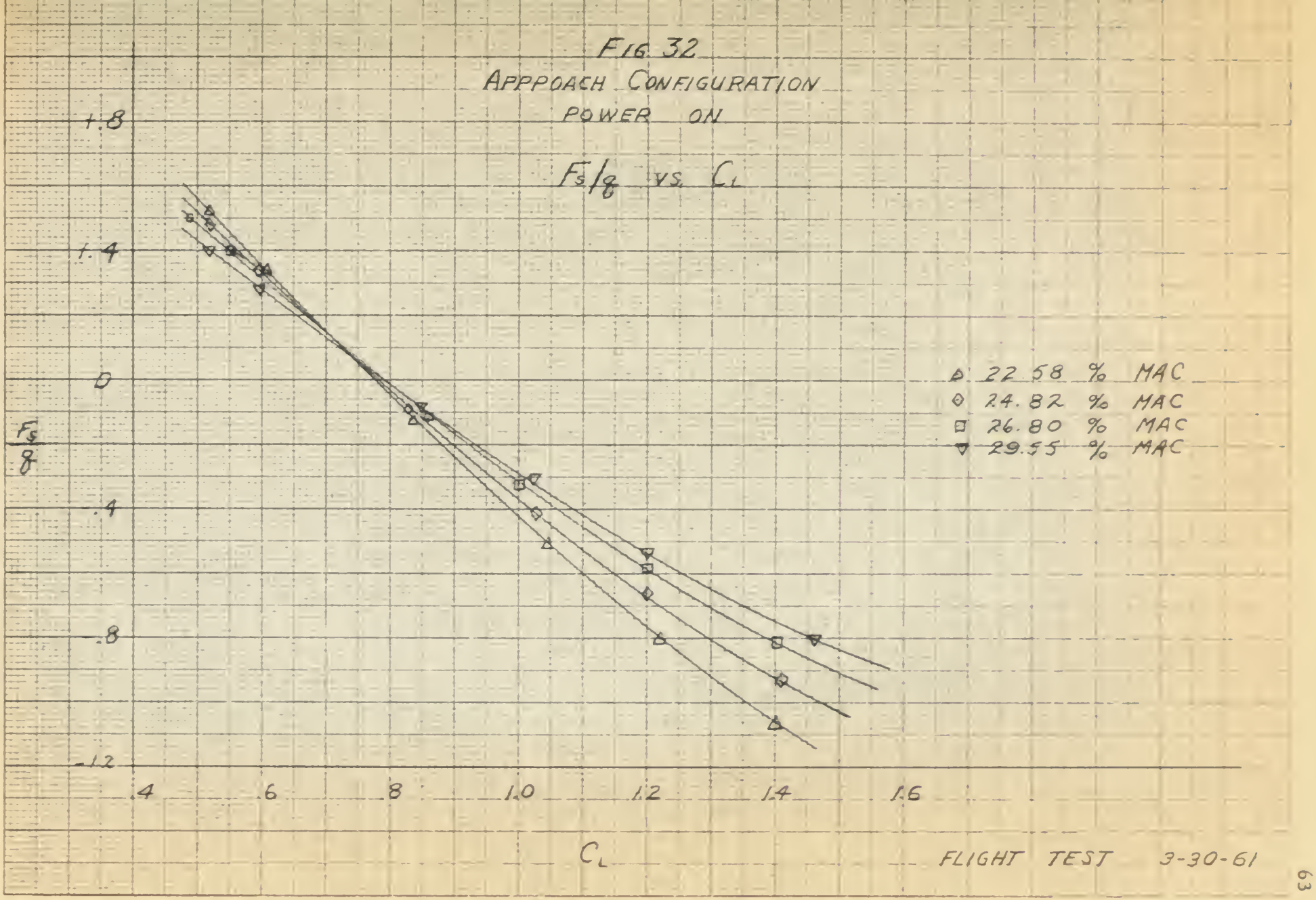

FLIGHT TEST 3-30-61

FIG 33

APPROACH CONFIGURATION

POWER ON

$\frac{d[F_s/q]}{dC_L}$ VS. % MAC

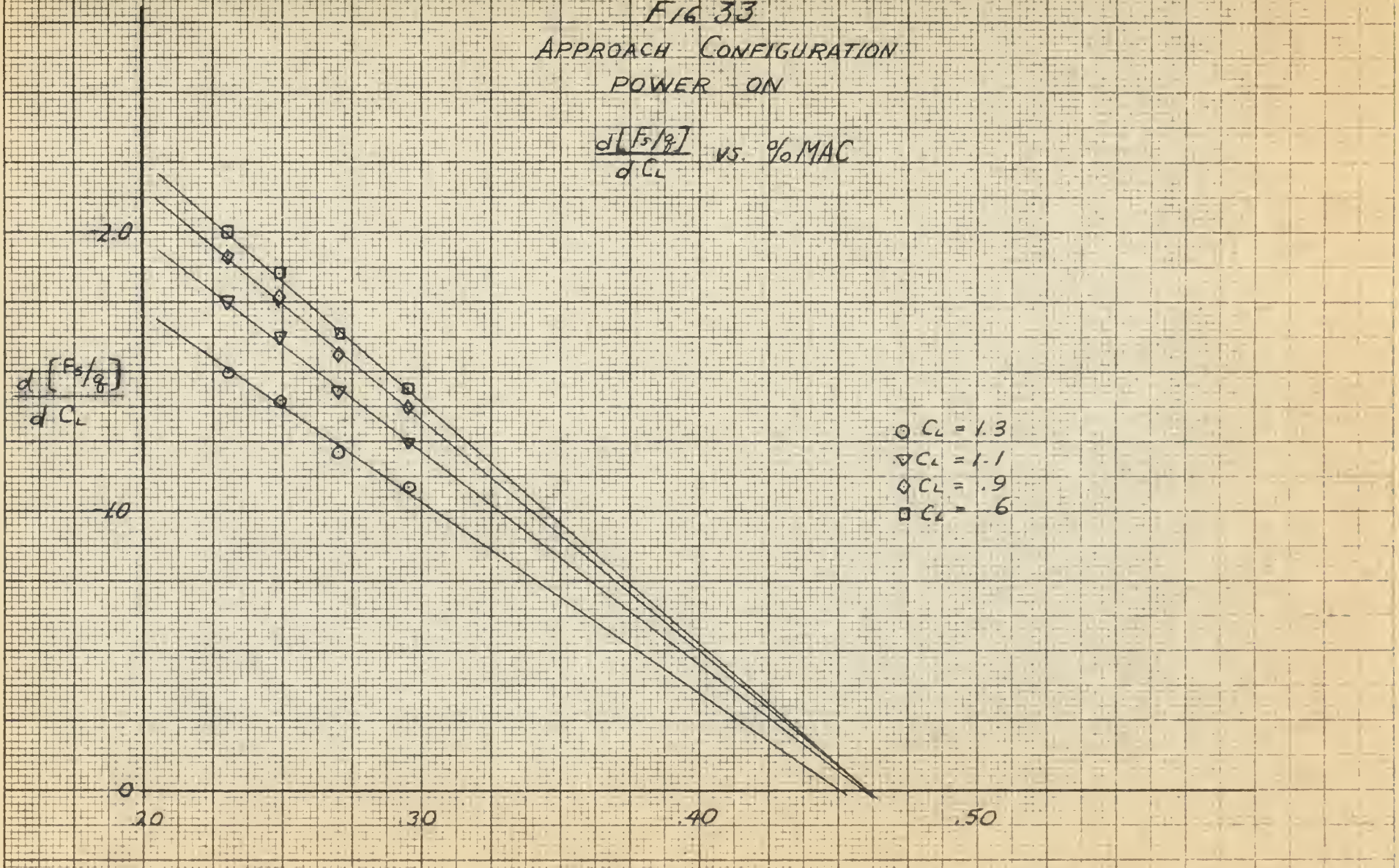

FLIGHT TEST 3-30-61

FIG. 34

APPROACH CONFIGURATION

POWER ON

N_o AND N_o' VS C_L

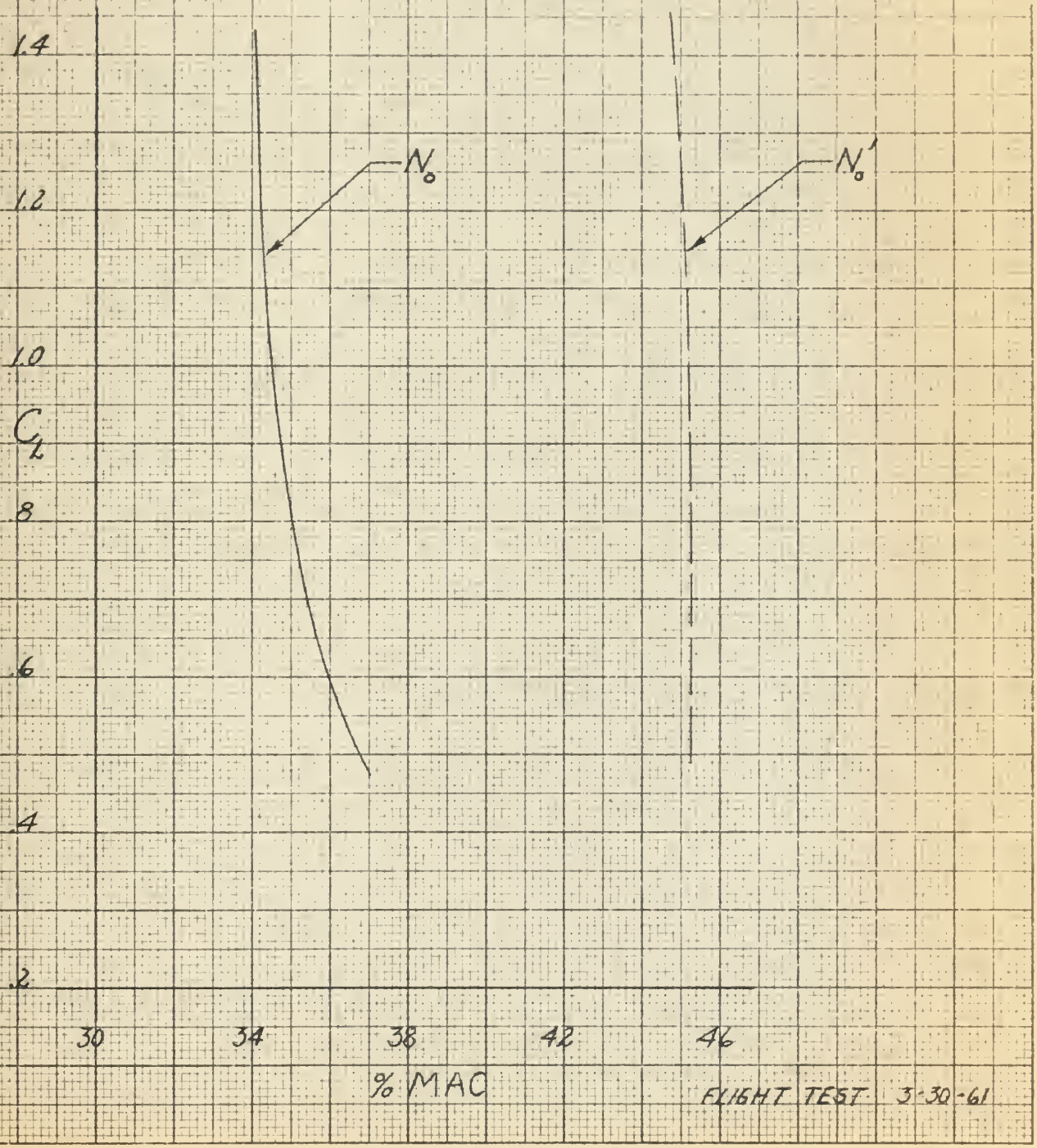

FLIGHT TEST 3-30-61

FIG. 35

APPROACH CONFIGURATION

POWER OFF

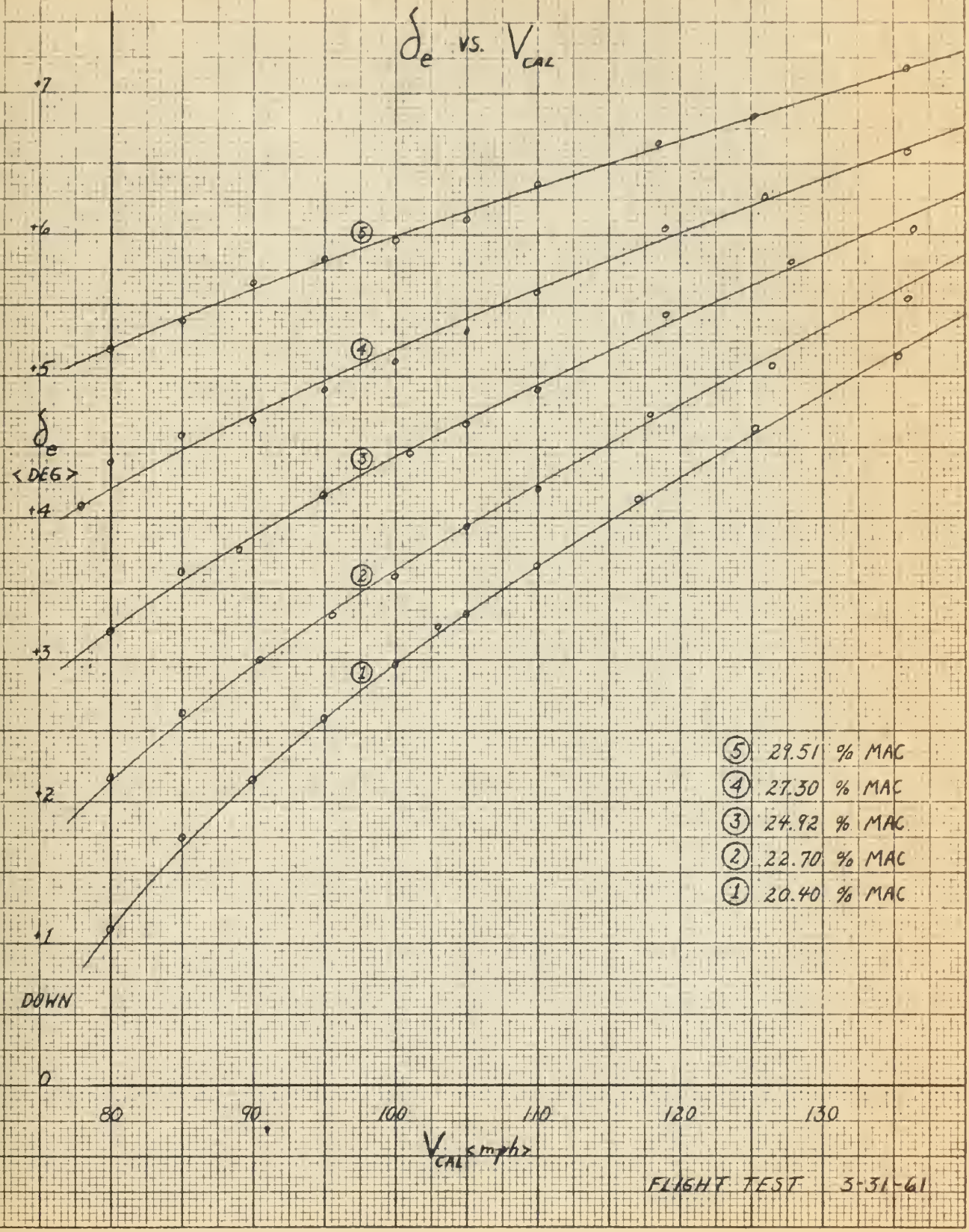

FLIGHT TEST 3-31-61

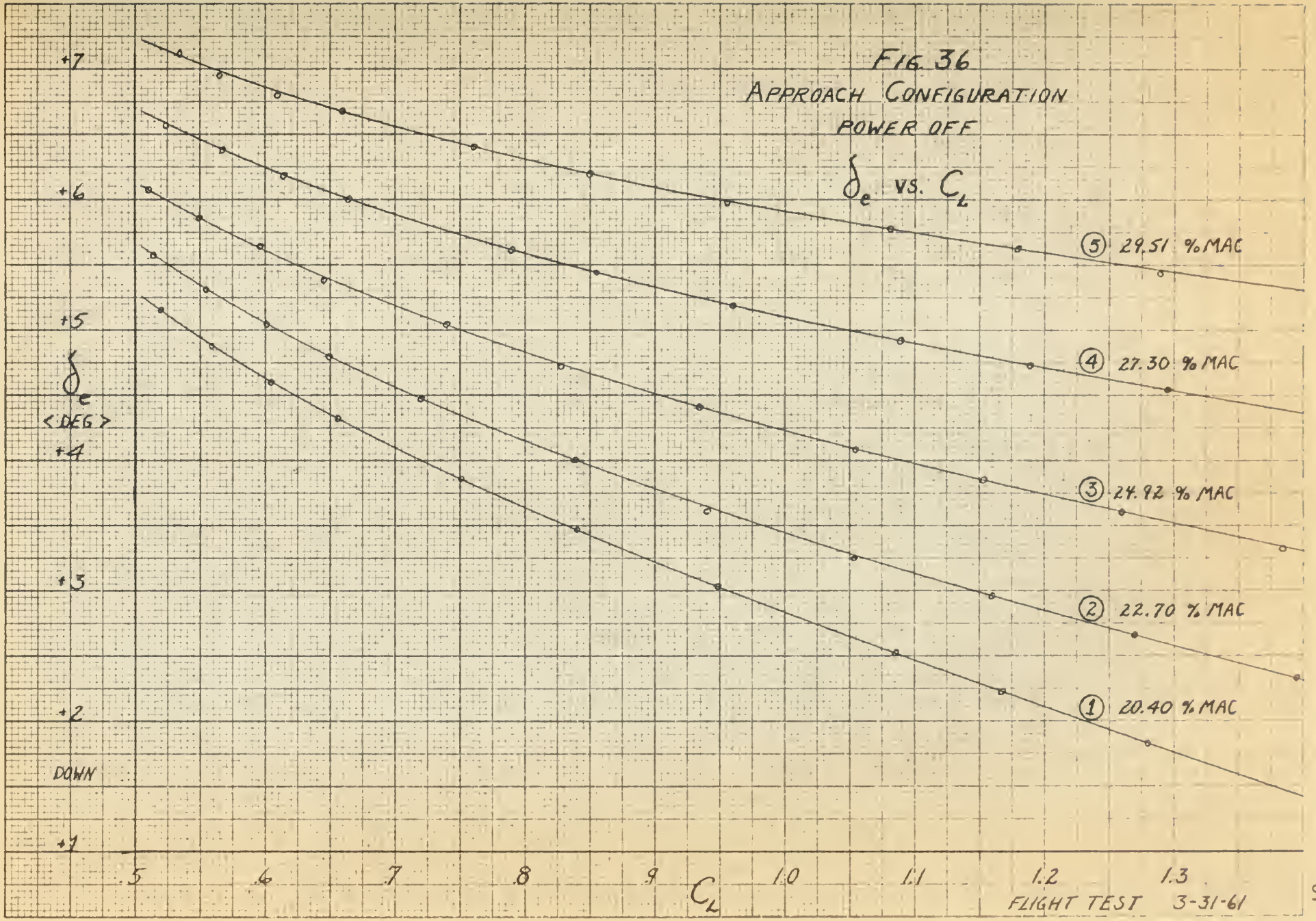
FIG. 36
APPROACH CONFIGURATION
POWER OFF
δ_e VS. C_L
⑤ 29.51 % MAC
④ 27.30 % MAC
③ 24.92 % MAC
② 22.70 % MAC
① 20.40 % MAC
+7
+6
+5
+4
+3
+2
+1
δ_e
<DEG>
DOWN
.5
.6
.7
.8
.9
1.0
1.1
1.2
1.3
C_L
FLIGHT TEST 3-31-61

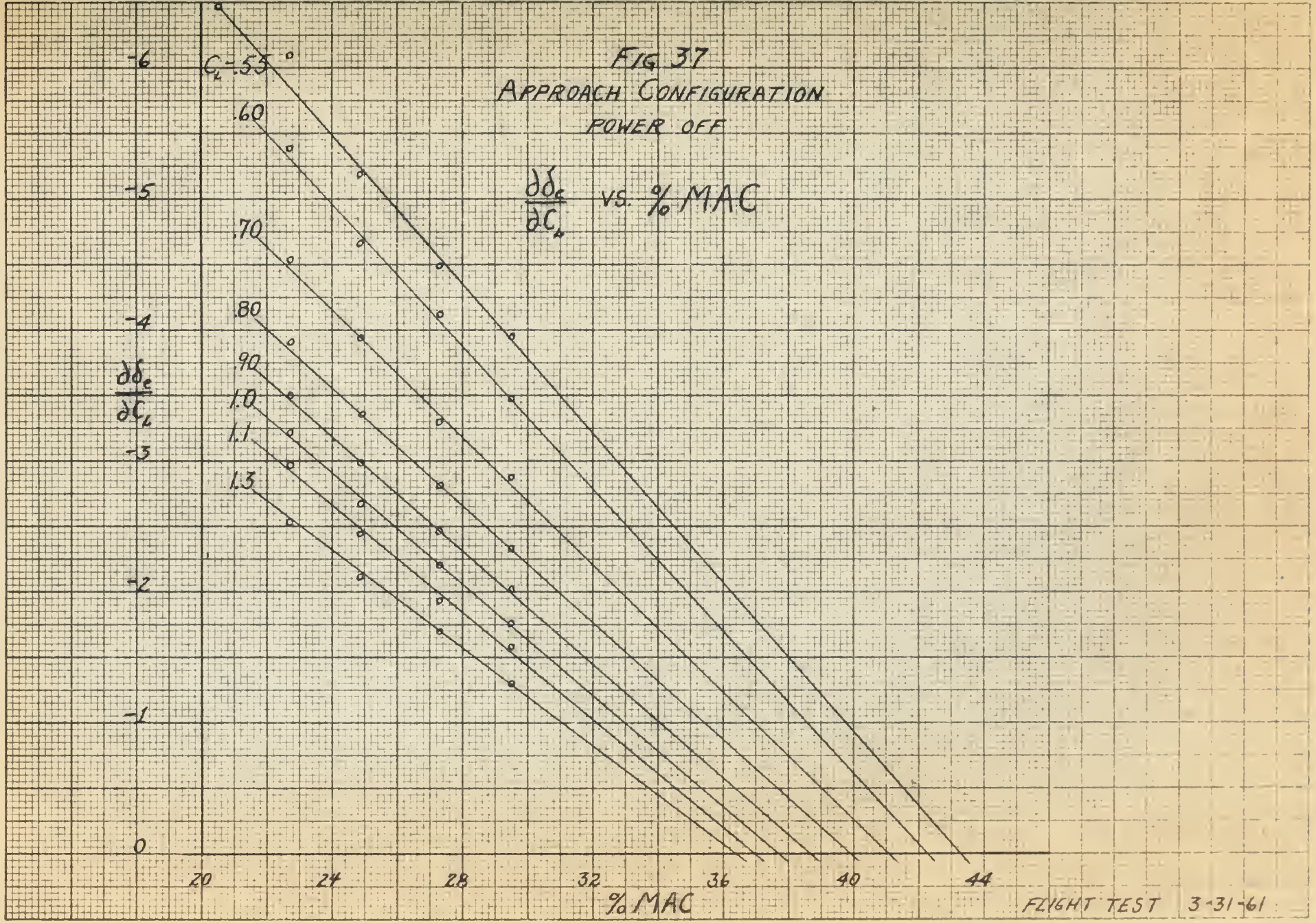
FIG 37
APPROACH CONFIGURATION
POWER OFF
$\frac{\partial \delta_e}{\partial C_L}$ VS. % MAC
C_L .53
.60
.70
.80
.90
1.0
1.1
1.3
$\frac{\partial \delta_e}{\partial C_L}$
-6
-5
-4
-3
-2
-1
0
20
24
28
32
36
40
44
% MAC
FLIGHT TEST 3-31-61

FIG. 38

APPROACH CONFIGURATION

POWER OFF

F_S VS. V_{CAL}

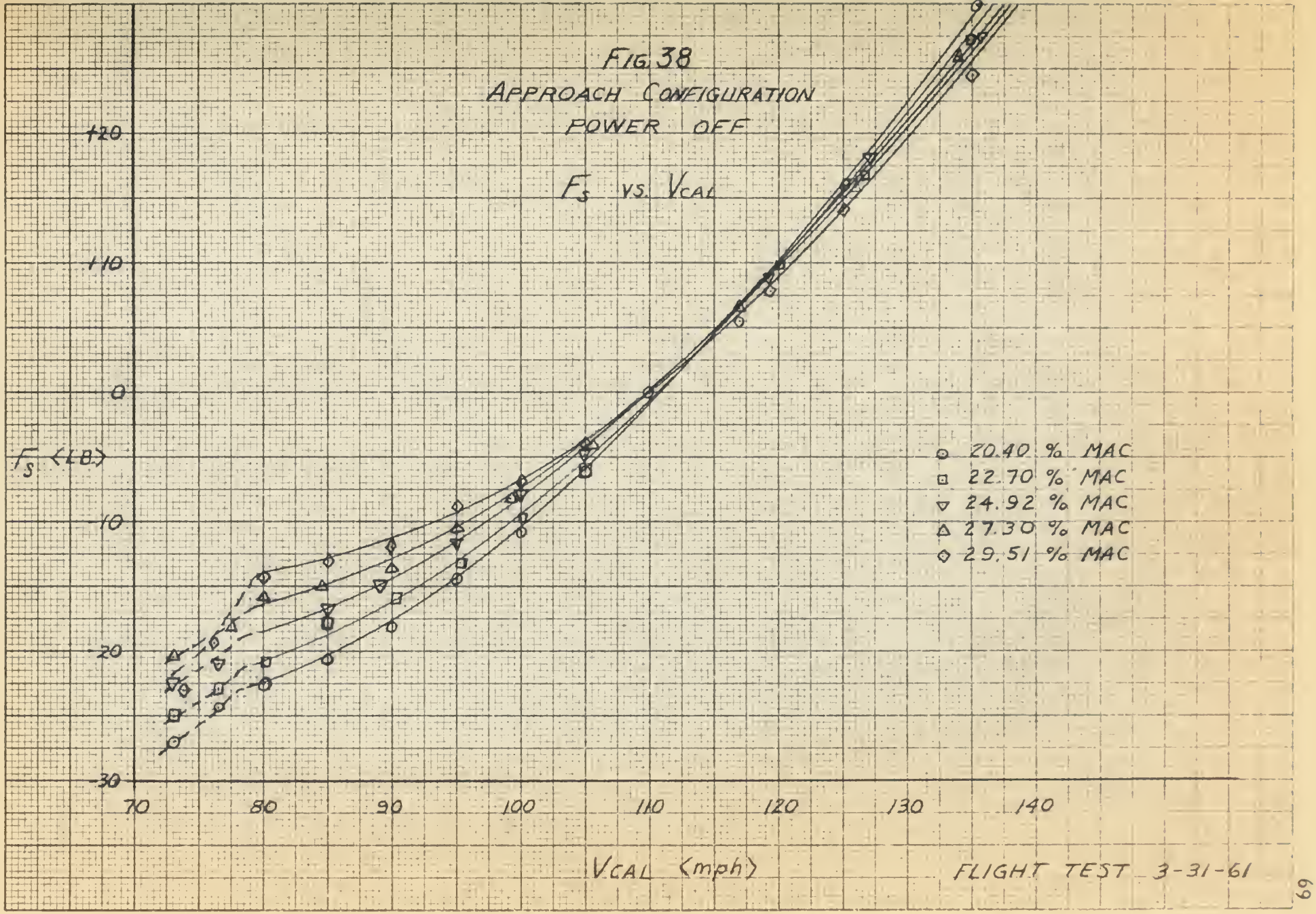

FLIGHT TEST 3-31-61

FIG. 39

APPROACH CONFIGURATION

POWER OFF

F_s/q VS. C_L

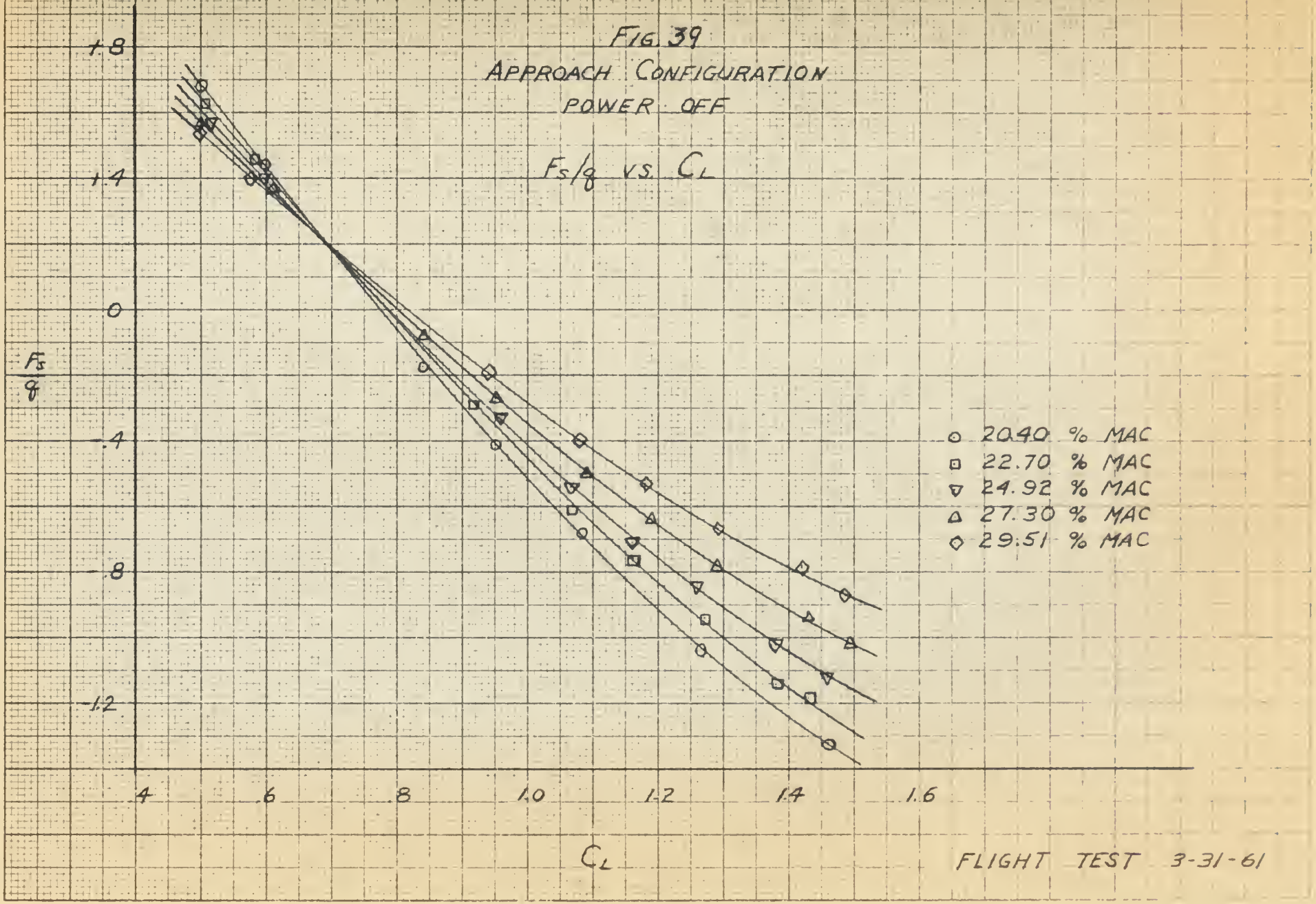

FLIGHT TEST 3-31-61

FIG. 40

APPROACH CONFIGURATION

POWER OFF

$\frac{d[F_s/q]}{dC_L}$ vs. % MAC

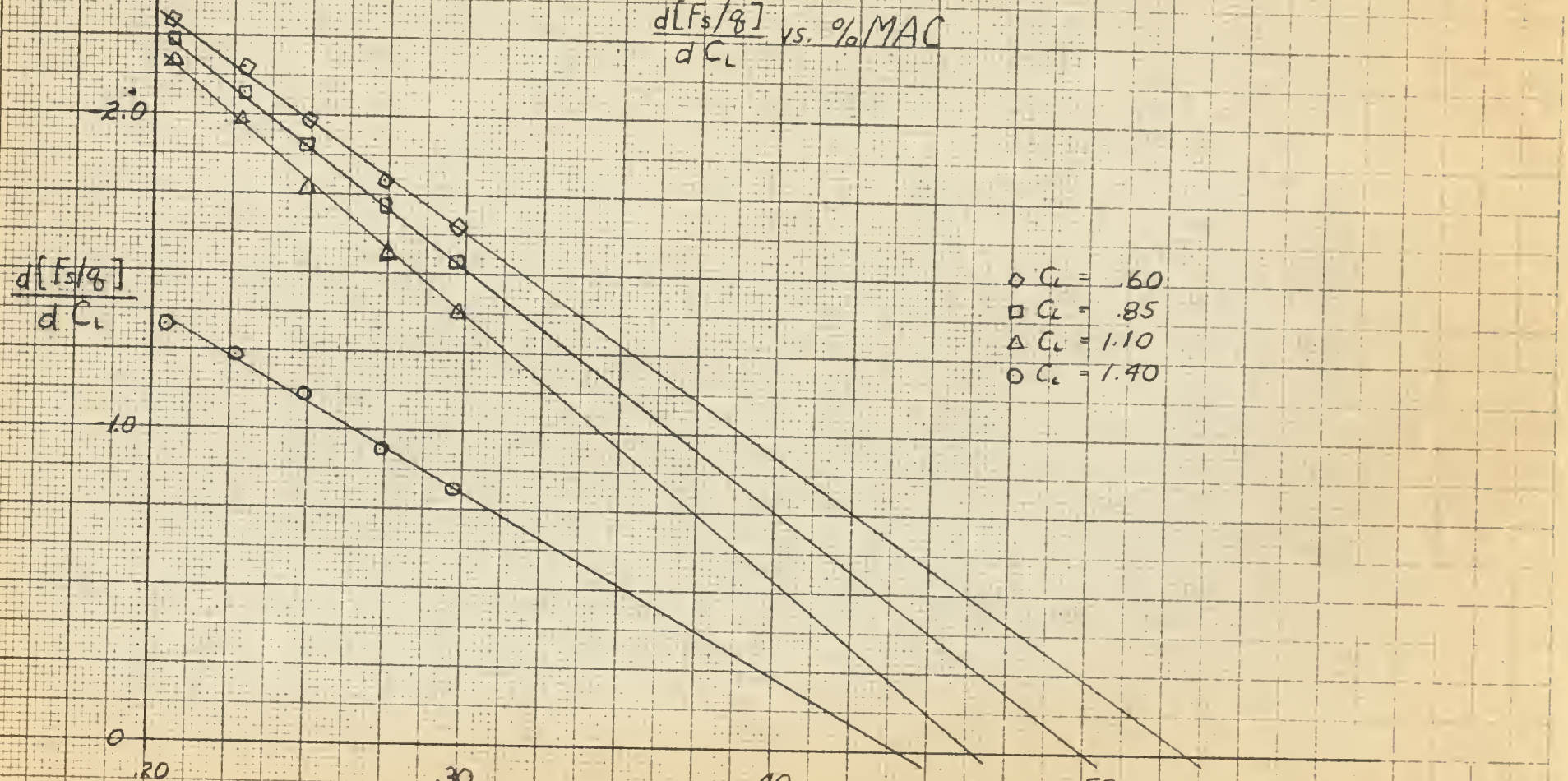

FLIGHT TEST 3-31-61

FIG. 41

APPROACH CONFIGURATION

POWER OFF

N_o AND N_o' VS. C_L

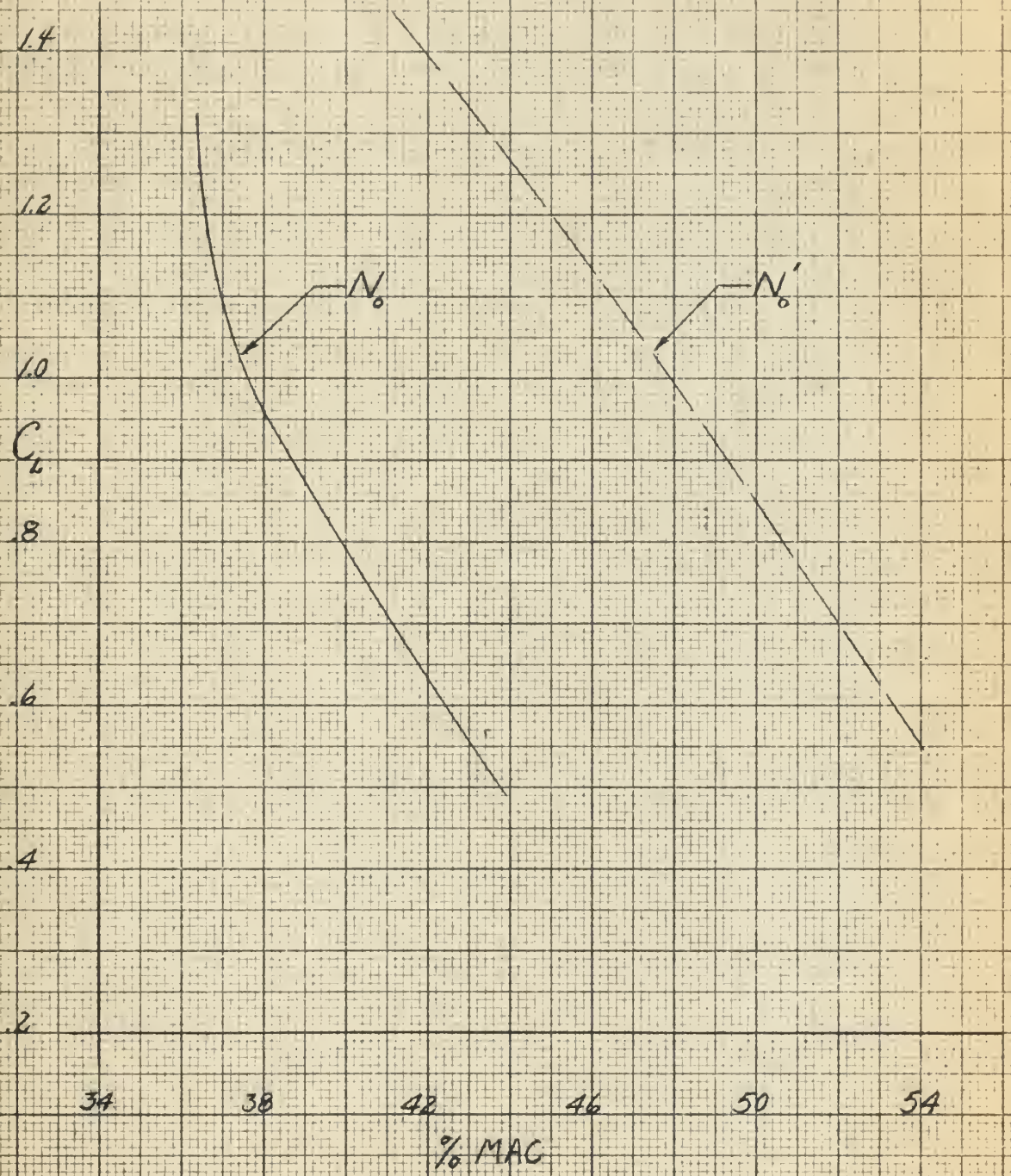

FLIGHT TEST 3-31-61

FIG. 42

NEUTRAL POINT SUMMARY

APPROACH CONFIGURATION

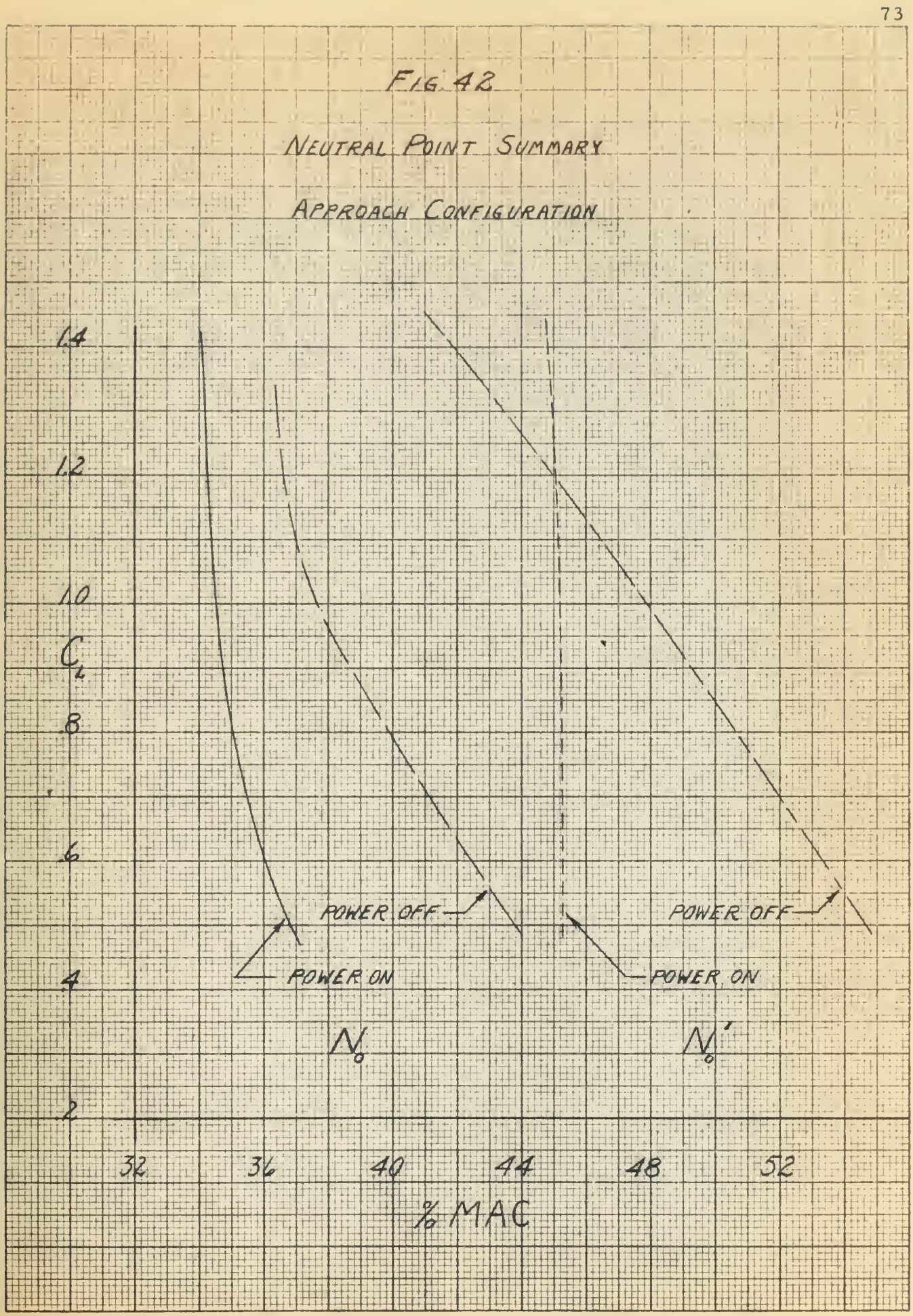

FIG. 43

CRUISE CONFIGURATION

POWER ON

δ_e VS. n

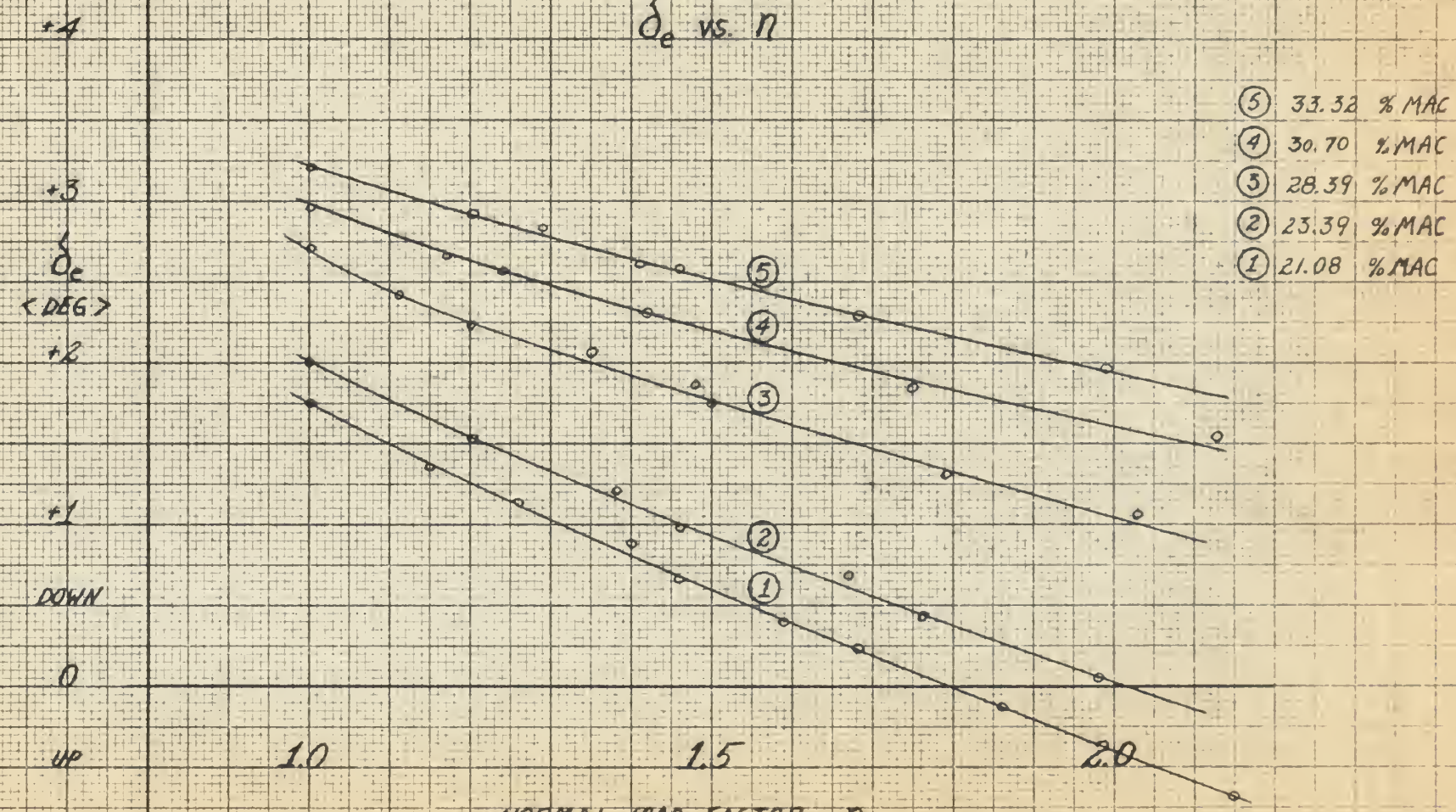

(5) 33.32 % MAC

(4) 30.70 % MAC

(3) 28.39 % MAC

(2) 23.39 % MAC

(1) 21.08 % MAC

FLIGHT TEST 4-4-61

FIG 44

CRUISE CONFIGURATION

POWER ON

δ_e VS C_{N_A}

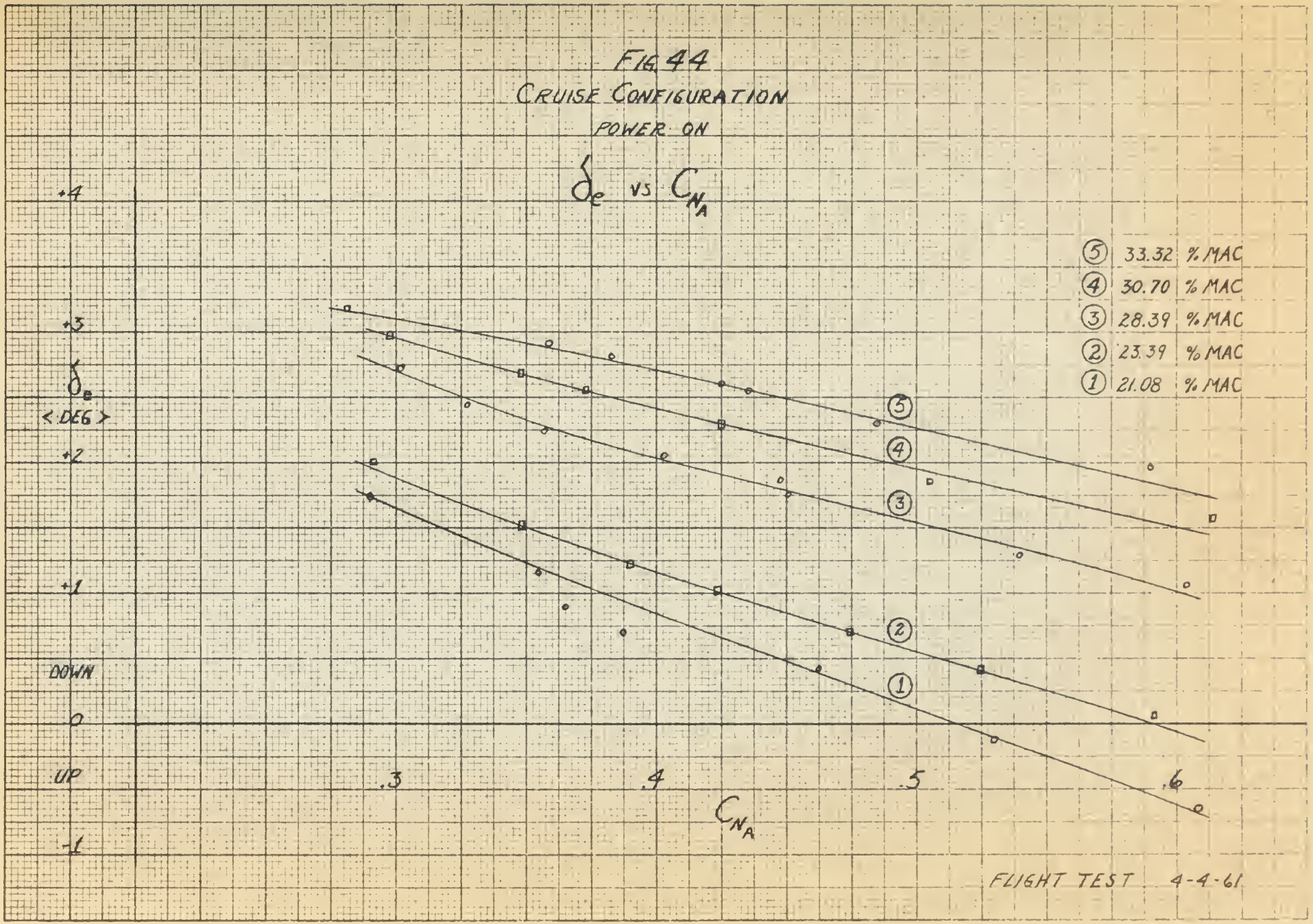

FLIGHT TEST 4-4-61

FIG 45

CRUISE CONFIGURATION

POWER ON

$\frac{\partial \delta_e}{\partial C_{N_A}}$ VS. %MAC

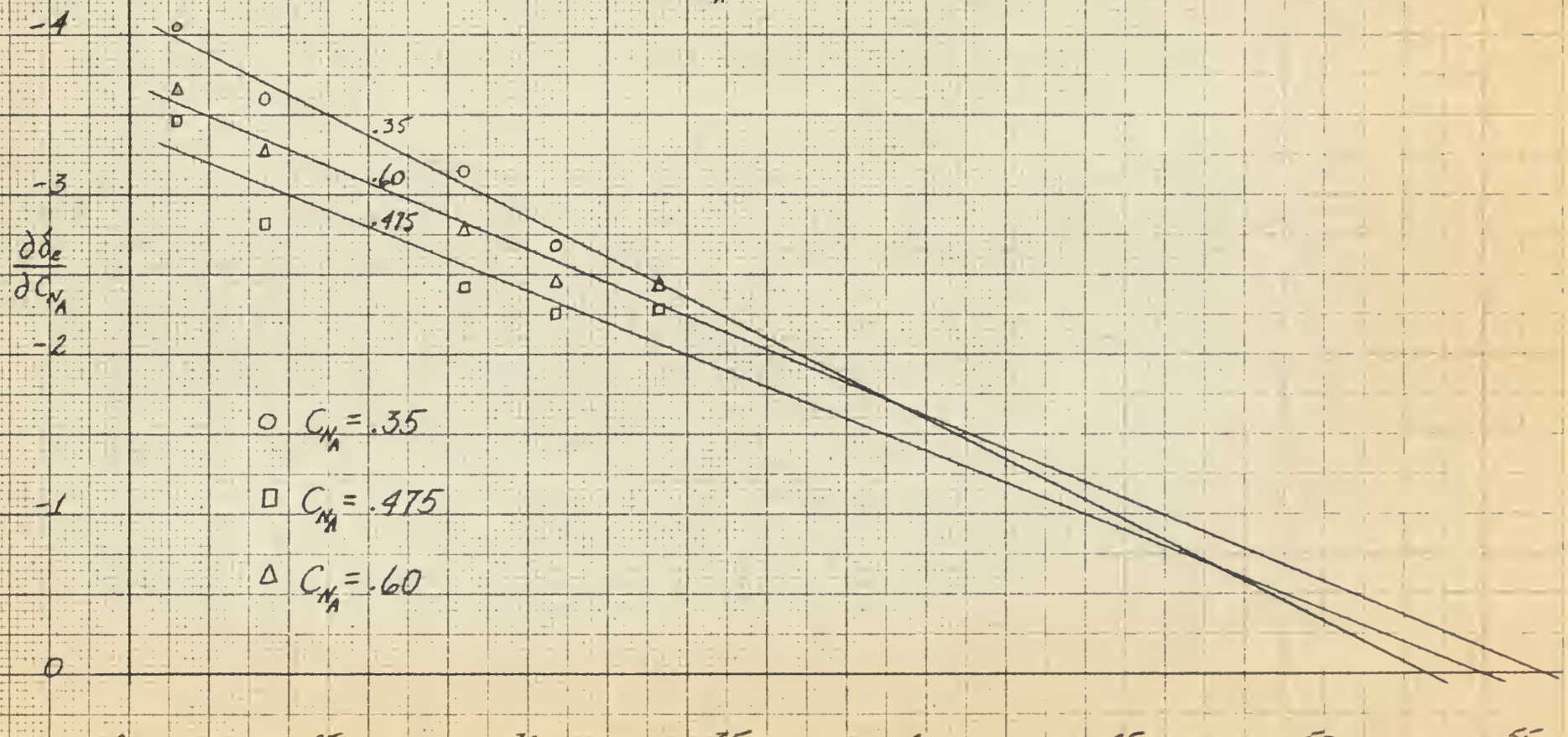

FLIGHT TEST 4-4-61

FIG. 46

CRUISE CONFIGURATION

POWER ON

F_S VS. n

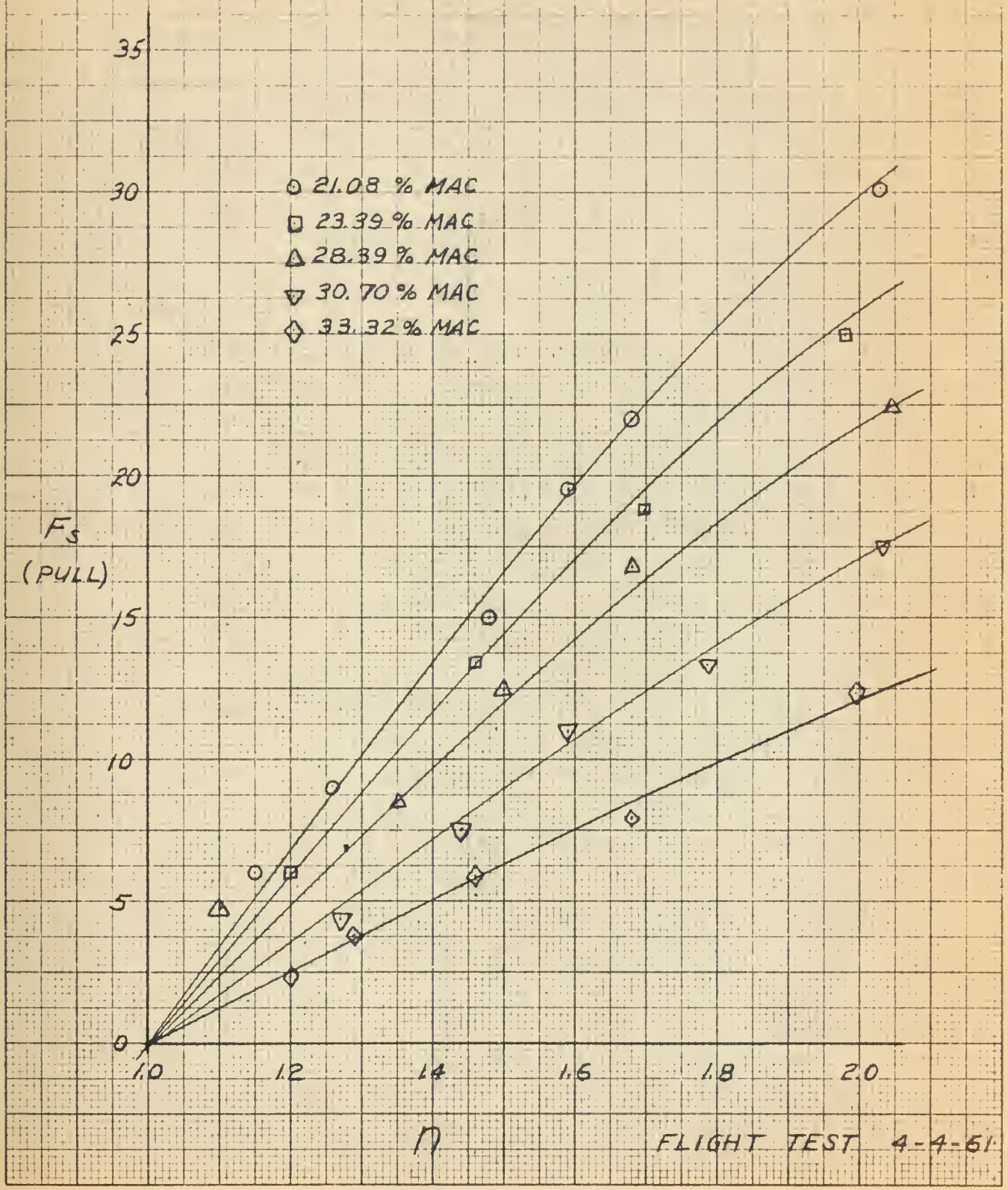

FLIGHT TEST 4-4-61

FIG 47

CRUISE CONFIGURATION

POWER ON

F_s/q VS. C_{N_A}

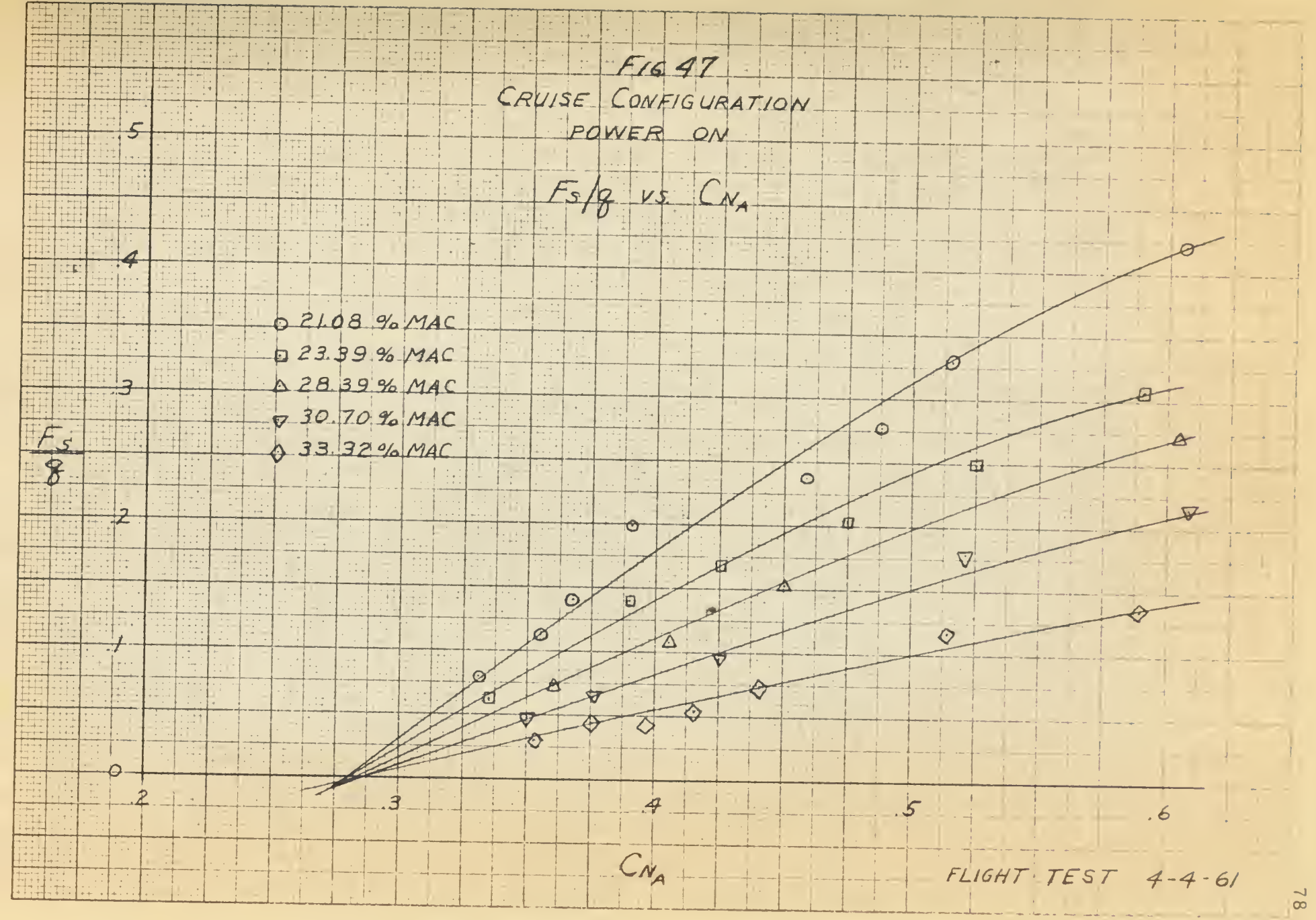

FLIGHT TEST 4-4-61

FIG. 48

CRUISE CONFIGURATION

POWER ON

$\frac{d[F_s/q]}{d C_{N_A}}$ vs. %MAC

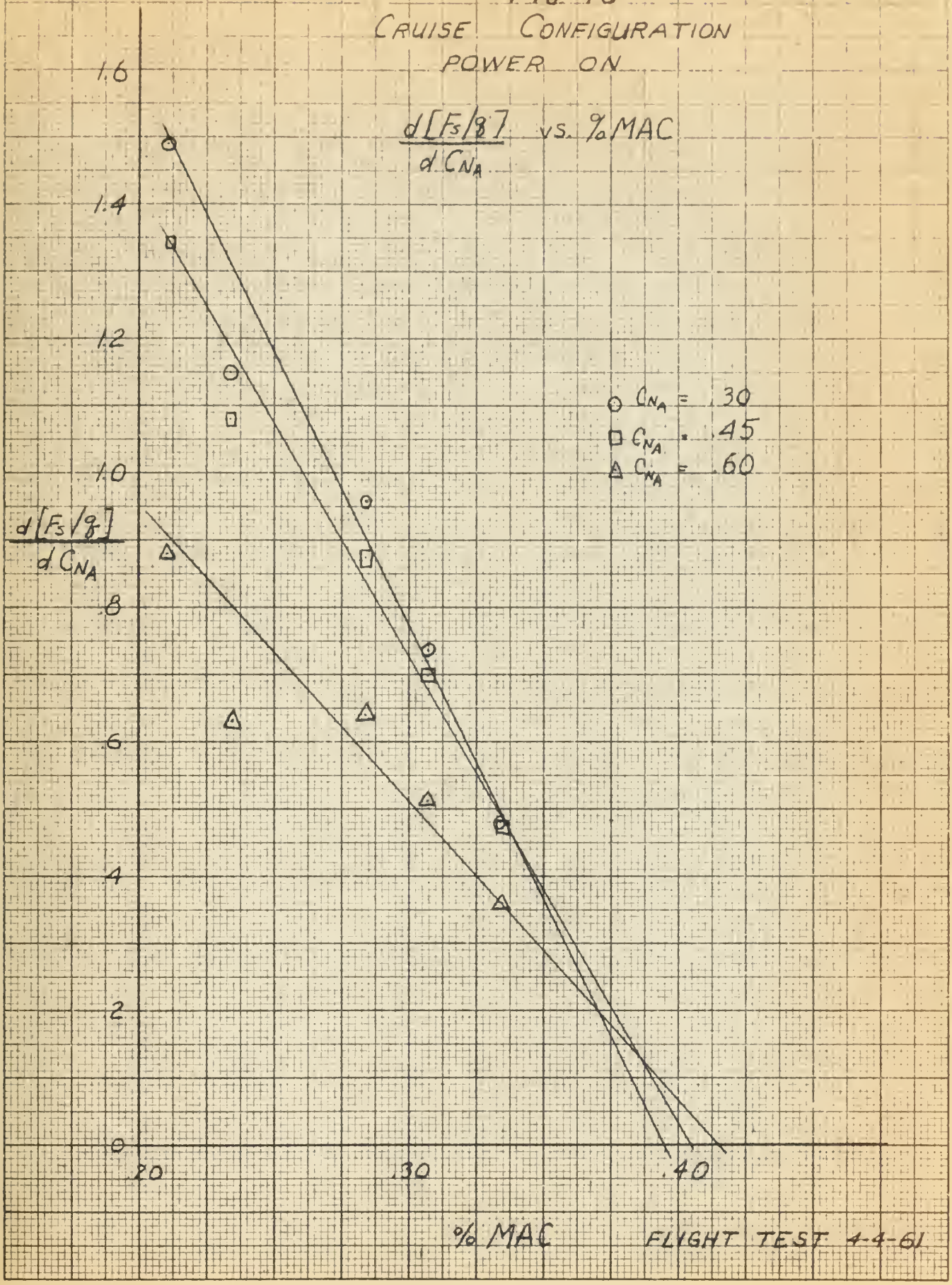

FLIGHT TEST 4-4-61

FIG. 49
MANEUVER POINTS

CRUISE CONFIGURATION

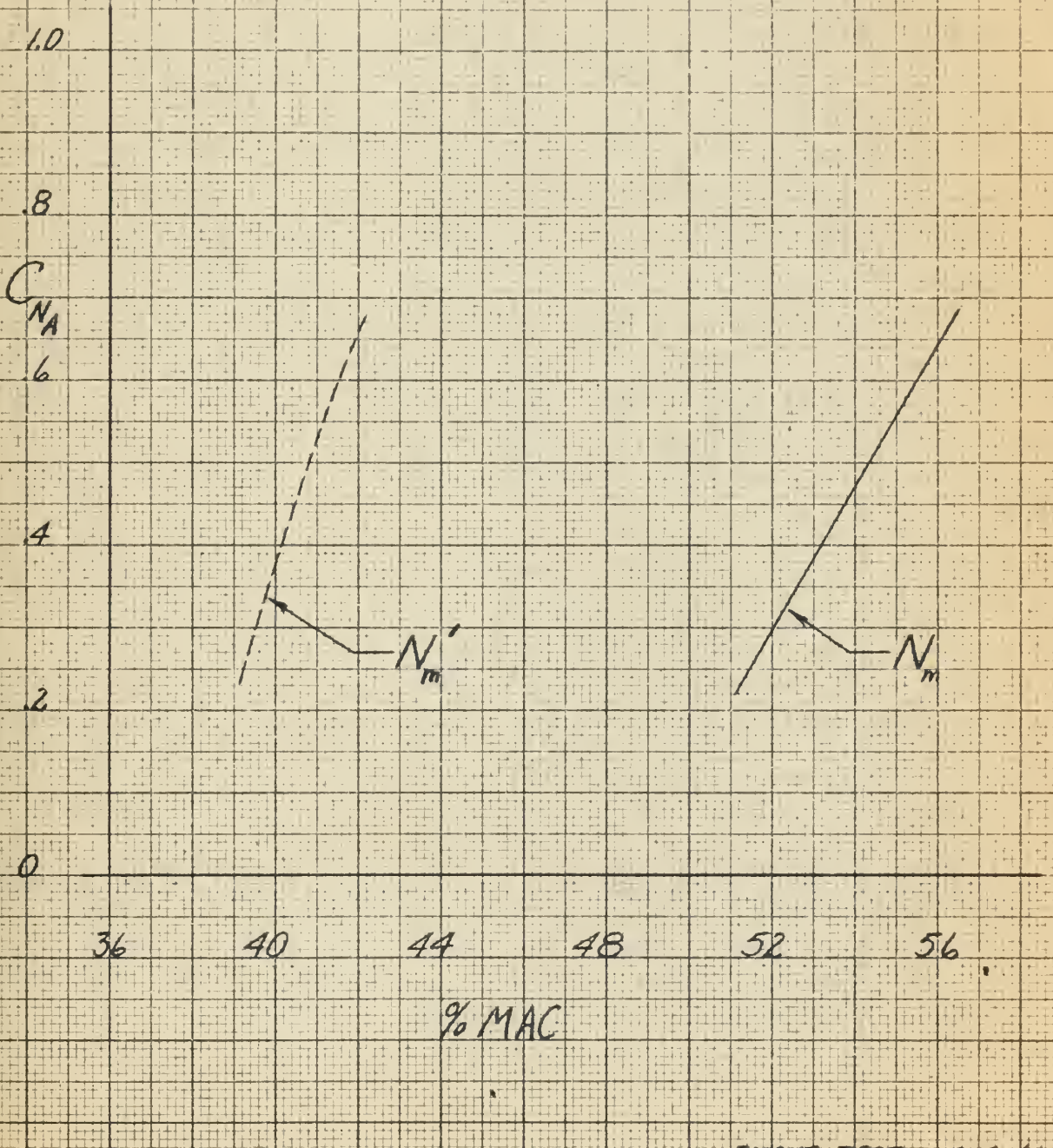

FLIGHT TEST 4-4-61

FIG 50

ELEVATOR POWER

C_{m_δ} VS C_L

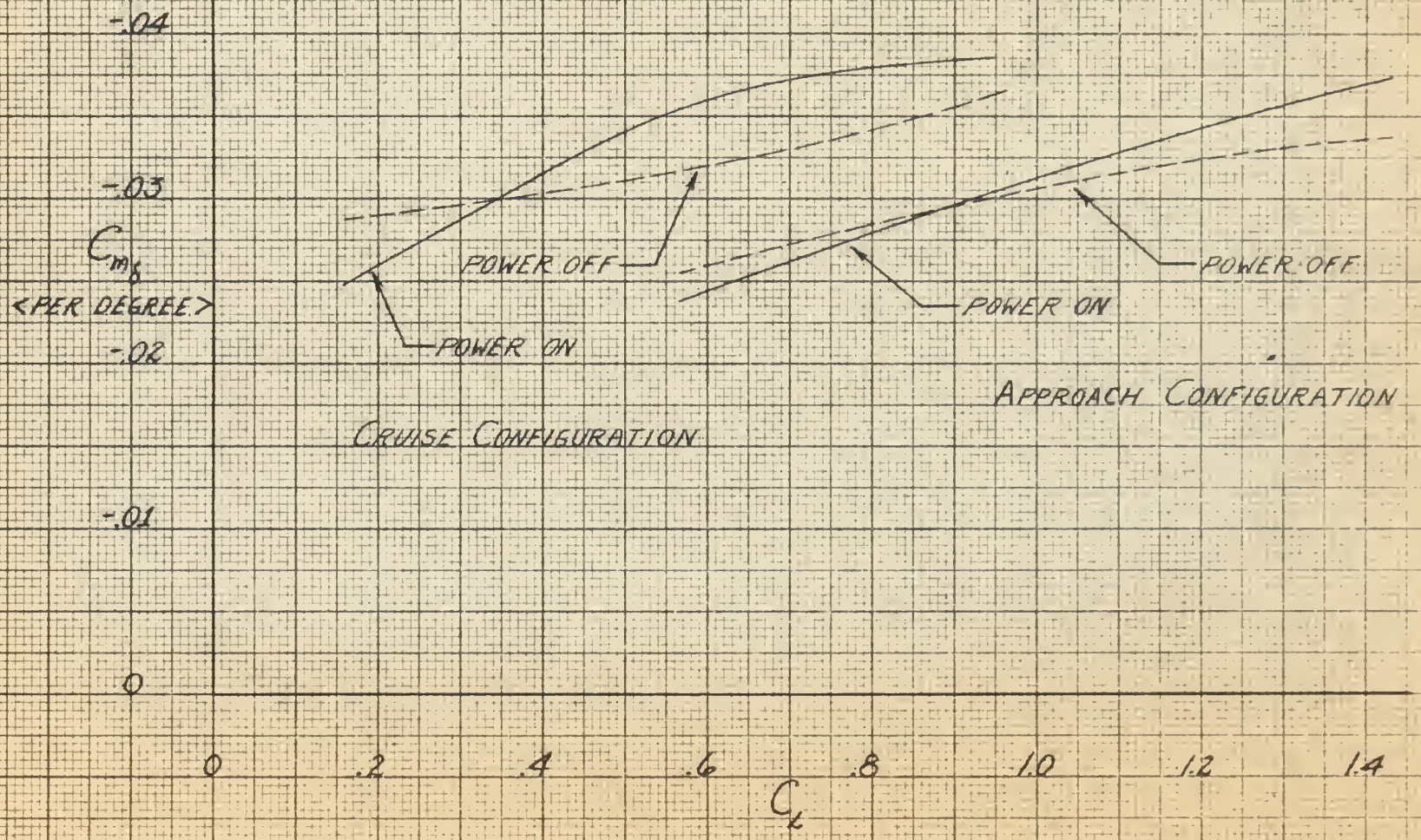

APPENDIX

THEORETICAL ANALYSIS

The theoretical determination of the various stability derivatives and parameters was based primarily on methods given in Ref. 6, and supported by various NACA reports. The neutral points, maneuver points, and elevator power were theoretically estimated for only the cruise configuration, using the actual flight conditions encountered in the flight tests.

For steady flight, the equation for the summation of moments about the airplane center of gravity can be written:

$$Cm_{c.g.} = C_{L_w} \frac{X_a}{C} + Cm_{ac} + Cm_{Fus,\,Nac} - C_{L_t} \overline{V}\,\eta_t + T_c \frac{2D^2}{S_w} \frac{Z}{c} + C_{n_p} \frac{\ell_p}{c} \frac{S_p}{S_w} = 0$$

For the purposes of this analysis, the center of gravity of the airplane and the aerodynamic center of the wing were assumed to be at the same location. Therefore,

$$\frac{X_a}{c} = 0$$

This appears to be a valid assumption, since it corresponds to the average center of gravity location during flight tests.

The stability derivative, $\frac{dC_m}{dC_L}$, can now be found by taking the derivative of the moment equation with respect to C_L.

$$\frac{dC_m}{dC_L} = \frac{dC_m}{dC_L}_{Fus,\ Nac} - C_{L_t} \bar{V} \frac{d\eta_t}{dC_L} - \frac{a_t}{a_w} \bar{V}\eta_t \left(1 - \frac{d\varepsilon}{d\alpha} - \frac{d\varepsilon_p}{d\alpha}\right)$$

$$+ \frac{dT_c}{dC_L} \frac{2D^2}{S_w} \frac{Z}{c} + \frac{dC_{n_p}}{dC_L} \frac{\ell_p}{c} \frac{S_p}{S_w}$$

The determination of the various derivatives are shown in the "Calculations" section of this appendix, and values of the various required airplane dimensions are shown in the table of airplane specifications. The tail lift coefficient, C_{L_t}, was found from solving the moment equation for tail force required to trim the airplane.

The control fixed neutral point, N_o, can now be evaluated, since

$$N_o = X_{c.g.} - \frac{dC_m}{dC_L}$$

In computing the control free neutral point, N_o', it is necessary to consider the effect of the stick force due to the downspring which is located in the elevator control system. This force, ΔP, was measured for several elevator positions, and the resulting calibration is shown in Fig. 11. The control free neutral point can now be estimated from:

$$N_o' = N_o + \frac{C_{m_\delta} C_{h_\alpha}}{a_w C_{h_\delta}} \left(1 - \frac{d\varepsilon}{d\alpha}\right) + \frac{\Delta P}{G_e S_e c_e} \frac{C_{m_\delta}}{C_{h_\delta} W/S}$$

The elevator power, C_{m_δ}, as shown in Ref. 1, can now be readily computed as:

$$C_{m_\delta} = - a_t \, \overline{V} \, \eta_t \, \tau$$

Values of C_{h_α} and C_{h_δ} were estimated from wind tunnel data in Ref. 7. The elevator control gearing ratio, G_e, was measured on the control system of the airplane and is shown in the airplane specifications.

The maneuvering points can now be calculated. For steady turning flight:

$$N_m = N_o - \frac{63 \, g \, \ell_t \rho}{2 \, W/S \, \tau} C_{m_\delta} \left(1 + \frac{1}{n^2} \right)$$

Also,

$$N_m' = N_o' + \frac{57.3}{W/S \, C_{h_\delta}} C_{m_\delta} \left[\frac{\rho}{2} \, g \ell_t \left(C_{h_\alpha} - \frac{1.1 \, C_{h_\delta}}{\tau} \right) \right] \left(1 + \frac{1}{n^2} \right)$$

where n is the normal acceleration.

In computing N_m', it must be remembered that the downspring does not affect the stick-free maneuvering point, and its contribution to N_o' must be neglected in the above equation.

The major results of this analysis have been extracted from the section of "Calculations" and are shown below in tabular form. The results are for the average conditions * encountered in the actual flight tests. A value of $n = 2$ was arbitrarily selected for maneuvering point computations.

PARAMETER	THEORETICAL VALUE
N_o	.477
N_o'	.634
N_m	.564
N_m'	.526
C_{m_δ}	-.0356

*V = 180 mph

W = 4200 lb.

h = 8000 ft.

Power = 135 Bhp @ engine

CALCULATIONS

a.) In addition to the information presented in the table of airplane specifications, the following data was used in the theoretical calculations:

a_w	= .0816	(Ref. 6)
a_t	= .069	"
τ	= .59	"
ρ	= .001868	"
$C_{m_{ac}}$	= -.010	"
$\frac{d\varepsilon}{d\alpha}$	= .36	"
$\left(\frac{dC_n}{d\alpha}\right)_{p\ T_c=0}$	= .095	"
$\frac{d\varepsilon_p}{d\alpha}$	= .0436	"
$\left(\frac{d\beta}{d\alpha}\right)_{prop}$	= 1.25	"
X_{ac}	= .245	"
C_{h_α}	= -.085	(Ref. 7)
C_{h_δ}	= -.74	"
η_p	= .85	(Ref. 8)
W	= 4200	Flight Test
V	= 180 mph	" "
h	= 8000 ft.	" "
C_T	= .28	" "

b.) Tail efficiency, η_t

Power effect

$$T_c = \frac{550\ SHP\ \eta_p}{\rho\ V^3\ D^2} \qquad \text{(Ref. 6)}$$

$$= \frac{550(135)(.85)}{.001868(264)^3(6.67)^2}$$

$$= .041$$

$$\left(\frac{V_s}{V}\right)^2 = 1 + \frac{8}{\pi}\ T_c$$

$$= 1 + 2.54(.041)$$

$$= 1.104$$

Fuselage Boundary Layer Effect

$$\left(\frac{V_t}{V}\right)^2 = (.93)^2 = .865 \qquad \text{(Ref. 9)}$$

From the three-view layout shown on Fig. 2, it is estimated the slipstream will affect one-half of the tail area. Therefore, the tail efficiency was found by averaging the slipstream effect and the fuselage boundary layer effect. Thus:

$$\eta_t = \frac{1.104 + .865}{2} = .985$$

c.) Fuselage and nacelle contribution to $\frac{dC_m}{dC_L}$

$$\left(\frac{dC_m}{dC_L}\right)_{Fus,\,Nas} = \frac{K_f\, w_f^2 L_f}{S_w\, ca_w} \qquad \text{(Ref. 6)}$$

$$= \frac{.09(4.6)^2(26.45)}{175(.0816)(5.09)} + 2\,\frac{.0295(2.93)^2(9)}{175(.0816)(5.09)}$$

$$= .1402$$

d.) Estimation of propeller effects

$$\frac{dT_c}{dC_L} = 1.5\, KC_L^{\frac{1}{2}}\, \eta_p \qquad \text{(Ref. 6)}$$

where $K = \frac{550\ Bhp\ \rho^{\frac{1}{2}}}{2(W/S)^{1.5} D^2}$ "

$$= \frac{550(135)(.001868)^{\frac{1}{2}}}{2(24)^{1.5}(6.67)^2}$$

$$= .142$$

$$\frac{dT_c}{dC_L} = 1.5(.142)(.85)(.28)^{\frac{1}{2}}$$

$$= .10$$

$$\frac{z}{c} = .066 \quad \text{(estimated from 3-view, Fig. 2)}$$

$$\frac{dC_{N_p}}{dC_L} = \left(\frac{dC_N}{d\alpha}\right)_p \left(\frac{d\beta}{d\alpha}\right)_p \frac{d\alpha}{dC_L} \qquad \text{(Ref. 6)}$$

d.) (continued)

$$\left(\frac{dC_n}{d\alpha}\right)_p = .147 \quad (T_c = .104) \qquad \text{(Ref. 10)}$$

$$\frac{dC_{N_p}}{dC_L} = \frac{.147(1.25)}{.0816(57.3)} = .04$$

$$\frac{d\eta_t}{dC_L} = .5\,\frac{d\left(\frac{V_s}{V}\right)^2}{dC_L} \qquad \text{(Slipstream affects only one-half of tail)}$$

$$\frac{d\left(\frac{V_s}{V}\right)^2}{dC_L} = \frac{8}{\pi}\,\frac{dT_c}{dC_L} = 1.74\,C_L^{\frac{1}{2}}\,\eta_p \qquad \text{(Ref. 6)}$$

$$= 1.74(.28)^{\frac{1}{2}}(.85) = .785$$

$$\frac{d\eta_t}{dC_L} = .5(.785) = .393$$

3.) Tail lift coefficient, C_{L_t}

Assuming constant derivatives,

$$C_{m_{c.g.}} = 0 = C_{m_{ac}} + C_L \left(\frac{dC_M}{dC_L}\right)_{Fus,\,Nac} + \frac{dC_{N_p}}{dC_L}\,\frac{\ell_p}{c}\,\frac{S_p}{S_w} + \frac{dT_c}{dC_L}\,\frac{2D^2}{S_w}\,\frac{Z}{c} - C_{L_t}\,\overline{V}\,\eta_t$$

e.) (continued)

$$C_{L_t} = + \frac{1}{(.89)(.985)} \left\{ - .01 + .28 \left[.14 + .1 \times 2 \times 2 \times \frac{44.5}{175} \times .066 + 2 (.147)(.251) \right] \right\}$$

$$C_{L_t} = + .0595$$

f.) Static margin,

$$\frac{dC_m}{dC_L} = \frac{a_t}{a_w} \bar{V} \left(1 - \frac{d\varepsilon}{d\alpha} - \frac{d\varepsilon_p}{d\alpha} \right) \eta_t - C_{L_t} \bar{V} \eta_t + \left(\frac{dC_m}{dC_L} \right)_{Fus, Nac} + 2 \frac{dT_c}{dC_L} \frac{2D^2}{S_w} \frac{Z}{c} + 2 \frac{dC_{N_p}}{dC_L} \frac{\ell_p}{c} \frac{S_p}{S_w}$$

$$= - \frac{.069}{.0816} .89 (1 - .36 - .0436) .985 - .0595 (.89)(.985) + .14 + 2 (.1)(2) \frac{(44.5)}{175} (.066) + 2 (.147)(.251)$$

$$= - .232$$

g.) Control-fixed neutral point, N_o

$$N_o = X_{c.g.} - \frac{dC_M}{dC_L}$$

$$= .245 - (- .232) = .477$$

h.) Elevator power, C_{m_δ}

$$C_{m_\delta} = a_t \overline{V} \eta_t$$

$$= -.069(.89)(.986)(.59) = -.0356$$

i.) Control-free neutral point, N_o'

$$N_o' = N_o + \frac{C_{m_\delta} C_{h_\alpha}}{a_w C_{h_\delta}}\left(1 - \frac{d\varepsilon}{d\alpha}\right) + \frac{\Delta P C_{m_\delta}(57.3)}{G_e S_e c_e C_{h_\delta} W/S}$$

$$= .477 + \frac{(-.0356)(-.085)}{(.0816)(-.74)}\left(1-.36\right) + \frac{42(-.0356)(57.3)}{.98(22.1)(1.3)(-.74)(24)}$$

$$= .477 + -.032 + .189$$

$$= .634$$

j.) Control-fixed maneuver point, N_m

$$N_m = N_o + \frac{63\rho \ell_t g C_{m_\delta}}{2\tau W/S}\left(1 + \frac{1}{n^2}\right)$$

$$= .477 - \frac{63(.001868)(14.6)(32.2)(-.0356)(1.25)}{2(.59)(24)}$$

$$= .477 + .087$$

$$= .564$$

k. Control-free maneuver point, N_m'

$$N_m' = N_o' + \frac{57.3}{(W/S)\, C_{h_\delta}} \frac{C_{m_\delta}}{} \left[\frac{\rho}{2} g \ell t \left(C_{h_\alpha} - 1.1 \frac{C_{h_\delta}}{\tau} \right) \right] \left(1 + \frac{1}{h^2} \right)$$

$$= .445 + \frac{57.3(-.0356)}{24(-.74)} \left[(.000934)(32.2)(14.6) \left(-.085 - \frac{1.1(-.74)}{.59} \right) \right] (1.25)$$

$$= .445 + .081$$

$$= .526$$